PROPERTIES OF THE TOMBUSVIRUS MOVEMENT PROTEIN AND RNAi SUPPRESSOR THAT INFLUENCE PATHOGENESIS

A Dissertation

by

YI-CHENG HSIEH

Submitted to the Office of Graduate Studies of
Texas A&M University
in partial fulfillment of the requirements for the degree of

DOCTOR OF PHILOSOPHY

August 2008

Major Subject: Plant Pathology

PROPERTIES OF THE TOMBUSVIRUS MOVEMENT PROTEIN AND RNAi SUPPRESSOR THAT INFLUENCE PATHOGENESIS

A Dissertation

by

YI-CHENG HSIEH

Submitted to the Office of Graduate Studies of
Texas A&M University
in partial fulfillment of the requirements for the degree of

DOCTOR OF PHILOSOPHY

Approved by:

Chair of Committee,	Herman B. Scholthof
Committee Members,	Linda A. Guarino
	T. Erik Mirkov
	Karen-Beth G. Scholthof
Head of Department,	Dennis C. Gross

August 2008

Major Subject: Plant Pathology

ABSTRACT

Properties of the *Tombusvirus* Movement Protein and RNAi Suppressor That Influence Pathogenesis. (August 2008)

Yi-Cheng Hsieh, B.S., Fu Jen Catholic University;

M.S., National Taiwan University, Taiwan

Chair of Advisory Committee: Dr. Herman B. Scholthof

Tomato bushy stunt virus (TBSV) provides a good model system to investigate molecular virus-host interactions in plants. P22 and P19 proteins encoded by TBSV contribute to multiple invasion-associated functions. Green fluorescence-mediated visualization of TBSV invasion in this study suggests that virus exit from inoculated epidermal cells is a crucial event. Close examination of one P22 mutant showed that it had lost the capacity to move between epidermis and mesophyll which was possibly due to an altered subcellular localization. P19 is a potent suppressor of RNA interference (RNAi) in various systems by forming dimers that bind 21-nucleotide (nt) duplex siRNAs (short interfering RNAs), to affect the programming of the RNA-induced silencing complex (RISC). P19 is attractive for biotechnological and research purposes to prevent RNAi of certain value-added genes in plants. To obtain a good plant-based expression platform, a suppression-active mutant P19 was expressed in transgenic *N. benthamiana* lines. This is the first example of P19 accumulating to detectable levels in a transgenic plant and initial results suggest it is actively suppressing RNAi. Furthermore, to investigate the correlation between siRNA binding of P19 and its various biological roles, predicted siRNA-interacting sites of TBSV P19 were modified, and the corresponding

TBSV mutants were used to inoculate plants. Substitutions on siRNA-contact sites on the central domain of P19 resulted in more severe symptoms in *N. benthamiana* compared to those affecting peripheral regions. All tested combinations of siRNA-binding mutations were associated with reduced accumulation of total TBSV-derived siRNAs, and loss of siRNA sequestration by P19. Additionally, some modifications were found to cause RNAi-mediated disappearance of viral and host materials in *N. benthamiana* but not in spinach. In conclusion, exit out of epidermal cells is a key host range determinant for TBSV and particular amino acids on P22 may influence this by regulating the proper subcellular localization. Mutant P19 transgenic plants were successfully established with minor physiological effects to be applied as a platform to study RNAi and to over-express proteins. Finally, a compromised P19-siRNA binding impacts symptom development, systemic invasion, integrity of virus plus host RNA and proteins, and that all in a host-dependent manner.

DEDICATION

I would like to dedicate this to my parents…..

ACKNOWLEDGMENTS

First of all, I would like to thank my academic adviser, Dr. Herman B. Scholthof, for his great mentoring and guidance for my graduate study in the Department of Plant Pathology and Microbiology at Texas A&M University. I also thank Dr. Karen-Beth Scholthof, my committee member for her critical reviewing of manuscripts and helpful advice. I would like to thank my other committee members, Dr. Linda Guarino and Dr. Erik Mirkov, for their suggestions and support.

I would like to give special thanks to our Associate Research Scientist, Dr. Rustem Omarov, for his training in techniques and collaboration in Chapter IV. I also appreciate Ms. Malika Shamekova's collaboration in Chapter II to establish some valuable constructs for our research. I want to thank Ms. Jessica Ciomperlik and Dr. Dong Qi for proofreading my manuscripts and assisting with chromatography and protoplast experiments. I would like to thank our student worker, Ms. Kristina Twigg, for diligently maintaining our common laboratory supplies.

Last but not least, I would like to thank my parents, sisters, and Ching-Jung Tsai for their encouragement. Without you, I would not be able to accomplish this task. Thank you.

TABLE OF CONTENTS

CHAPTER Page

Page

LIST OF TABLES

LIST OF FIGURES

FIGURE Page

FIGURE Page

CHAPTER I

INTRODUCTION

General

Viruses can generally be defined as "a set of one or more nucleic acid templates, encapsidated in protective coats of protein (or lipoprotein) which are enable to support viral replication within suitable host cells" (Hull, 2002). The major criteria used by Hull for classification is based on the defined molecular features of viruses, including virion properties (structure and physicochemical properties of virus particle), replication and genome organization (properties of viral nucleic acids), antigenic properties (viral proteins and serological relationships), biological properties (viral transmission and virus-affiliated activities in the plant). Moreover, according to nucleic acid properties plant viruses can be classified as DNA viruses (dsDNA and ssDNA viruses) and RNA viruses (dsRNA, ssRNA, plus-stranded (+), and negative-stranded (-) ssRNA).

The simple composition of viruses generally restricts the amount of genetic material (DNA/RNA) they can carry. Therefore, efficient utilization of these limited genomic nucleic acids is critical for viral life cycles and biological performance. Hence, the coding sequences of viruses are well packed and positioned compactly to increase the efficiency in use of nucleic acids to translate viral proteins. However, this composition implies some challenges in order to overcome the constraints of the eukaryotic monocistronic criteria for translation. For this, viruses have developed several tactics to express viral proteins, which can be categorized as generation of subgenomic RNAs (sgRNAs), translation of

---

This dissertation follows the style of Plant Cell.

polyproteins, formation of multipartite genomes, internal initiation, leaky scanning, non-AUG start codon, trans-activation, translational shunt, read through, frameshifting, differential splicing, translation of both viral and complementary strands. The control of translation is further attributed to the 5'-cap, 3'-poly (A) tail, and 5'-untranslated region (UTR) to increase the translational levels of downstream genes. Furthermore, single gene products may have more than one function by interacting with other host- and virus-encoded proteins, or with regulatory non-coding or coding nucleotide sequences for RNA synthesis (Hull, 2002).

Although DNA is generally more stable than RNA, to the date there are many more RNA than DNA plant viruses; in fact more than 90% of plant viruses are represented by RNA molecules (Hull, 2002). Among these, most contain a positive sense single-stranded RNA that can function as messenger RNA (mRNA) for efficient translation of early viral proteins (usually replication-associated proteins). In addition, viruses use the (+) RNA as templates for genome replication, and they are encapsidated and protected within the virus particles (Gamarnik and Andino, 1998). Nevertheless, the limited size of the RNA genome (usually less than 20 kb) encompasses all the signals for translation, replication, and encapsidation, which include the genes as well as *cis*-acting RNA elements that are all perfectly-packed into these small RNA molecules and that are critical for the virus life cycle (Duggal et al., 1994). The virus used in this research (as introduced below) is an example of such an efficiently operating (+) sense RNA virus that serves as a model system in studies on plant-virus interactions (Yamamura and Scholthof, 2005).

Tombusviruses

There are eight genera of viruses in the family *Tombusviridae* which include *Aureusvirus*, *Avenavirus*, *Carmovirus*, *Dianthovirus*, *Machlomovirus*, *Necrovirus*, *Panicovirus*, and *Tombusvirus* (Stuart et al., 2004). The genomes of viruses in this family are positive-sense single-stranded RNAs. The viral genome is monopartite, except for viruses in the genus *Dianthovirus* which contains bipartite genomes.

The viruses of the family *Tombusviridae* contain neither 5'-cap structures nor 3'-poly-(A) tails on their genomic RNAs (Takeda et al., 2005). These viruses do not encode proteins containing a helicase motif that is conserved in many eukaryote infective viruses (Koonin and Dolja, 1993). Symptom induction by some viruses in the *Tombusviridae* family is associated with subviral RNAs which include defective-interfering RNA (DI RNA) and satellite RNA (Rubio et al., 1999; Simon et al., 2004).

Studies on these viruses began with serological and cytopathology, but in the late 1900's they were further examined regarding the sequence homology to study the relationships. For example, seven viruses in the *Tombusvirus* genus which include *Artichoke mottle crinkle virus* (AMCV), *Carnation Italian ringspot virus* (CIRV), *Cymbidium ringspot virus* (CyRSV, or CymRSV), *Eggplant mottle virus* (EMCV), *Petunia asteroid mosaic virus* (PAMV), *Pelargonium leaf curl virus* (PLCV), and *Tomato bushy stunt virus* (TBSV) were used as standards to define some tentative members. The results demonstrated that AMCV, CIRV, EMCV, PAMV, PLCV, and TBSV are serologically related while CymRSV is distantly related to TBSV (Gallitelli et al., 1985).

In our laboratory, TBSV is used to study the mechanism behind tombusviral invasion of different hosts. TBSV was first reported in *Lycopersicon esculentum* (tomato) from

England in 1935 (Smith, 1935). The symptoms were described as bushy growth, reduced yield of fruits with chlorotic blotching, ring and line patterns on *Lycopersicon esculentum*. In some natural host plants (for example, *Capsicum annuum, Solanum melongena, Tulipa* spp.) mottling, crinkling, necrosis, deformation of the leaves, stunting growth, petal necrosis, no fruit production or few spotted and deformed fruit were also observed. TBSV can be transmitted by mechanical inoculation, grafting, plant contact, seed (relatively lower), and possibly from pollen to the seed. Transmission of TBSV does not involve a vector.

TBSV is characterized by relatively small, isometric T=3 virus particles that encapsidate a ss (+) sense RNA genome of ~4.8 kb (Olson et al., 1983). The infectivity range of TBSV is very broad and includes plant species in more than twenty families. TBSV serves as a classical model system for investigation of fundamental principles of virus replication and translation (Nagy and Pogany, 2000), the occurrence and genesis of DIs (Hillman et al., 1987; Scholthof et al., 1995c), host-virus protein interactions (Desvoyes and Scholthof, 2002; Yamamura and Scholthof, 2005), and intercellular virus movement (Scholthof et al., 1995b).

The 5' to 3' gene arrangement on the TBSV RNA genome includes *p33*, *p92* (both replication-associated), *p41* (coat protein), and the 3′-proximal open reading frames (ORFs) known as *p22* and *p19* that encode a ~22 kDa (P22) and a ~19 kDa (P19) protein, respectively (Fig. I-1). P22 is a cell-to-cell movement protein (MP) and P19 has multiple roles in TBSV pathogenicity (Hearne et al., 1990; Scholthof et al., 1995b; Scholthof, 2006). The *p19* ORF is entirely nested in the ORF for *p22*, resulting in simultaneous translation of two distinct proteins. Moreover, the overlapping sequence between *p19* and *p22* is considerably conserved among tombusviruses further indicating that this region of

the genome performs crucial biological functions. Therefore, the 3'-proximal ORFs, with a particular emphasis on the biological events regulated by P19, are the major focus of this study.

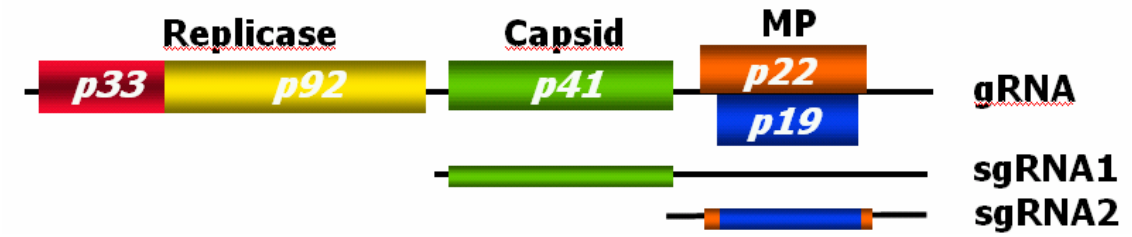

Fig. I-1. Composition of the TBSV genome.
The figure shows the 4,775-nucleotide single-stranded plus-sense genomic RNA (gRNA) of TBSV. Genes of TBSV are named corresponding to their predicted encoded protein sizes (in kDa). These proteins play roles in viral replication (replicase), virus encapsidation (capsid), and virus spread or movement (movement protein, MP). There are two 3' co-terminal subgenomic RNAs (sgRNAs) produced during virus replication for translation of *p41* and *p22/p19*, respectively (Hearne et al., 1990; Scholthof, 2006).

Viral movement

The successful viral invasion of plants comprise several characteristic processes including but not limited to: entry of virus into plant cells, amplification of viral genome in the early stage of infection, translation of viral proteins, viral cell-to-cell movement via plasmodesmata, and subsequent long-distance movement of virus thorough the vascular system (Dawson, 1992; Lucas, 1995; Carrington and Whitham, 1998; Lucas, 2006). Cell-to-cell movement is further divided into two distinct phases which are intracellular and intercellular. Intercellular transport goes through plasmodesmata and intracellular trafficking accompanies viral replication (Carrington et al., 1996; Hull, 2002). Within infected cells, virus accumulation is completely dependent on the host protein-synthesizing machinery and host proteins are thought to be involved in virus movement by interacting with viral MPs. Five cell-to-cell movement strategies of plant viruses were classified (Carrington et al., 1996; Hull, 2002):

a) *Tobacco mosaic virus* (TMV) strategy: TMV encodes an insoluble membrane-bound movement protein (MP, P30) that binds ssRNA in a non-sequence specific manner (Citovsky et al., 1992; Citovsky et al., 1993) and increases the size-exclusion limit (SEL) of plasmodesmata to transport the virus particles or ribonucleoprotein complexes intercellularly (Ding et al., 1992; Waigmann et al., 1994). It is now thought that the moving complex may be a replication complex (Asurmendi et al., 2004; Kawakami et al., 2004).
b) The tubule strategy: Formation of tubules with viral MPs to extend the cell wall and plasmadesmata, therefore, viral complexes are able to traffic through modified plasmodesmata (Carrington et al., 1996).

c) Triple-gene block (TGB) strategy: Different TGB products are involved in different phases of cell-to-cell movement. One TGB product (TGB1) of potexviruses increases the SEL of plasmodesmata, together with the viral coat protein to from a complex interacting with viral RNA, and intracellularly transport through plasmodesmata. Other TGB products (TGB2, 3) are required for intercellular transport (Lough et al., 1998).

d) Potyviral strategy: Pin-wheel inclusions associate with cell wall and array virus particles (confirmed with CP detection and EM) to move through the opening of plasmodesmata (Roberts et al., 1998).

e) Geminiviral strategy: Movement out of the nucleus is assisted by viral proteins (coat protein) and cell-to-cell movement (through plasmodesmata) is mediated by other virus-encoded proteins (Lazarowitz and Beachy, 1999).

Furthermore, viruses can also be simply categorized depending on the need for coat protein or virus particles for movement (Scholthof, 2005). TBSV follows the TMV strategy for cell-to-cell movement and does not need the CP for this process (Scholthof, 2005).

In addition to cell-to-cell movement, long-distance spread via phloem for systemic transport plays a crucial role for rapid delivery of infective viral materials through out the whole plant. Based on a report on TMV (Bennett, 1940), once virus enters the phloem movement may occur at the "velocity" of 1.5 cm/h.

Based on the observation that many plant viruses are able to replicate in protoplasts isolated from non-host plant tissues (Wang et al., 1996), it was postulated that cell-to-cell movement and long-distance viral spread together are major determinants for infectivity on hosts. Furthermore, long-distance movement is also influenced by viral proteins other

than MPs or CPs which include P19 of TBSV (Scholthof et al., 1995b), helper component proteinase (HC-Pro) of potyviruses (Cronin et al., 1995), and the 2b protein of *Cucumber mosaic virus* (CMV) (Ding et al., 1995). All these virus-encoded proteins act as movement elements to assist long-distance spread of viruses. Moreover, some of these long-distance movement proteins are required for efficient amplification of the viral genome, and most are the major determinants for symptom development. Most intriguingly, all these proteins function as suppressors of post-transcriptional gene silencing (PTGS) within plants (Anandalakshmi et al., 1998; Brigneti et al., 1998; Voinnet et al., 1999; Kasschau et al., 2003). These virus-encoded suppressors of gene silencing are able to perturb this plant defense mechanism (discussed in more detail later), thus providing a mechanistic explanation for their contributions to invasion (Scholthof, 2005). For full systemic infection, most viruses need coat protein (CP) but whether that is related to movement of viruses or alternative CP-RNA complexes depends on the virus-host combination (Callaway et al., 2001). Particular aspects of viral movement, especially the importance of exit from inoculated epidermal cells are discussed in Chapter (II).

RNA interference

RNA interference (RNAi) is a post-transcriptional RNA silencing process in eukaryotes that serves as a regulatory mechanism to target specific RNAs for catalytic degradation or translation inhibition (Grishok et al., 2001; Scholthof, 2006). RNAi commonly results in elimination of mRNAs for particular genes. Based on the mechanism of RNAi, organisms are able to protect their genomes from foreign gene insertion (transposons) and pathogenic invasion (viruses). In fact, RNAi is considered as

part of an ancient straightforward defense system (Plasterk, 2002; Robinson, 2004; Dykxhoorn and Lieberman, 2006).

The initiation of the RNAi pathway is currently thought to consist of two major significant events. The first step involves the recognition of double-stranded (ds) RNA by Dicer-like protein complexes. Viral replication in plants often leads to accumulation of abundant levels of single-stranded RNA with hairpins and double-stranded RNAs with replicative forms (Molnar et al., 2005). These highly-structured RNA molecules are thought to be used as the substrates for initial steps in RNAi (Fig. I-2). The second important event is the cleavage of dsRNAs, which yields duplex short interfering RNAs (siRNAs) with 3' overhangs (Fig. I-1) (Zou and Yoder, 2005), by the action of a RNase III enzyme-like Dicer (Fire et al., 1998; Bernstein et al., 2001). Particularly, this cleavage procedure is an ATP-dependent reaction and these siRNAs are incorporated in a complex to form the RNA-induced silencing complex (RISC). One strand of the dsRNA remains incorporated with RISC and thus is used for the recognition of homologous sequences that are then cleaved by the hydrolytic activities of RISC, to achieve gene silencing.

Based on these general understandings of RNAi, *Tomato bushy stunt virus* (TBSV) and *Nictotiana spp.* are routinely used in our laboratory to study RNAi in the context of virus-host interactions. TBSV is a convenient model to study RNAi because during the course of infection in plants it enormously enriches dsRNA substrates for Dicer-mediated cleavage and results in readily detectable amount siRNAs (Omarov et al., 2006; Scholthof, 2006). It has further been shown that TBSV-siRNAs associate with a virus-specific RISC-like complex that cleaves viral RNAs resulting in the recovery of plants from infection (Omarov et al., 2007). This model is illustrated in Fig. I-2 and the

importance of TBSV P19 that is shown in this figure will be explained in the following section.

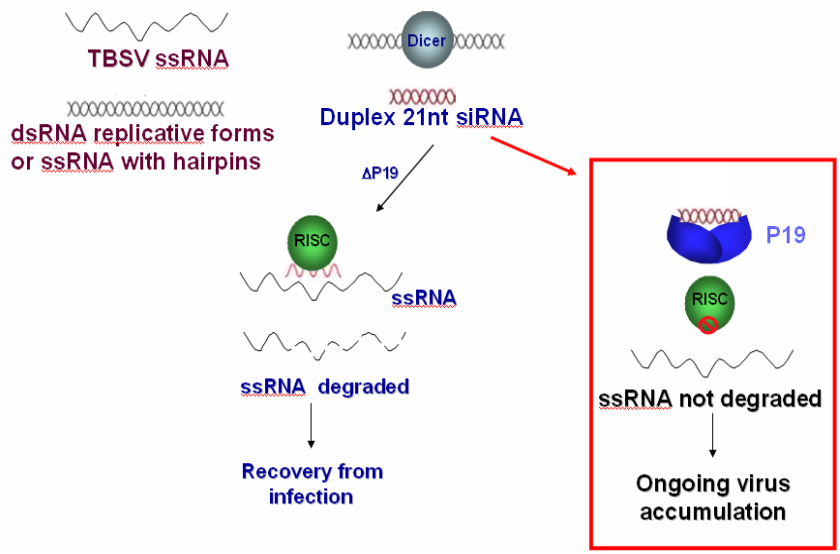

Fig. I-2. A model for suppression of RNA silencing in the context of TBSV infection. A current model of the RNAi pathway (Zou and Yoder, 2005) includes recognition of replicative forms of dsRNA or structured ssRNA by Dicer for siRNAs generation that are used to program the RNA induced silencing complex (RISC). TBSV P19 plays an important role by sequestering duplex siRNAs which presumably prevents programming of RISC that in turn suppresses RNAi-mediated RNA degradation, to permit ongoing virus accumulation (Omarov et al., 2006; Omarov et al., 2007).

Suppressors of RNA interference

As mentioned in a previous section on viral movement, some long-distance movement proteins which include HC-Pro, 2b, and P19 are able to suppress RNAi. Intriguingly, these suppressors also determine symptom development and function at different steps of RNAi (Beclin et al., 1998; Brigneti et al., 1998; Voinnet et al., 1999; Lakatos et al., 2006). Among these, the multiple activities of P19 are the areas of focus in our laboratory. These activities include the elicitation of a hypersensitive response (HR) in *N. tabacum*, promoting cell-to-cell movement in pepper, long distance spread in pepper and spinach, and induction of severe symptom development in most hosts. Even though P19 is dispensable for the initiation of TBSV infection in *N. benthamiana,* it is crucial for viral RNA maintenance (Chu et al., 2000; Qiu et al., 2002; Qu and Morris, 2002; Omarov et al., 2006; Scholthof, 2006). Furthermore, some effects of P19 are directly related to its ability of binding viral siRNA (Fig. I-2) (Omarov et al., 2006). However, it still remains unknown how this property relates to the different host-dependent activities of P19, and this is a major topic of the research described in Chapter IV.

Since P19 activities were found to be influenced by the host background, it was hypothesized that this protein may interact with one or more host factors (Chu et al., 2000). Subsequent yeast-two hybrid screening with a *N. tabacum* cDNA library resulted in identification of Hin19 protein that specifically interacts with P19 in a biological relevant manner (Park et al., 2004). Based on the GenBank search and results from western blots, Hin19 has high similarity with an analogous protein in *N. benthamiana*. The N-proximal 120 amino acids of Hin19 show 60-65% identity to *Arabidopsis* ALY-like proteins that are involved in nuclear export or transcriptional co-activation (Uhrig et

al., 2004; Canto et al., 2006) that are also known as RNA export factor (REF) binding proteins (Yamamura and Scholthof, 2005). The most striking feature of Hin19 is the presence of the conserved RNA recognition motif that is a signature block of RNA binding proteins. These proteins are involved in a variety of post-transcriptional events.

TBSV P19 was the first suppressor for which the target molecule on RNAi pathway was identified (Takeda et al., 2005). Furthermore, some P19-mediated activities (as suppression of RNAi) are also controlled by specific self-interactions (Park et al., 2004). This was later structurally confirmed by X-ray crystallographic studies (Vargason et al., 2003; Ye et al., 2003). The structure of P19 dimers involves formation of the P19 dimeric complex with duplex siRNAs (Fig. I-3). Recent work from our laboratory showed that P19 can form dimers in absence of siRNAs indicating that protein dimerization is an independent intrinsic property of the viral protein (Park et al., 2004; Omarov et al., 2006). The sequence-nonspecific sequestration of siRNAs is thought to be responsible for the ability of P19 to suppress RNAi (Fig. I-2). Currently, P19 has become an extensively used tool to study the mechanism of RNAi in various eukaryotic model systems (Voinnet et al., 2003; Zou and Yoder, 2005; Scholthof, 2006).

Even though P19 has been used in several systems to suppress RNAi for bio-technological purposes (elaborated in Chapter III), its toxic effects in plants, with severe

negative consequences, have been observed (Silhavy et al., 2002; Omarov et al., 2006; Scholthof, 2006). Our previous studies revealed that a non-toxic P19 mutant (P19/R43W) partially retains suppression activities while greatly decreasing the severity of symptoms in plants (Omarov et al., 2006). Based on these properties of P19/R43W, this P19 TBSV mutant may represent a unique and suitable biotechnological tool to permit enhancing foreign gene expression in plants by suppressing RNAi activity without causing lethal necrosis. This is the focus of the work described in chapter III.

In conclusion, the research of this dissertation has three major components. The first deals with the correlation between host-range and cell-to-cell movement as well as how a single conserved amino acid of P22 is crucial for this purpose (Chapter II). Then, work is described towards using a mutant P19 which is suppression-active but less toxic to plants, to determine its suitability for application in elevating expression of foreign genes (Chapter III). The third component focuses on the siRNA binding by P19 that controls suppression of RNAi in TBSV infected plants, with a particular emphasis on host-specific effects (Chapter IV).

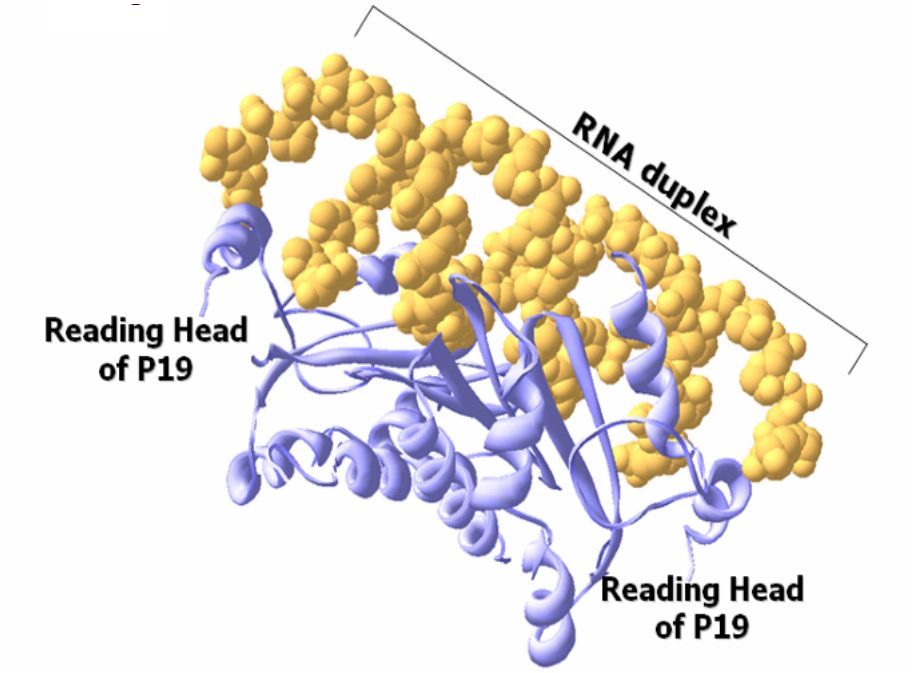

Fig. I-3. P19/siRNA structure.
P19 dimers “measure” and bind 21 nt siRNA duplexes. Two α-helical 'reading heads' extend from opposite ends of the p19 homodimer. The amino acids between position 39 and 43, in particular the tryptophan residues are thought to recognize the 3’-end of RNA duplex. This recognition, following by stacking these terminal base pairs of siRNAs, is thought to be critical for siRNAs sequestration of P19 dimer (Ye et al., 2003).

CHAPTER II

TOMBUSVIRUS EGRESS FROM INOCULATED EPIDERMAL CELLS IS A CRITICAL HOST RANGE DETERMINANT THAT REQUIRES A CONSERVED AMINO ACID ON P22

Introduction

Establishment of a successful systemic infection for plant viruses relies on multiple events such as replication in the initially inoculated cells (which for mechanically transmitted viruses is often an epidermal cell), local spread via plasmodesmata, and the distant distribution via the vascular system. Therefore, a comprehensive understanding of plant virus infections requires a detailed characterization of viral movement and the underlying molecular/biochemical mechanisms (Lucas, 1995; Waigmann et al., 1998; Oparka and Cruz, 2000; Scholthof, 2005).

The primary transport of viral components is assisted by virus-encoded movement proteins (MPs) and presumably by host factors, and this can be defined as cell-to-cell movement (Lucas, 2006). In general, many plus-stranded RNA plant viruses have movement strategies that depend on five shared common biochemical properties of the MPs that as originally reported for the MP of *Tobacco mosaic virus* (TMV). First, MPs are capable of binding nucleic acids to form non-virion ribonucleoprotein complex (RNPs) that are trafficked through plasmodesmata, the pores that provide intracellular (symplastic) connections between plant cells (Kiselyova et al., 2001; Lucas and Lee, 2004). Second, MPs associate with microtubules in the cytoskeleton and accumulate at the cell wall to temporarily increase the size exclusion limit of plasmodesmata (Heinlein et al., 1995;

Heinlein et al., 1998; Ashby et al., 2006). Third, the phosphorylation of MPs by host kinases may regulate translation of the viral proteins and control the localization of the viral ribonucleoprotein complexes translocation to and through plasmodesmata (Balachandran et al., 1995; Sokolova et al., 1997; Hofius et al., 2001). Fourth, dimerization of conventional, movement proteins is essential for these MPs to function in cell-to-cell spread (Brill et al., 2004). Fifth, MPs are shown to interact with host factors (Oparka and Cruz, 2000; Scholthof, 2005), and even though for most their precise role is not known, a few have been demonstrated to play a direct role in cell-to-cell movement (Jimenez et al., 2006; Kaido et al., 2007; Yoshii et al., 2008). Others seem to have a role in defense responses and/or protein degradation (Conrath et al., 1998; Bucher et al., 2001; Heinlein, 2002; Liu et al., 2002a; Liu et al., 2002b; Liu et al., 2004; Zeng et al., 2006).

Some of the above listed properties are also shared by MPs of viruses that form tubules that grow through the plasmodesmata (Scholthof, 2005). MPs behave as intrinsic membrane proteins with a tendency to self congregate and promote aggregation of endoplasmic reticulum (ER) during virus replication. Importantly, as shown for TMV, the MP is critical to form virus replication complexes (VRCs) in association with cellular membranes such as ER and traffic these VRCs through plasmodesmata (Asurmendi et al., 2004; Liu et al., 2005). Therefore, it seems that MPs do not simply traffic viral RNA, but instead transport whole replication units.

In general, a simple categorization of viral movement can be based on the requirement of CP or virion (Scholthof, 2005). Plant viruses may not require CPs to move, or utilize CPs as auxillary MPs, or alternatively they need CPs because they move as particles or particle-like CP-containing complexes.

Tomato bushy stunt virus (TBSV), the type member of the genus *Tombusvirus* in the *Tombusviridae*, is a plus-sense single-stranded RNA virus that serves as a useful model system to study key aspects of virus-host interactions (Yamamura and Scholthof, 2005). The TBSV-encoded MP, P22, is an insoluble membrane-bound protein that is encoded by the 3' proximal region (*p22*) of the TBSV genome and it is known that this protein is required for cell-to-cell movement (Scholthof et al., 1995b). P22 is able to bind viral RNAs and move viral material through the plasmodesmata (Chu et al., 1999; Desvoyes and Scholthof, 2002).

In a previous study, eight mutants of *p22* were constructed to result in the substitution of one or more amino acids in locations that were predicted to be exposed on the surface of the folded protein (Chu et al., 1999; Park et al., 2002). These modifications were performed without changing the *p19* gene which is a gene encoding the suppressor of RNA silencing that is nested within the *p22* gene (Scholthof, 2006). Intriguingly, all eight P22 mutants were capable to replicate and generate TBSV sgRNAs but three P22 mutants (including an E103A substitution), were unable to establish successful infections. They failed to move from the initially inoculated to uninfected neighboring cells (Chu et al., 1999). Further tests indicated that the defect in movement correlated with the inability of the mutant proteins to interact with a host transcription factor (Desvoyes et al., 2002). How this host factor contributes to P22 functionality is not yet known. Based on our current understanding of TBSV, CP is not mandatory for systemic infection in the few experimental hosts tested thus far, although the presence of CP accelerates the progression of the infection (Scholthof et al., 1993; Desvoyes and Scholthof, 2002; Qu and Morris, 2002).

Thus far, general principles on TBSV movement such as those described above were uncovered through experiments with only a few hosts such as *Nicotiana benthamiana*. However, the movement pattern and requirements have not yet been investigated for most hosts, which seems an important oversight considering the vast host range of TBSV (Yamamura and Scholthof, 2005). Within this framework, the first part of the present study on TBSV movement examined the infectivity and tissue specificity of an infectious TBSV construct containing the gene for green fluorescent protein (GFP) substituted for CP (TBSV-GFP), in different hosts. This provided a powerful tool to examine suitability of plants for infection (replication plus movement) because the occurrence of green fluorescent spots can be rapidly observed and measured. Using this system, ~30 plant species were tested. For some susceptible species the results indicated that the ability to penetrate from epidermal cells into the underlying mesophylls is an important determinant for the ability of TBSV to infect plants beyond the site of inoculation.

Secondly, during a periodic NCBI online multiple protein sequences alignment a serendipitous observation was made that the valine (V) at position 124 on TBSV (P22/V124) is a very but not completely conserved amino acid on P22 among tombusviruses, suggestive of a residue that is involved in interaction with a host component. Therefore, for the second part of this study the aim was to change TBSV P22/V124 to alanine (A), and to also make a higher impact substitution to leucine (L). These mutants were introduced on wtTBSV cDNA, TBSV cDNA with defective *p19*, TBSV-GFP, and on constructs for which *gfp* was fused with *p22* (GFP-P22). Transcripts obtained from these constructs were compared for *in vitro* translation assays, viral replication in protoplasts, P22 localization, and cell-to-cell movement. The data showed that the V124A mutation (as it naturally occurs on P22 of *Cymbidium ringspot virus*-

CymRSV) had negligible effects whereas the V124L mutation did not affect protein accumulation or replication but specifically prohibited effective exit of virus from initially inoculated epidermal cells. This appeared to correlate with a somewhat compromised ability of GFP-P22/V142L to locate towards the cell surface of transfected protoplasts.

The combined results show that egress of TBSV from epidermal cells into underlying tissues is an important host range determinant and that cell-to-cell movement out of the initially infected epidermal cells and subsequent movement, requires a proper subcellular localization of P22 that depends on an amino acid at position 124 that is conserved among most species within the genus *Tombusvirus*.

Materials and methods

*Dpn*I-mediated site-directed mutagenesis. A QuikChange kit (Stratagene, La Jolla, CA) was used for site-directed mutagenesis and standard molecular biology protocols were followed for the isolation and manipulation of plasmid DNA (Sambrook et al., 1989). The plasmids used to generate mutants were a pUC119 phagemid derivative with the full TBSV cDNA insert (pTBSV100) (Hearne et al., 1990). TBSV-GFP and TBSV-P22-GFP were kindly provided by T. Rubio and A. Jackson (UC Berkeley). The significance of these constructs is explained in Results. All mutant constructs were made specifically to yield amino acid substitutions on P22 while keeping P19 intact.

Inoculation and analysis of plants and protoplasts. *In vitro* generated transcripts of pTBSV-100-derived cDNAs expressing wtP22, P22/E103A, P22/V124L, and P22/V124A, TBSV-GFP, and GFP-P22 were prepared essentially as reported earlier

(Hearne et al., 1990). The plasmids (1 μg) were linearized at the 3'-terminus of the viral cDNA sequence by digestion with *Sma*I, and transcripts were synthesized with T7 RNA polymerase. *N. benthamiana* plants were inoculated using standard procedures (Scholthof, 1999). For the RNA accumulation tests in protoplasts, about 4×10^5 *Nicotiana benthamiana* protoplasts were used per transfection. Methods described previously (Scholthof et al., 1995c) were followed for preparation and transfection of protoplasts and to monitor RNA accumulation using hybridization probes that were generated by using random primers with plasmid pTBSV-100 or from a *p19* PCR product.

RNA analysis. At 1 dpi, transfected *N. benthamiana* protoplasts were readily spun down at 70 centrifugation force (xg). Total RNA was extracted on ice by adding 300 μl RNA extraction buffer (200 mM ammonium carbonate pH 9.0, 2% SDS, 2 mM EDTA, 200 μg/ml bentonite), immediately followed by twice phenol/chloroform extraction (1:1, vol/vol) and precipitated with 10 M ammonium acetate solution (1:1, vol/vol) at 4 °C for 1 hour. The resulting pellets were washed with 70% ethanol, then resuspended in RNA suspension mix (10 mM DTT, 80 units/100μl RNasin), and used for northern blot hybridization. Total RNAs were separated in 1% agarose gel in 1× Tris-borate-EDTA (TBE) (Sambrook et al. 1989). Equal loading of samples was verified by ethidium bromide staining of the gels. The RNAs were then transferred to nylon membranes (Osmonics, Westborough, MA). TBSV gRNA and sgRNAs were detected by hybridization with [^{32}P]dCTP-labeled TBSV-specific probes, essentially as previously described (Scholthof et al., 1993).

Western blot analysis. Protein samples were separated by SDS-PAGE in 15% polyacrylamide gels and transferred to nitrocellulose membranes (Osmonics, Westborough, MA). After transfer, the membranes were stained with Ponceau S (Sigma, St. Louis, MO) to verify protein transfer efficiency. The TBSV P22 and P19 antibodies were diluted 1:5,000. Alkaline phosphatase–conjugated goat anti-mouse antiserum (Sigma, St. Louis, MO) was used as a secondary antibody at a dilution of 1:1,000, and the immune complexes were visualized by hydrolysis of tetrazolium-5-bromo-4-chloro-3-indolyl phosphate as the substrate. In some experiments horseradish peroxidase-conjugated to goat anti-mouse antiserum (Bio-Rad, Hercules, CA) was used as a secondary antibody at a dilution of 1:5,000, and the immune complexes were visualized by enhanced chemioluminescence detection kit (Pierce, Rockford, IL).

In vitro translation. The *in vitro* translation assay of TBSV sgRNA2 was performed by using TNT T7 Coupled Wheat Germ Extract System (Promega, Madison, WI) which directly incorporates transcription in the translation mixture. TBSV sgRNA2 was amplified with an added sequence of the T7 promoter on the 5'-primer for PCR amplification to obtain a product representing sgRNA2. The forward primer to add the T7 promoter sequence is shown upstream of the sgRNA2 sequence in italics for TBSV T7-sgRNA2-F: 5'-ccggaattcctaatacgactcactata*ggaacaagaccagttcatggatactgaat*-3'; the reverse primer, TBSV sgRNA2-R: 5'-gggctgcatttctgcaatgt-3' is located at the 3'-end of TBSV sgRNA2. The PCR program for use with this primer were set initially to dissociate secondary structure of template DNAs and primers at 94°C 5 min, following by 25 cycles of reaction (94°C, 1 min; 55°C, 1 min; 72°C, 5 min), and terminated at 72°C 10 min. Approximately 0.2 - 2 μg of DNA templates from T7-sgRNA2 PCR were subsequently

added to the TNT Extract reactions and incubated 1.5 hours at 30°C. The subsequent protein separation was carried out in 15% polyacrylamide gels and transferred to nitrocellulose membranes (Osmonics, Westborough, MA) to detect the yield and content of proteins.

Agrobacterium-mediated transient expression (agroinfiltration) in *N. benthamiana*. The single amino acid substitutions on pKYLX7-P22 construct (provided by Dr. James E. Schoelz) was performed and then transformed into *Agrobacterium* C58 and EHA strains by electroporation (GIBCO-BRL Cell-Porator system (LCT)). The subsequent western detection was used to detect P22 and P19 in *N. benthamiana*.

Fluorescent imaging. GFP signals on the inoculated *N. benthamiana* leaves were monitored with a 100 W handheld long-wave ultraviolet (UV) lamp (UV products, Black Ray model B100AP, Upland, CA). Fluorescence microscopy was performed using the Olympus BX51 microscope (Olympus, America, Melville, NY, USA) with Olympus DSU spinning disc confocal imaging system. Fluorescent protoplasts, and selected inoculated leaf tissues with green fluorescent signals under UV observation that were carefully sectioned/peeled, and were used for fluorescent microscopy to study the viral cell-to-cell movement and subcellular localization. An Olympus DP70 camera was used for the capturing the image with different interference contrast (DIC) and wide field fluorescence. A Q-imaging MicroPublisher RTV 5.0 camera (Q-Imaging, Burnaby, B.C. Canada) was used for Z-axis-sectioning imaging. The GFP signal was excited and detected at the wavelength of 488 and 507 nm, respectively. Pictures were processed by NIH Image J (http://rsb.info.nih.gov/nih-image).

Results

TBSV-GFP visualization on different plants

The TBSV infectivity assays were conducted by using a TBSV cDNA construct in which the CP was partially replaced with the C3 version of the 26 kDa green fluorescent protein (GFP). The *gfp* cDNA was inserted in-frame between the *Not*I and *Bal*I sites within TBSV cDNA resulting in a fusion of *gfp* to the 5'-*cp* fragment and the presence of ~ 1 kb non-expressed CP RNA sequences downstream of the *Bal*I site (Fig II-1). Infectious viral RNA transcripts were rub-inoculated onto various plant species as listed in Table II-1 and as shown for selected examples in Fig. II-2.

Generally, plants inoculated with infectious TBSV-GFP developed characteristic green fluorescent symptoms emerging (under UV-light) at 2 dpi. Even though symptoms were seen in upper leaves of some susceptible hosts at 5-7 dpi, no green fluorescence occurred in those leaves. Loss of foreign genes due to recombination events during virus replication is a common occurrence for TBSV (Scholthof et al., 1993; Desvoyes and Scholthof, 2002). I have also seen such recombination occurring as evidenced by the ability of the virus to accumulate a reconstituted, although truncated, CP protein (data not shown). These recombination events were less apparent when the remaining CP RNA sequences present on TBSV-GFP downstream of the *Bal*I site (Fig. II-1), were removed. In recent experiments, this new construct yielded green fluorescent spots on inoculated leaves that were similar, or perhaps even larger, than those obtained with TBSV-GFP, yet infections in upper tissues most often still lacked GFP expression (M. Shamekova and Y. Hsieh, personal communication).

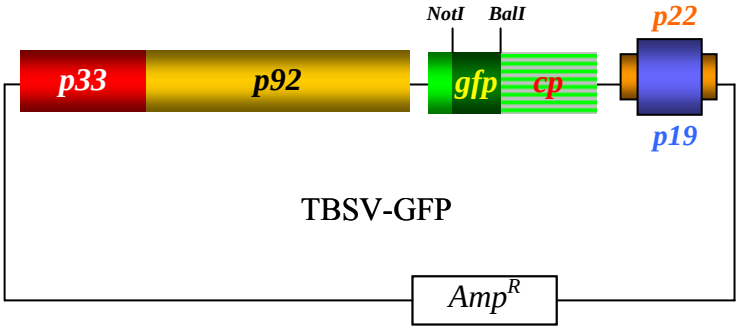

Fig. II-1. A schematic representation of the TBSV-GFP construct. TBSV-GFP was constructed with the pTBSV100 backbone which contains full-length cDNA of TBSV genome. This figure indicates that the TBSV *cp* is partially replaced by *gfp* sequence with ~ 1 kb untranslated downstream CP sequences remaining (indicated by thin gray lines). The selection marker for pTBSV100 and TBSV-GFP is ampicillin resistance gene (Amp^R).

Table II-1. Plants tested for TBSV infection and observation of green fluorescent spots

Plant species	TBSV infection	GFP foci
Abelmoschus esculentus (Okra)	Local lesions	●
Allium fistulosum (green onion)	No infection observed	○
Allium cepa (onion)	No infection observed	○
Amaranthus cruenta	Local lesions	●
Beta vulgaris var. *cicla* (swisschard)	Systemic infection	●
Beta vulgaris (Beet)	No infection observed	○
Capsicum annuum (pepper)	Systemic infection	●
Collinsia heterophylla	No infection observed	○
Cucurbita maxima (pumpkin)	Systemic infection	●
Cucumis sativus (cucumber)	Systemic infection	●
Cucumis melo reticulates (Cantaloupe)	Systemic infection	●
Digitalis purpurea	No infection observed	○
Fagopyrum esculentum (buckwheat)	Local lesions	●
Lactuca sativa (lettuce)	Local lesions	●
Musa acuminata (banana)	No infection observed	○
Nicotiana benthamiana	Systemic infection	●
Nicotiana cleverandii	Systemic infection	●
Nicotiana excelsior	Systemic infection	●
Nicotiana groseei	Local lesions	○
Panicum miliaceum (proso millet)	No infection observed	○
Paphiopedilum (lady's slipper orchid)	No infection observed	○
Phacelia campanularia	Systemic infection	●
Phaseolus vulgaris (Garden Beans Blue Lake Bush)	Local lesions	●
Raphanus sativus (radish)	No infection observed	○
Setaria italica (foxtail millet)	No infection observed	○
Solanum lycopersicum (tomato)	Systemic infection	●
Spinacia oleracea (spinach)	Systemic infection	●
Vigna unguiculata (cowpea)	Local lesions	●

Note. Plant species tested for types of TBSV infection and green florescent foci.
GFP expression (fluorescence) initiated from TBSV-GFP on the inoculated leaves is indicated by black circles. Open circles indicates lack of GFP fluorescence. GFP signals were not visible on upper leaves due to the instability of foreign insert even when these upper leaves showed systemic symptoms. However, for the purpose of this study, GFP spots on inoculated leaves of plants can be used as an indicator to separate non-host and host plants of TBSV. Categorization of TBSV infection is based on symptom development and infectivity of TBSV-GFP. TBSV infection and GFP expression would vary by quality of RNA transcripts, age of plants, and plant growth condition.

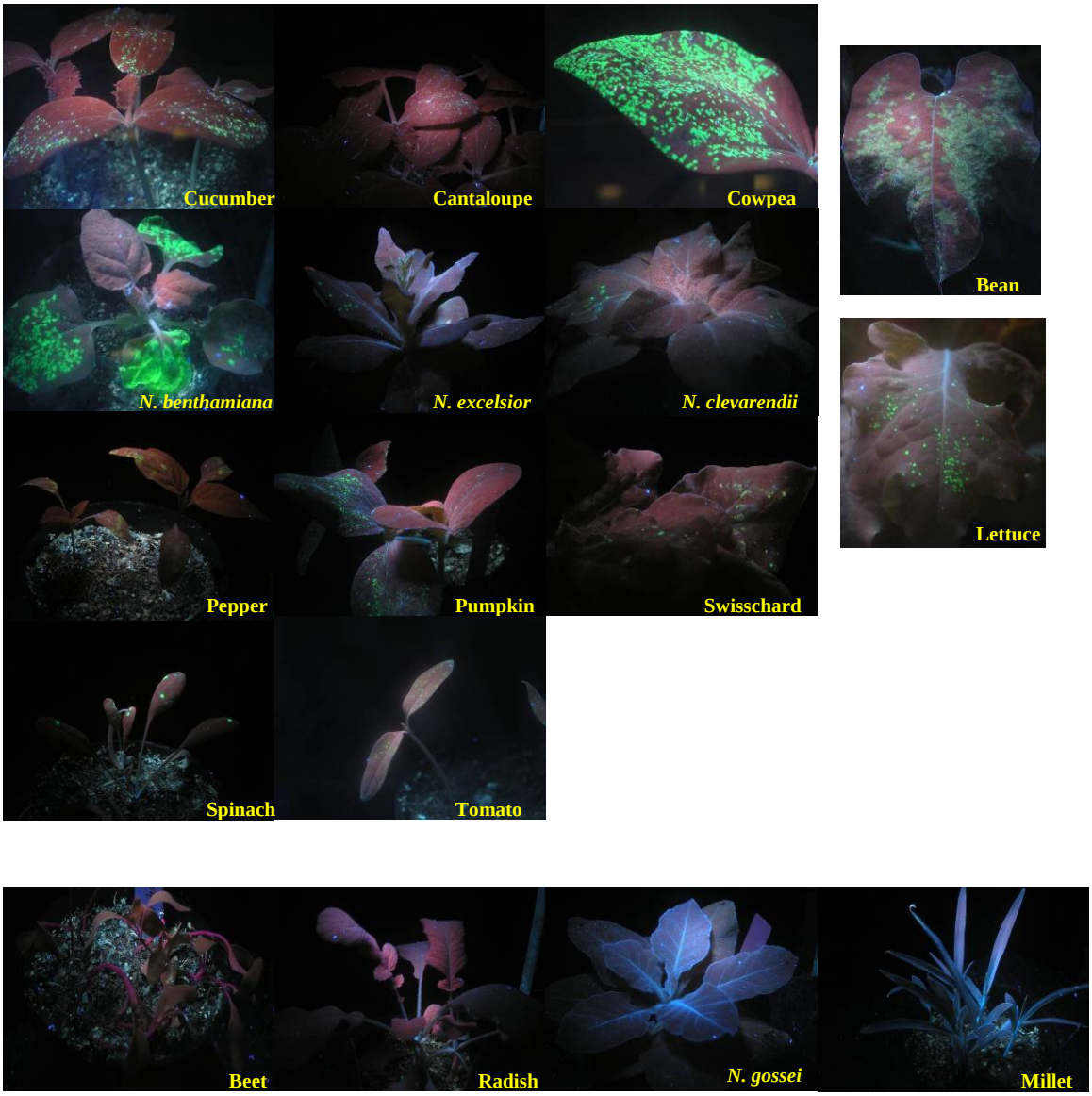

Fig. II-2. Host-specific infectivity of TBSV-GFP.
The top panels (from cucumber through tomato) show representative examples of hosts that display varying levels of GFP expression and associated foci number and size. The four examples on the bottom (beet-millet) represent plants that did not exhibit GFP expression upon inoculation with TBSV-GFP.

The recombinogenic nature of TBSV-GFP constructs precluded visualizing systemic infections with GFP observation, therefore, the visual tracking of the virus movement by monitoring green fluorescence was limited to inoculated leaves. Upon TBSV-GFP inoculations, a number of host-plants developed readily detectable GFP spots, whereas on others no green fluorescent signals were detected (Table II-1). Previously it was determined that millet supports TBSV replication (H. Scholthof, unpublished data) confirming that the inability of TBSV-GFP to cause an infection in millet and probably other non-hosts is due to the inability to move cell-to-cell. Furthermore, in a few instances local lesions were observed upon infection with TBSV, but no green spots were visible with TBSV-GFP.

Tissues of selected plants infected with TBSV-GFP were further analyzed for GFP cellular localization using microscopic imaging. During these tests, a correlation surfaced between GFP cellular localization and ability of the virus to cause systemic infection. For example, inoculated leaves of *N. benthamiana,* which is a host for systemic TBSV invasion, displayed intense and thorough GFP signals in mesophyll as well as epidermal cells (Fig. II-3). Contrastingly, in plants supporting only local TBSV infections, such as cowpea (Scholthof, 1999) and particularly lettuce (B. Seaberg and Y. Hsieh, unpublished data), the presence of GFP expression was mainly limited to small spots mostly comprised of epidermal cells (Fig. II-3).

These observations indicate that the capacity of TBSV to penetrate and infect mesophyll cells is an essential and critical prerequisite event to accumulate viral components towards subsequent phloem loading to establish overall successful TBSV systemic invasion of the host plant.

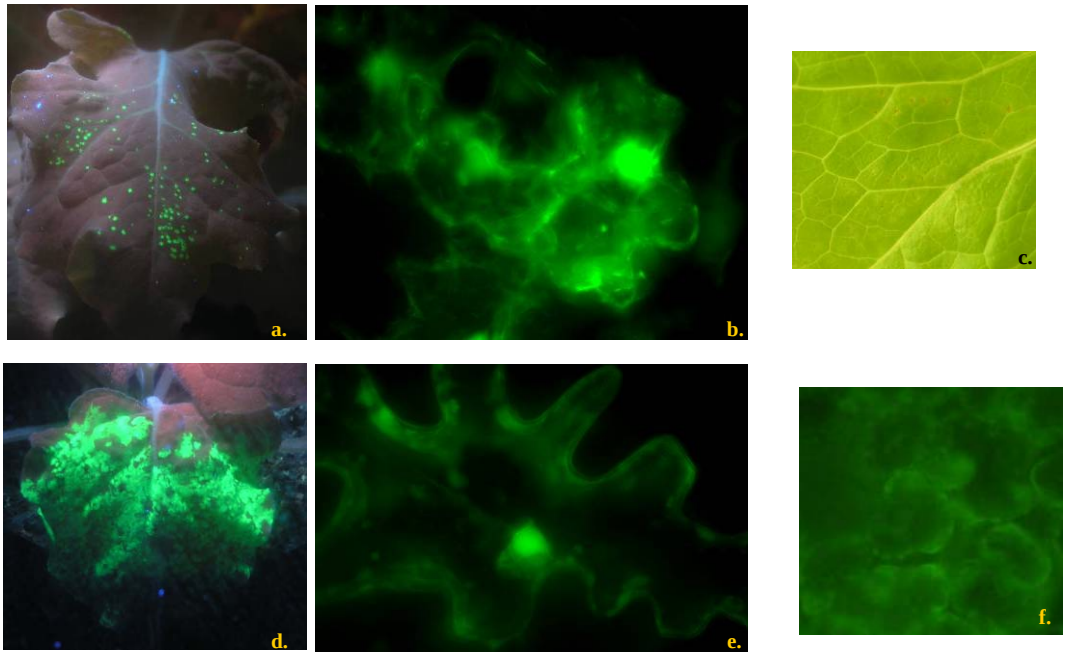

Fig. II-3. Localization of TBSV-GFP invasion on inoculated leaves of lettuce and *N. benthamiana.* The figure indicates the GFP signals on leaves and epidermal cells of inoculated leaves. a, b: lettuce (a is the same image as in Fig. II-2); d, e: *N. benthamiana*. c: bright light image showing pin-point local lesions on lettuce. f: green fluorescent mesophyll cells in *N. benthamiana* that are positioned underneath the initially inoculated and infected epidermal cell(s); such massive invasion of mesophyll cells was not observed for lettuce. (b) shows the folded epidermal cell with TBSV-GFP infection. The intensities and sizes of GFP spots correlate to numbers of infected epidermal cells (horizontal-area) plus mesophyll cells (vertical-brightness).

Effects of single amino acid substitutions on TBSV P22

During a separate mutagenesis study on *p19* (Chapter IV) an additional serendipitous mutation was introduced in some constructs that resulted in substitution of valine at position 124 on P22 (V124). All *p19* mutants carrying this additional *p22* mutation at position 124 seemed non-infectious (data not shown). The comparative analysis of the P22 amino acid sequence of *Tombusvirus* members reveals that valine at position 124 is relatively conserved (Fig. II-4). However, *Cymbidium ringspot virus* (CymRSV) contains alanine instead of valine in the position of P22/124 and three out of sixteen *Tombusvirus* species had other substitutions (Fig. II-4). The nature of these amino acids (predominantly A and V) and the fact there is no complete conservation as opposed to other residues does not suggest a conserved biochemical RNA- or membrane-binding role but is more suggestive for interaction with specific host factors. This led me to examine the hypothesis that V124 is crucial for infectivity and most likely for proper cell-to-cell movement due to interaction with one or more host elements.

To test the functional involvement of V124 in TBSV movement, site-directed-mutagenesis was first performed on the wild-type pTBSV-100 infectious clone to yield p22/V124A and p22/V124L. *N. benthamiana* plants inoculated with constructs containing the V124L mutation remained healthy without any sign of even local infection, whereas those inoculated with transcripts from p22/V124A or wild-type caused a lethal infection (data not shown). These results suggested that the V124L mutation rendered the virus non-infectious. I have ruled out that the non-infectious nature of the virus containing the V124L mutation is due to non-intended lethal mutations elsewhere on the genome because mutagenesis of the V124L expressing genome to restore it to V124V re-created a wild-type phenotype (Fig. II-5A).

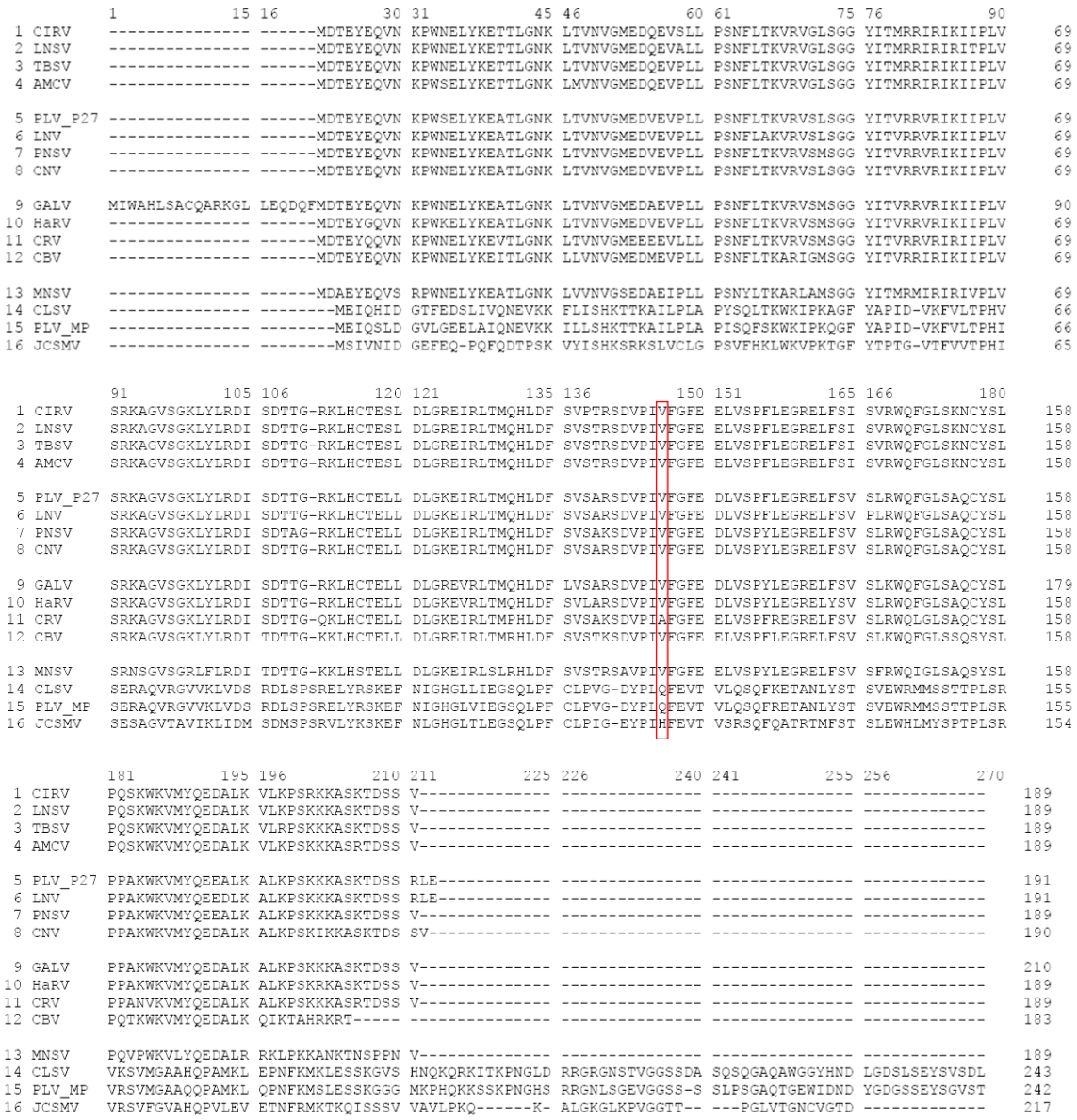

Fig. II-4. Multiple alignment of tombusvirus movement P22 proteins.
The abbreviations of tombusvirus and their full names are listed as following:
CIRV: *Carnation Italian ringspot virus*; LNSV: *Lettuce necrotic stunt virus*; TBSV: *Tomato bushy stunt virus*; AMCV: *Artichoke mottled crinkle virus*; PLV_P27: *Pear latent virus*; LNV: *Lisianthus necrosis virus*; PNSV: *Pelargonium necrotic spot virus*; CNV: *Cucumber necrosis virus*; GALV: *Grapevine Algerian latent virus*; HaRV: *Havel river virus*; CRV: *Cymbidium ringspot virus*; CBV: *Cucumber Bulgarian virus*; MNSV*: Maize necrotic streak virus;* CLSV: *Cucumber leaf spot virus*; PLV_MP: *Pothos latent virus*; JCSMV: *Johnsongrass chlorotic stripe mosaic virus*. The position of V residue that was specifically modified is aligned with its correlatives and indicated by red box.

A.

TBSV P22/V124L **TBSV P22/V124L→wtP22** **TBSV wtP22** **Mock**

B.

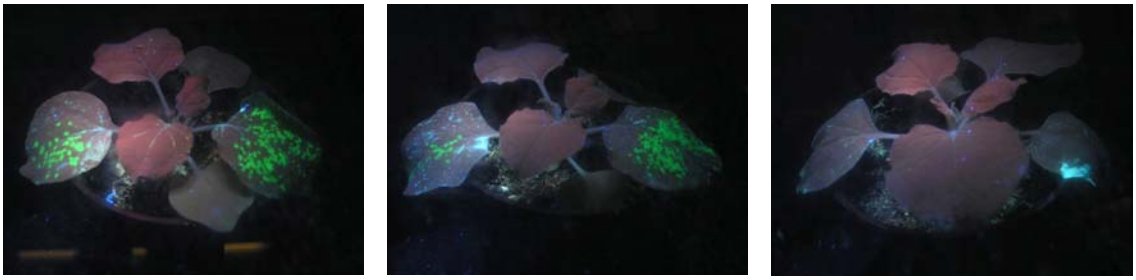

TBSV-GFP **TBSV-GFP P22/V124A** **TBSV-GFP P22/V124L**

Fig. II-5. Effect of modifications on P22/V124 on the capacities of wtTBSV (A) and TBSV-GFP (B) constructs to infect *N. benthamiana*. (A) In this experiment, modifications of P22 were first performed on a construct with full-length wtTBSV cDNA. The TBSV P22/V124L mutant displayed a null phenotype (image on left). However, a wild-type-like phenotype was observed when this specific substitution was restored back to wtP22 (second image from left). (B) Infection with TBSV-GFP (with wtP22) and TBSV-GFP P22/V124A resulted in abundance of green fluorescent spots on inoculated leaves but not for TBSV-GFP P22/V124L. Only three small green fluorescent spots (not really visible in the picture) were observed for TBSV-GFP P22/V124L inoculation.

To determine whether the non-infectivity associated with the V124L mutation was due to a defect in movement, the same mutations were introduced in the TBSV-GFP background. The two P22 mutants (TBSV-GFP-P22/V124L and TBSV-GFP-P22/V124A) were examined for viral movement, as monitored by detection of GFP fluorescence under UV light. The wild-type P22 and P22/V124A expressing TBSV-GFP constructs both showed intensive GFP signals on inoculated leaves (Fig. II-5B). However, the construct with substitution of P22/V124L did not yield any detectable GFP signal on plants (Fig. II-5B).

To investigate if the V124L perhaps exerted a host-specific effect on virus movement, other TBSV hosts, such as pumpkin and cowpea were inoculated with P22/V124L. The results obtained upon inoculations of pumpkin and cowpea were very similar to those obtained on *N. benthamiana,* as illustrated for cowpea (Fig. II-6). All tests indicated that this specific modification (P22/V124L) abolished infectivity of TBSV and compromised expression of green fluorescent spots on inoculated leaves (Fig. II-5 and -6).

Occasionally, a few small green spots would appear on *N. benthamiana* plants with virus expressing P22/V124L (Fig. II-5, -6, and -7) albeit not nearly as large as seen for wild-type P22 of P22/V124A (Fig. II-6 and –7). Microscopic observation of these P22/V124L associated small spots indeed revealed a cluster of infected, mostly mesophyll cells (Fig. II-7). Regions on inoculated leaves that did not exhibit green fluorescent spots by normal visual inspection were subjected to similar microscopy. Examination of such regions showed that in these inoculated tissues infected with TBSV-GFP-P22/V124L epidermal cells could be found that were infected but no spread of GFP expression occurred to underlying mesophyll cells, in contrast to what was observed for P22/V124A and wtP22 (Fig. II-8).

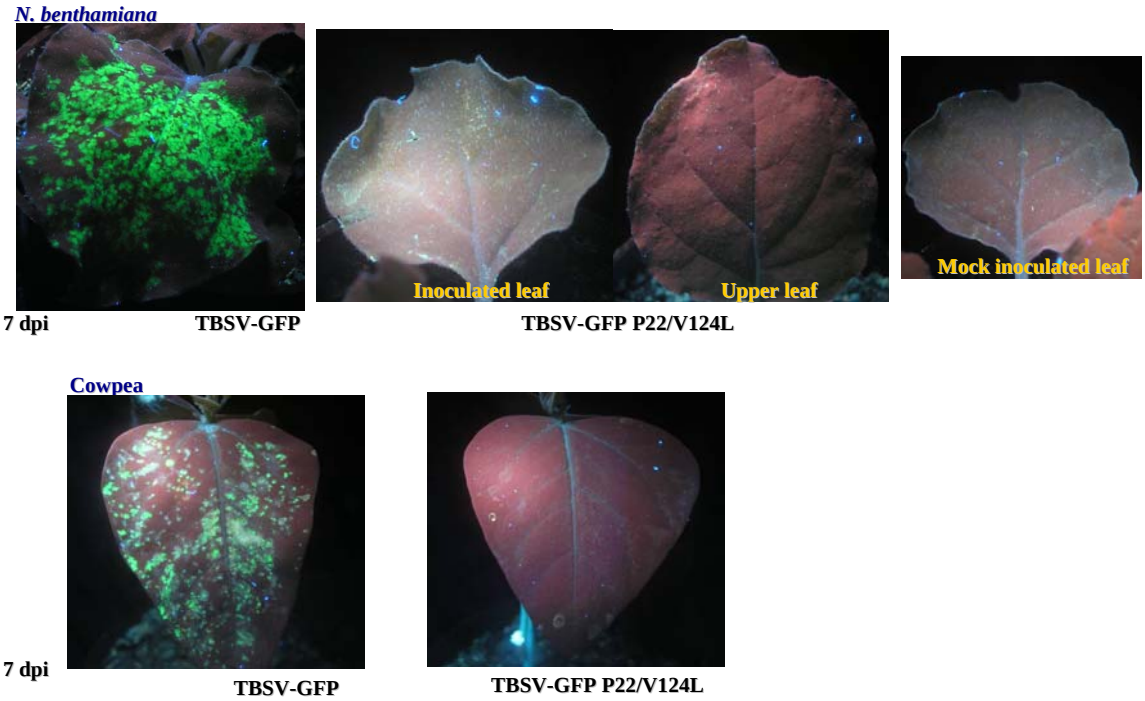

Fig. II-6. The effect of P22/V124 mutations on the ability of TBSV-GFP to infect *N. benthamiana* and cowpea. Inoculated *N. benthamiana* leaves with TBSV-GFP P22/V124L occasionally displayed small green fluorescent spots; these were selected for Fig. II-7.

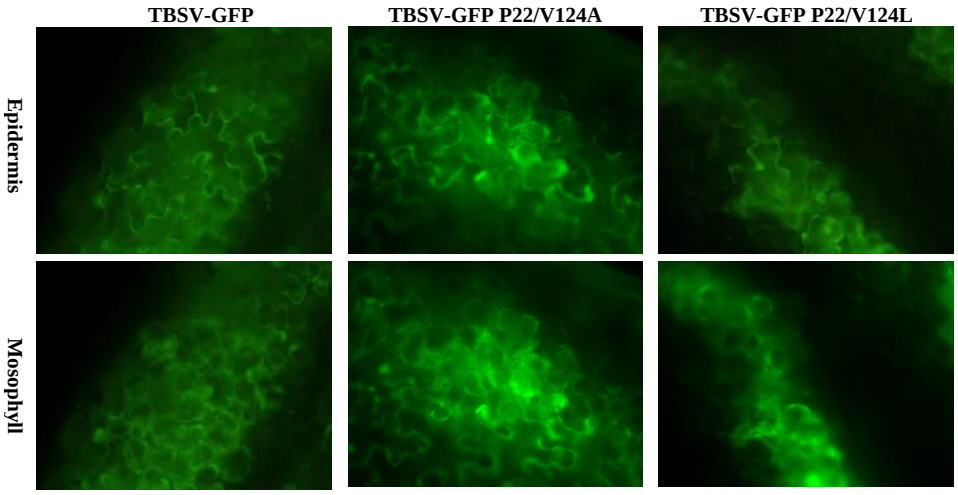

Fig. II-7. GFP signals obtained upon inoculation of *N. benthamiana* with TBSV-GFP expressing either wtP22 or the mutant versions, as indicated on top. Images in all cases are from regions on the leaves showing green fluorescent spots that were further selected because they were visible by naked eye (see also Fig. II-6). These tissues were then prepared for fluorescent microscopy as shown in the panels. For the top panels, the focal plane was on the epidermal layer whereas the panels below focus on underlying mesophyll.

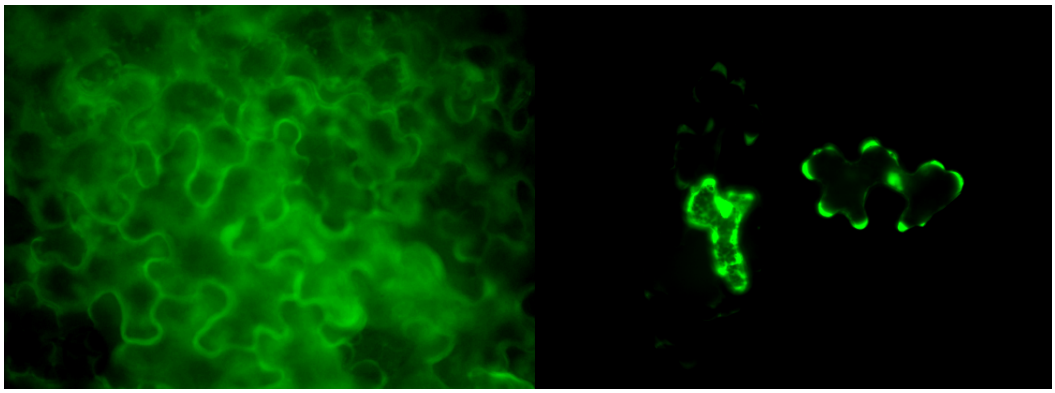

TBSV-GFP P22/V124A **TBSV-GFP P22/V124L**

Fig. II-8. Localization of GFP signals upon inoculation of *N. benthamiana* with TBSV-GFP expressing P22/V124A or P22/V124L. The image on the right was from a leaf section not showing any green fluorescent regions visible by naked eye (in contrast to the image in Fig. II-7). TBSV-GFP P22/V124L shows singly infected cells or perhaps restricted cell-to-cell movement between neighboring epidermal cells. Meanwhile, TBSV-GFP P22/V124A inoculated leaves displayed thorough distribution of GFP spots that include invaded mesophyll cells.

Effects of the P22/V124L mutation on localization

It is known that nucleotide mutations, especially those towards the termini, can have effects on gene expression and replication. Even though the positive results obtained with V124A do not suggest that a *cis*-acting region is involved, this could not be ruled out because it was shown previously that sequences within and adjacent to the *p22* ORF can affect RNA accumulation in a nucleotide-specific manner (Scholthof and Jackson, 1997; Park et al., 2002). To rule out possible effects of the P22/V124L on gene expression and on protein stability, I first compared the mutants for protein expression levels. For this, PCR templates for T7 polymerase transcription were generated by using a forward primer containing the T7 promoter. This permitted the *in vitro* transcription of sgRNA2 mimicks. These T7-sgRNA2s of TBSV P22 derivatives were subjected to wheat germ *in vitro* translation system. The amount of P22 and P19 detected by authoradiography did not reveal substantial differences in total amounts and P22/P19 ratio, when comparing *p22* mutant constructs (Fig. II-9).

To start investigating the effects of P22 mutations (P22/V124L and P22/V124A) on protein subcellular localization, GFP-P22 constructs were made with an infectious TBSV cDNA clone in which *gfp* is fused to the 5' end of *p22* to yield GFP-P22, GFP-P22/V124L and GFP-P22/V124A. Also a GFP-P22/E103A control was generated for inclusion because that is known to be movement negative mutant presumably because of faulty interactions with a host transcription factor (Desvoyes et al., 2002). *N. benthamiana* protoplasts were transfected with viral transcripts, and for reasons mentioned above, first a replication assay was conducted. For this purpose, viral RNAs were analyzed at 1 dpi by northern blot hybridization. The result showed no significant differences in the levels of viral genome accumulation for all analyzed samples (Fig. II-

10). Collectively, the viral genomes containing the *gfp-p22* fusions replicated less efficiently than TBSV-GFP (CP substitution) presumably to effects on the structure of the 3' end of the genome (Park et al., 2002); which is in agreement with results obtained by others (T. Rubio, unpublished data).

Fluoresence microscopy of transfected protoplasts inoculated with GFP-wtP22 and GFP-P22/V124A revealed predominant spotted localization of GFP-P22 to cell membranes and the cell surface (Fig. II-11). Contrastingly, movement deficient P22/V124L as well as the previously characterized P22/E103A (Chu et al., 1999; Desvoyes et al., 2002) exhibited a more uniform scattering of GFP-P22 signals throughout the cytosol (Fig. II-11). Although results should be verified with independent biochemical fractionation experiments, these initial tests offer the possibility that the impaired capacity of the P22/V124L mutant to systemically infect plants correlates with an altered subcellular protein localization of the protein. Importantly, the fluorescent signal intensity obtained with V124L is comparable to that seen for others, demonstrating that *in vivo* the V124L has not caused protein instability.

I conclude that the conserved P22/V124 on most tombusviruses is critical for proper intracellular targeting, and subsequent cell-to-cell movement. The substitution to alanine does not abolish its activity but the more drastic change to leucine compromises its localization, which prevents effective cell-to-cell movement. The detailed mechanism how this change resulted in the null phenotype still needs further examination.

Overall the results in this Chapter suggest that the ability of TBSV to exit out of initially inoculated epidermal cells is a key determinant controlled by the host and by conserved features on P22.

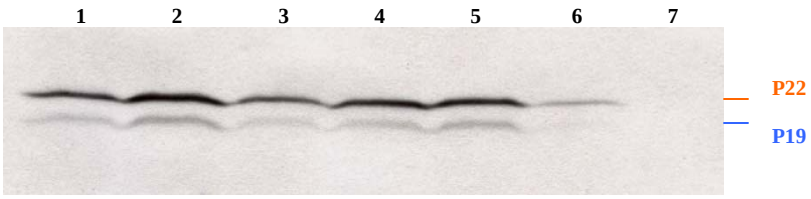

Fig. II-9. *In vitro* translation of *in vitro* transcribed TBSV sgRNA2 from P22 derivatives in the TBSV-GFP backbone. 1: TBSV-GFP; 2: TBSV-GFP P22/V124L; 3: TBSV-GFP P22/V124A; 4: TBSV-GFP P22/E103A; 5: TBSV-GFP P19/S113C; 6: TBSV-GFP P19/Q107P+S113T (simultaneously carried P22/V124L substitution); 7: no transcripts added. The two P19 mutants in lanes 5 and 6 are relevant to Chapter IV.

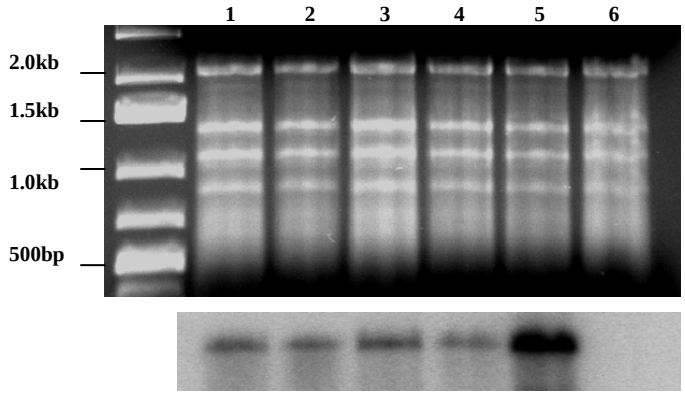

Fig. II-10. Detection of TBSV RNAs in transfected *N. benthamiana* protoplasts. The EtBr-stained gel on top shows the equal yield of total RNA collected at 1dpi. The northern blot on the bottom shows the accumulation of gRNA based on hybridization with random primed full-length TBSV cDNA (the sgRNAs were poorly visible in this experiment). The tested P22 derivatives include 1: P22/V124L, 2: P22/V124A, 3: P22/E103A, 4: wtP22, all on the infectious construct expressing the GFP-P22 fusion, 5: TBSV-GFP (of approximately similar size) was included as a positive control, 6: Mock transfected protoplast.

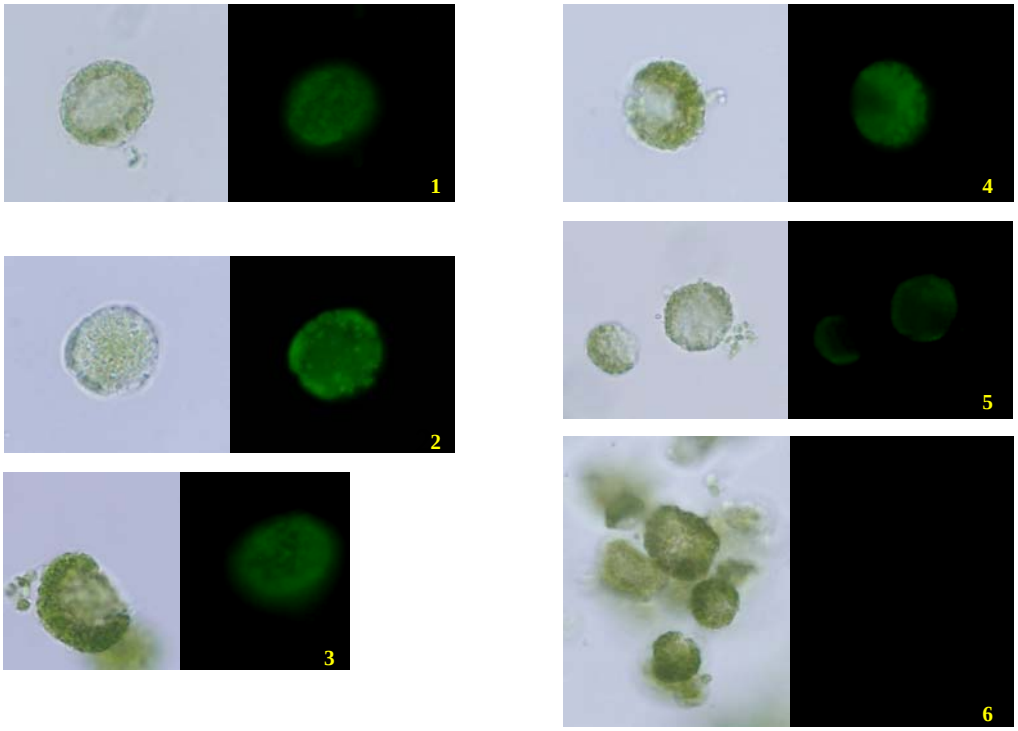

Fig. II-11. Subcellular localization of the GFP-P22 fusion proteins.
N. benthamiana protoplasts were freshly prepared and transfected with infectious RNA transcripts made from the constructs either expressing the GFP-P22 fusion, which included 1: P22/V124L, 2: P22/V124A, 3: P22/E103A, 4: wtP22, or in lane 5 from the TBSV-GFP construct which is the CP substitution vector expressing wtP22. Panel 6 shows Mock transfected protoplasts. Samples were observed under bright field (left) to verify the survival of protoplasts, and under UV light (right) to observe the GFP signals in these single cells at 2 dpi.

Discussion

Host range and cell-to-cell movement

The results in this study show that TBSV-GFP is able to establish at least local infections in a variety of plants in different families. The substantial number of species that tested positive agrees with the notion that TBSV has an extensive host range for local movement (Martelli et al., 1988; Yamamura and Scholthof, 2005). Furthermore, since the CP gene is defective on TBSV-GFP it can be concluded that the CP is not required to establish local infections in many plants. Thus, TBSV firmly belongs to the Type I viruses that do not require the CP for cell-to-cell movement (Scholthof, 2005). The experiments also indicate that TBSV-GFP is a useful tool to determine if a plant is a host because positive results only occur upon replication and cell-to-cell movement. Traditional infectivity tests with wild-type TBSV would need sensitive and laborious detection techniques because onset or absence of symptoms is not a reliable indicator, and the detection of TBSV proteins and/or RNA in some local lesion hosts is technically challenging because the host defenses clear the viral material (Scholthof et al., 1995a). However, it has to be noted that only positive results with TBSV-GFP are meaningful. No firm conclusions can be drawn for those plants not showing green fluorescence because that could be due to poor infectivity with transcripts, poor penetration of UV illumination, an inability to replicate, compromised movement, requirement of CP, rapid deletion of GFP, or a combination of causes.

Comparison of the movement profile of TBSV-GFP in *N. benthamiana* and lettuce (and cowpea) suggest that the ability of TBSV-GFP to egress effectively from initially inoculated epidermal tissue is an important component that might involve specific host components. In this context, it is noteworthy that lettuce does not express HFi22 (Seaberg,

2008), which is a host protein that interacts with P22 (Desvoyes et al., 2002). It is also intriguing that lettuce and cowpea respond with the onset of local chlorotic/necrotic lesions upon infection with TBSV or TBSV-GFP. Whether this is the cause or a result of the restricted movement remains to be determined.

Effects of the V124L mutation on P22

Considering the conservation of the V at position 124 on the cell-to-cell movement protein P22 of most but not all tombusviruses, and its possible participation in a host-dependent manner to movement, this residue was targeted for substitution. The results showed that substitution to A (as it naturally occurs for P22 of CymRSV) did not alter the phenotype and the resulting virus moved as efficiently as comparable TBSV derivatives expressing wtP22. However, the V124L substitution rendered the virus non-infectious. Based on the possible indirect interactions involving TBSV P19, CP, and P22 (Yamamura and Scholthof, 2005), the P22 mutations were made in various virus genetic backgrounds: i) with TBSV-GFP (not expressing CP), and with TBSV CP expressing constructs either ii) with wt*p19* or iii) defective for *p19* expression (data not shown). The results in all cases confirmed the observation made with TBSV-GFP that P22/V124L was unable, whereas P22V124A was able, to cause systemic TBSV infection and this was independent of the presence of CP or P19. Additional tests showed that the mutation did not affect translation, P22 accumulation, or replication. Collectively, the data provided evidence that upon rub-inoculation the V124L substitution compromised cell-to-cell movement out of the initially inoculated epidermal cells. Attempts were made to complement the movement defect of V124L by prior agroinfiltration with constructs expressing wtP22 but this showed little effect (data not shown). This may be because of

timing issues or perhaps the dominant-negative nature of the V124L substitution. Nevertheless, the results confirm that P22 is required and sufficient for cell-to-cell movement of TBSV (Chu et al., 1999). The absence of movement associated with V124L also prevented the onset of local lesions on indicator hosts, which agrees with the observation that cell-to-cell movement is a pre-requisite for local lesion induction by TBSV (Chu et al., 1999; Desvoyes et al., 2002).

For the most part, the V124L mutation prevented egress from the inoculated epidermal cells, even though the observed clustering of a few epidermal cells suggested that movement between epidermal cells could still occur. It is possible that the V124L mutation simply slows down movement and that the restriction is a reflection of the host defenses that can take over when movement is slow or inefficient. However, *N. benthamiana* is a very promiscuous host that is not known for effective induction of defense responses (Yang et al., 2004; Whitham et al., 2006). Therefore, I favor the interpretation that the movement defect associated with V124L is caused by a direct deficiency in a specific biochemical or cell biological mechanism.

Occasionally, small green fluorescent spots were observed in *N. benthamiana* inoculated with TBSV-GFP expressing V124L; these clusters were mostly comprised of GFP expression in mesophyll cells. These are probably the result of the occurrence of complementary mutations that sometimes arise during TBSV replication (Scholthof and Jackson, 1997). However, an attractive possibility that deserves testing is that during rub-inoculation on a few spots on the leaf this procedure leads to wounding of mesophyll cells followed by virus inoculation directly into these cells. Thus the virus bypassed the need to exit any epidermal cells even though some movement from mesophyll cells into epidermal cells may occur (Fig. II-7). More evidence is needed to substantiate a

conclusion, but it is possible that the V124L mutation does allow cell-to-cell movement between and out of mesophyll cells but not out of epidermal cells.

Our previous studies indicated that even with comparable accumulation of P22 to wtP22, one specific P22 derivative-P22/E103A was no longer strictly insoluble but also present in the soluble fraction (Chu et al., 1999; Desvoyes et al., 2002). This indicated that the function of P22 is related to proper subcellular distribution. These previous results were based on biochemical fractionation studies and I thought it to be more informative to examine the distribution *in vivo* in infected cells. For this, the wtP22 and the mutant versions were expressed in protoplasts as fusion proteins with GFP from an infectious TBSV construct. The results indicated that both P22/V124L and P22/E103 exhibited localization of GFP that slightly diverged from the normal tight association with membranes and towards the surface observed for *N. benthamiana* protoplasts infected with virus expressing wtP22 or V124A as fusion products with GFP. These results have to be considered within the context that protoplasts consist mostly of mesophyll cells, and if the effect of the V124L mutation is predominantly noticeable in epidermal cells as postulated earlier, the full effect may be masked in the present protoplast experiments.

Future experiments are planned to express V124L in plants using agroinfiltration (Chapter III), or to over-express it in *E.coli* followed by purification (Desvoyes et al., 2002). This will provide the tools to verify the sub-cellular localization in infiltrated epidermal tissue, and to test for self-interaction and or RNA binding of P22/V124L as those are biochemical properties of movement proteins (Lucas, 2006), as also demonstrated for wtP22 (Desvoyes et al., 2002).

Experiments have ruled out the possibility that the movement defect of V124L is due to *cis*-acting RNA elements at the position of the codon for V124, and *in vitro* and *in vivo* protein accumulation tests have shown that even if the V124L causes mis-folding, it is not subject to accelerated degradation. Even though it cannot yet be entirely ruled out that the V124L mutation affects RNA binding or P22 self-interaction (and as indicated above such experiments are planned), usually such interactions are governed by charged residues rather than V or A. The results do seem to suggest however, that the deviation in subcellular localization correlates with the movement defect. Therefore, the results support the interpretation that the specific single amino acid substitution from non-polar (V) to hydrophobic (L) changes the electrostatic or folding property of P22 resulting in a movement defect because of faulty interaction(s) with one or more host elements.

Conclusion

The invasion of different plant species with TBSV was visualized on the whole-plant, cellular, and subcellular levels. The results suggest that the difference between plants that are non-host, local lesion hosts, and those susceptible to a systemic infection, resides mostly in the extent and level at which P22-associated viral complexes are permitted to move intra- and intercellularly. TBSV is not able to move in non-host plants; hosts displaying local lesions contain the virus mainly in and around the epidermal cells; systemic invasion occurs when viral spread can occur freely between epidermis and mesophyll cells to permit subsequent vascular as well as systemic spread. In addition, modifications on P22 may result in different localization of P22 causing loss of cell-to-cell movement out of the initially infected epidermal cells.

Thus, it appears that for the mechanically transmitted TBSV, the ability of the virus to egress from the inoculated epidermal cells is an important host range determinant that might be specified by specific contributions of P22 residues. Although virus spread is considered a vital host range determinant the importance of the ability to exit the epidermal cells as a key process, is a concept that has not previously been given a great deal of attention.

CHAPTER III

EFFECT OF TRANSIENT AND TRANSGENIC EXPRESSION OF A MUTANT P19 ON FOREIGN GENE EXPRESSION IN PLANTS

Introduction

Tomato bushy stunt virus (TBSV) is a superb model system for studying molecular virus-host interactions including RNA silencing and its suppression (Yamamura and Scholthof, 2005; Scholthof, 2006). The 3'-proximal region of the plus-sense single-stranded (ss) RNA genome of TBSV contains two nested open reading frames (ORFs) that are denoted as *p19* and *p22*. These overlapping genes encode two separate unrelated proteins; the cell-to-cell movement protein (P22) and the pathogenicity protein (P19).

P19 is a particularly intriguing multifunctional protein because it is a very critical host-range determinant, it is an important contributor to viral symptoms, and it has host-dependent effects on virus invasion (Chu et al., 2000). Recent studies suggest that these biological effects may be related to the activity of P19 as a suppressor of post-transcriptional gene silencing (i.e., RNA silencing) and virus-induced gene silencing (VIGS) (Silhavy et al., 2002; Lakatos et al., 2004; Park et al., 2004; Omarov et al., 2006; Scholthof, 2006). To enable this suppression function, P19 self-interacts to form dimers that specifically sequester 21 bp siRNAs in a sequence-nonspecific manner (Vargason et al., 2003; Ye, Malinina, and Patel, 2003). This prevents programming of an RNA silencing-associated RNA induced silencing complex (RISC) and during infections this blocks the antiviral RNA silencing and consequently viral RNA is not subjected to degradation (Omarov et al., 2007).

The different host-dependent biological activities are modulated by the same central region in concert with activity-dependent separate external regions on the 172 amino acid of P19 protein (Chu et al., 2000; Scholthof, 2006). Substitutions of residues in the central region (71-72) had pleiotropic effects, including inactivation of suppressor function, that were attributed to possible effects on structural integrity (Chu et al., 2000; Qiu et al., 2002; Turina et al., 2003). The importance of the central region for maintaining structure was later verified (Vargason et al., 2003; Omarov et al., 2006). Some structural effects may directly affect functionality but could also influence protein stability. This is especially relevant since it is known that the capability of P19 for its biological activities and suppression requires its relative high levels of accumulation during infection (Scholthof et al., 1999; Qiu et al., 2002).

Amino acids at the extreme N-, and C-terminal ends of P19 were predicted to be exposed on the surface of the polypeptide (Chu et al., 2000). For the most part this agrees with the structure (Fig. III-1) and thus these residues could potentially be available for interaction with host-specific proteins. Intriguingly, however, there was no significant measurable biological effect of substitutions within the termini on the biological activities upon infection of plants (Chu et al., 2000). In contrast, mutations outside the central region for instance at 43 (P19/R43W) prevented lethal necrosis on *N. benthamiana* (Chu et al., 2000). This suggested that this region on the N-terminal portion of P19 mediates host-dependent interactions.

Further studies suggested that the symptom attenuation and reduced viral pathogenesis associated with P19/R43W correlated with a somewhat “loosened” binding of P19 to siRNAs that is otherwise quite strong (Omarov et al., 2006). Examination of the structure revealed that the substitution of Arg43 (R43) with Trp (W) in P19/R43W likely

interfered with the establishment of a hydrogen bond between the caliper residue at position 42 and the 5′-phosphate of the 21-bp siRNA, or otherwise causes inappropriate exposure of the hydrophobic Trp residues. Nevertheless, it was shown that P19/R43W retained the silencing suppression activity, as demonstrated by its ability to prevent virus-induced silencing of GFP in GFP-transgenic plants (Qiu et al., 2002), and to prevent TBSV RNA from RNA silencing-mediated degradation during infection of plants (Omarov et al., 2006). Importantly, this activity is maintained even though P19/R43W is far less symptomatic than wtP19 which is typically associated with the induction of lethal symptoms.

Several plant viruses are known to suppress gene silencing in different steps of RNAi (Ding et al., 1995; Brigneti et al., 1998; Voinnet et al., 1999; Voinnet et al., 2000; Qiu et al., 2002; Qu and Morris, 2002; Kasschau et al., 2003; Qu et al., 2003; Chapman et al., 2004; Lu et al., 2004; Omarov et al., 2006). However, P19 is the best characterized suppressor and it has the major advantage that it can be used as a tool to study the mechanism of RNA silencing in several eukaryotic systems because it binds siRNAs in an non-sequence specific manner (Bernstein et al., 2001; Ding et al., 2004; Scholthof, 2006).

High levels of foreign gene expression, whether transgenically, transiently, or by means of a virus vector, is often compromised by the onset of RNA silencing (Scholthof, 2007). This has been a major stumbling block for plant biotechnology endeavors focused on value-added protein production or crop improvement. Therefore, it is highly desirable to obtain a plant platform that is permissive for high levels of foreign protein expression without the deleterious effects of RNA silencing. P19 has recently shown promise in several systems to suppress RNA silencing of foreign genes for biotechnological

purposes, however, its toxic effect in plants has severe negative consequences on plant performance and development (Silhavy et al., 2002; Papp et al., 2003; Dunoyer et al., 2004). Considering that the non-toxic P19/R43W TBSV mutant retained suppression activities while decreasing the severity of symptoms in plants, we hypothesized that P19/R43W could represent a suitable alternative biotechnological tool to suppress RNA silencing activity to permit enhancement of foreign gene expression in plants. This technology could potentially also be useful for similar purposes in other transgenic organisms (Dunoyer et al., 2004; Scholthof, 2006).

It was previously shown that transient (i.e., non-transgenic) co-expression of P19 prevents the onset of silencing of simultaneously introduced foreign genes, resulting in greatly (~50-fold) enhanced transient expression levels of the target foreign gene (Voinnet et al., 2003). Based on these findings, we developed a similar assay to compare the suppression ability of P19 encoded by three different tombusviruses. In this assay *Agrobacterium* with a plasmid expressing P19 is co-infiltrated with agrobacteria expressing GFP resulting in substantially increased levels of GFP compared with control treatments in absence of any suppressor. These results showed the viability of our assay to test for the ability of P19 to suppress RNA silencing. We then used this same test to demonstrate that P19/R43W could be expressed transiently, following agroinfiltration, and that this was sufficient to enhance GFP expression.

Based on the positive results with the transient assay, it was thought that P19/R43W-expressing transgenic *N. benthamiana* plants may provide a good system to continuously and stably elevate levels of foreign gene expression *in planta*. Here I report that upon regeneration of such transgenic plants, P19/R43W is expressed in a temperature and growth-stage dependent manner. Even though some developmental aberrations are

observed that varied by the age of plants and growth conditions, the plants yield fertile seeds. Preliminary tests indicate that the transgenically expressed P19/R43W is actively suppressing RNA silencing leading to delay in VIGS and increased susceptibility to virus infection. Effects on expression levels of introduced foreign genes remain to be determined but based on the results thus far it seems promising that the P19/R43W-transgenic *N. benthamiana* plants will yield a viable platform for increased expression of foreign genes and to provide a tool for further investigation of RNAi mechanisms in *N. benthamiana*.

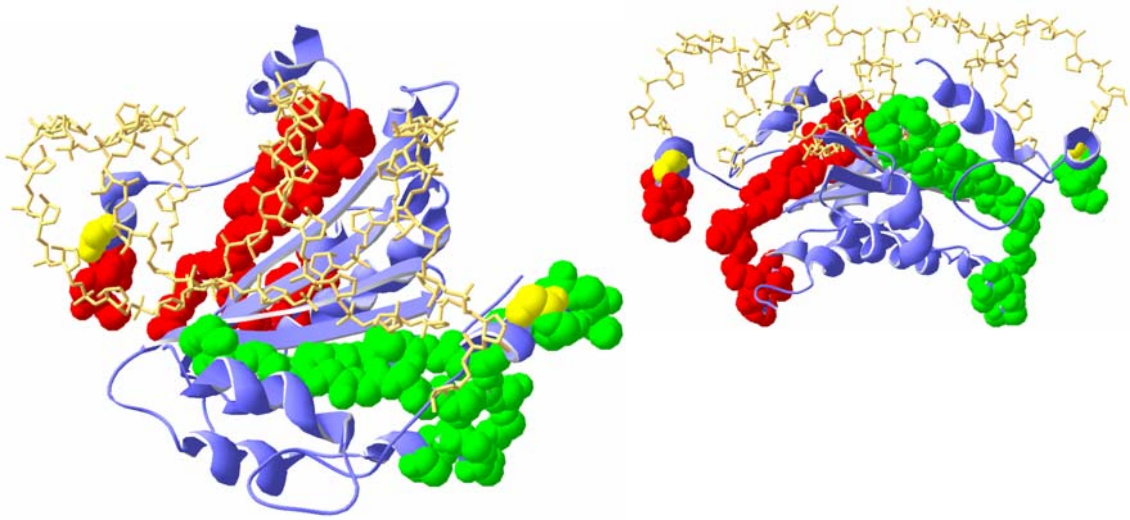

Fig. III-1 . Three dimensional views of the location of R43 in the P19/siRNA structure.
The red and green regions indicate the amino acids in two P19 monomers that were examined for P19 functions by introducing mutations (chapter IV). The yellow balls on the P19 dimer indicate the location of P19/R43 which is close to the Trp reading head of P19 that measures 21nt siRNAs. The blue ribbon presents the backbone of the P19 dimer and the siRNA duplex is shown as the gold chain. The protein structure profile was downloaded from NCBI protein structure database and viewed/modified by DeepView/Swiss-PdbViewer v3.7.

Materials and methods

Constructs and *Dpn*I mediated site-directed mutagenesis PCR. *Tombusvirus p19* genes from *Cucumber necrosis virus* (CNV), *Cymbidium ringspot virus* (CymRSV), and *Tomato bushy stunt virus* (TBSV) were constructed in the binary T-DNA plant transformation vector pKYLX7 and cloned in *Agrobacterium* strain *Agl-1* (provided by Dr. James E. Schoelz, University of Missouri-Columbia). The QuikChange kit (Stratagene, La Jolla, CA) was used for site-directed mutagenesis and standard molecular biology protocols were followed for the isolation and manipulation of plasmid DNA (Sambrook et al., 1989). For construction of pKYLX7-R43W, plasmid pKYLX7-p22 (expressing both P22 and P19) was first mutated to inactivate the start codon of P22 (pKYLX-p22 stop-F primer- 5'-ctcgaga**G**ggatactgaatacgaa-3'; pKYLX-p22 stop-R primer- 5'-ttcgtattcagtatccCtctcgag-3') to solely express P19, subsequently was verified by western blot analysis).

pKYLX7-R43W was obtained by site-directed mutagenesis PCR (P19/R43W-F primer- 5'-actgagtgg**T**ggctacataacgatgagacgaattcgaat-3'; P19/R43W-R primer- 5'-tatgtagcc**A**ccactcagtccaactcggactttcgtcag-3') without subcloning. All mutations were verified by sequencing. Plasmids for transient expression that expressed TBSV P19 were: pCB301-p19 (provided by S. Kamoun, Norwich research park, Norwich, UK), pJL-p19 (provided by J. Lindbo, Ohio State Univ., Wooster), and pCass4N-P19 (provided by S. Gowda, Univ. Florida, Lake Alfred). The construct pCass4N-P19/R43W was generated using the mutagenesis protocol and primer described for pKYLX7-R43W. The relevant properties of the T-DNA vector expressing GFP (Qiu et al., 2002) is shown in Fig. III-2.

Agroinfiltration of *N. benthamiana* followed by western blotting and imaging. The T-DNA vectors were transformed into *Agrobacterium* C58 and EHA strains by electroporation (GIBCO-BRL Cell-Porator system). Media for overnight induction contained 200 μM MES, pH 5.85 [monohydrate 2-(*N*-morpholino) ethanesulfonic acid] and 19.5 μM acetosyringone. The *Agrobacterium* infiltration buffer included 10 mM MES (pH 5.85), 10 mM $MgCl_2$, and 2.25 mM acetosyringone. Agrobacteria were infiltrated into expanded leaves at the abaxial surface of ~4 week old *N. benthamiana* plants using a simple syringe.

The infiltrated leaves were extracted with Tris-EDTA (TE) buffer and protein samples were separated by standard SDS-PAGE in 15% polyacrylamide gels and transferred to nitrocellulose membranes (Osmonics, Westborough, MA). The membranes were stained with Ponceau S (Sigma, St. Louis, MO) to verify the efficiency of protein transfer. The antisera against TBSV proteins were applied at the dilution of 1:5,000, respectively. Alkaline phosphatase–conjugated goat anti-mouse or rabbit antiserum (Sigma) was used as the secondary antibody and applied at a dilution of 1:1,000. The immune complexes were visualized by hydrolysis of tetrazolium-5-bromo-4-chloro-3-indolyl phosphate (BCIP) as the substrate in the presence of nitro-blue tetrazolium chloride (NBT). In some experiments, horseradish peroxidase-conjugated to goat anti-mouse antiserum (Bio-Rad, Hercules, CA) was used as the secondary antibody at the dilution of 1:5000, and the immune complexes were visualized by using the enhanced chemioluminescence detection kit (Pierce, Rockford, IL). Mouse monoclonal IgG_{2a} GFP antibody [GFP (B-2): sc-9996, Santa Cruz Biotechnology, CA] was used to quantify GFP expression.

GFP signals on the inoculated *N. benthamiana* leaves were monitored with a 100 W handheld long-wave ultraviolet (UV) lamp (UV products, Black Ray model B100AP, Upland, CA). An Olympus DP70 camera was used for the image acquisition of DIC and wide field fluorescent images.

Inoculation and analysis of plant tissues. TBSV virions purified from infected *N. benthamiana* plants infected with *in vitro* generated transcripts of full-length TBSV cDNAs expressing wtP19 and defective P19 (ΔP19) were used for inoculation. Plants were inoculated with virus plus 1% Celite, 50 mM KH_2PO_4 (pH 7.0), following standard procedures (Scholthof et al., 1993).

Transgenic plants. Plasmid pKYLX7-R43W was sequenced to confirm its identity and sent to the Ralph M. Parsons Foundation Plant Transformation Facility, U. C. Davis, for transformation of *N. benthamiana*. Fourteen lines were regenerated by this facility, which were labeled as 072106-001 to 072106-009, 072106-011 to 072106-015 (072106-019 was missing). For our purposes, these lines were later abbreviated as 43-1, etc. Healthy non-transgenic *N. benthamiana* plants regenerated at same facility from the same callus were used as negative controls. These P19/R43W transgenic *N. benthamiana* plants were grown in the laboratory on light shelves at ambient temperature (~25-28°C) with 14 hours photoperiod. Seeds from parental transgenic plants were harvested separately from each plant. The F1 seed was germinated in MS (Murashige and Skoog) medium (Life Technologies, Rockville, MD) with 30 μg/ml kanamycin. For reasons described in results, plants were grown under two conditions, either ~25-28°C or ~18-20°C.

Results

Establishment of a rapid transient expression system to measure the ability of tombusvirus P19 proteins to suppress RNA silencing

In the first set of experiments the intention was to develop a transient expression system that would permit rapid identification of active suppressors by testing their ability to enhance the expression of co-introduced GFP. The activities of P19 encoded by three tombusviruses (CNV, CymRSV, and TBSV) were compared. Towards this end, *N. benthamiana* plants were infiltrated with *Agrobacterium* expressing green fluorescent protein (GFP) (Fig. III-2) together with *Agrobacterium* constructs expressing P19. The treated plants were observed for green fluorescent signals and protein accumulation beginning at 2 dpi. Representative examples are shown at 5 and 7 dpi (Fig. III-3) and at 7 and 17 dpi (Fig III-4).

As shown in Fig. III-3, the maximal GFP expression obtained without P19 expression was at 5 dpi and then the fluorescence started to fade. In contrast, co-infiltration of the constructs expressing P19 together with GFP suppressed RNA silencing, evidenced by an increase of GFP signal with a maximum GFP fluorescence at 7 dpi (Fig. III-3). All three tombusvirus P19 proteins extended and enhanced the levels of GFP expression (Fig. III-

3). CNV P19 was able to maintain GFP expression for extra two days, TBSV P19 could uphold GFP signals for 14 days, and CymRSV P19 preserved the ability to suppress gene silencing and extend expression of fluorescent protein for more than 20 days (data not shown).

The western blot assays of GFP and P19 protein expression (Fig. III-4) showed that compared to the controls with GFP only (lanes 4-5) the levels of GFP proteins were increased by co-expression of P19 (lanes 1-3) at 7 dpi. This effect was even more substantial at 17 dpi (Fig. III-4B). At 7 dpi, P19 of all three tombusviruses was detectable albeit at different levels. However, the antiserum is specific to TBSV P19 and thus quantitative comparisons are not reliable. At 17 dpi, only CymRSV and TBSV P19 were detected which corresponded with the highest level of GFP for these treatments.

In conclusion, the transient expression system using GFP fluorescence and accumulation provided a relatively rapid manner to evaluate the ability of (potential) suppressors to enhance foreign gene expression.

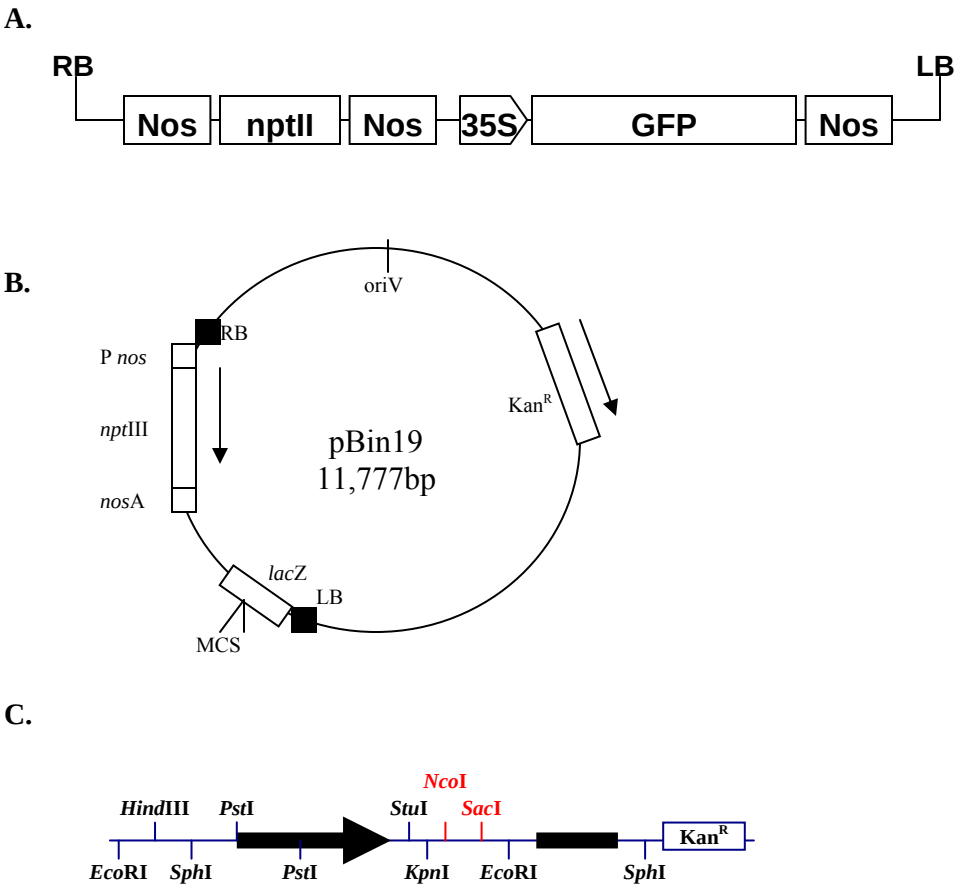

Fig. III-2. Organization of T-DNA constructs used for transient expression of GFP and P19. (A) GFP expression construct. 35S: CaMV 35S promoter; Nos: nopaline synthase terminator. *Agrobacterium tumefaciens* strain C58C1 was used to carry the 35S:GFP construct. (B) pBIN19 construct contains replication origin (oriV), kanamycin resistance gene (Kan^R), T-DNA left border (LB), T-DNA right border (RB), *nos* promoter (P *nos*), *nos* terminator (*nos* A), *npt*III, *lac*Z with multiple cloning sites (MCS). (C) pCass4N is a pBIN19-based (~11Kb) construct. TBSV *p19* was cloned between the *Nco*I and *Sac*I sites of pCass4N and named pCass4N-P19.

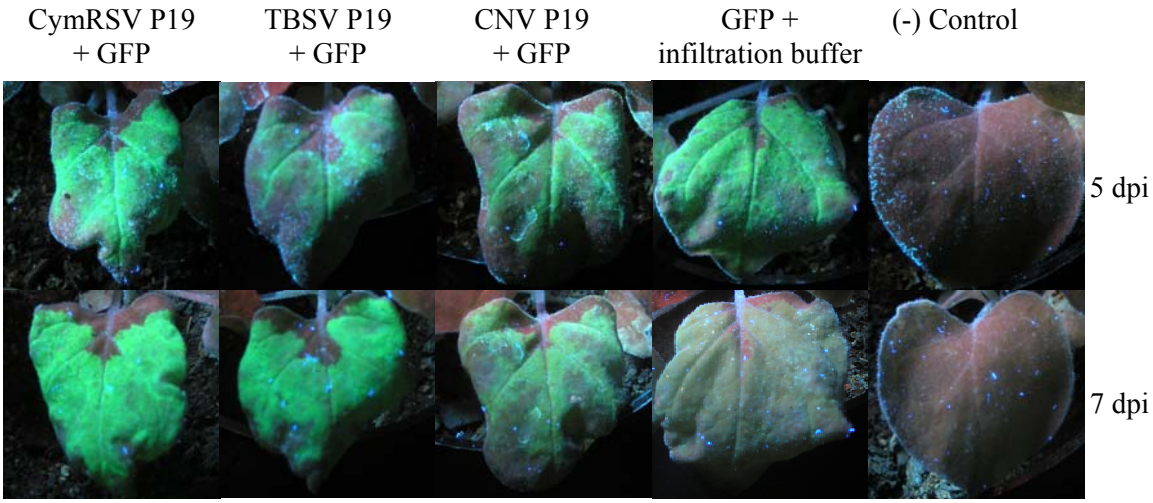

Fig. III-3. Transient GFP expression upon co-infiltration of tombusvirus P19 expressing constructs.
Compared to 5 dpi infiltrated (top panel) and 7 dpi infiltrated *N. benthamiana* leaves (bottom panel), all samples (except the negative (-) control only infiltrated with infiltration buffer) showed similar amounts of GFP fluorescence at 5 dpi. Nevertheless, different levels of GFP expression were observed at 7 dpi. At 7 dpi, co-infiltration with GFP- and CymRSV P19-expressing agrobacteria showed most intense GFP expression, TBSV P19 displayed intermediate GFP signals, CNV P19 gave much lower GFP expression, while GFP signals faded away on infiltrated leaves only treated with GFP-expressing *Agrobacterium* and buffer.

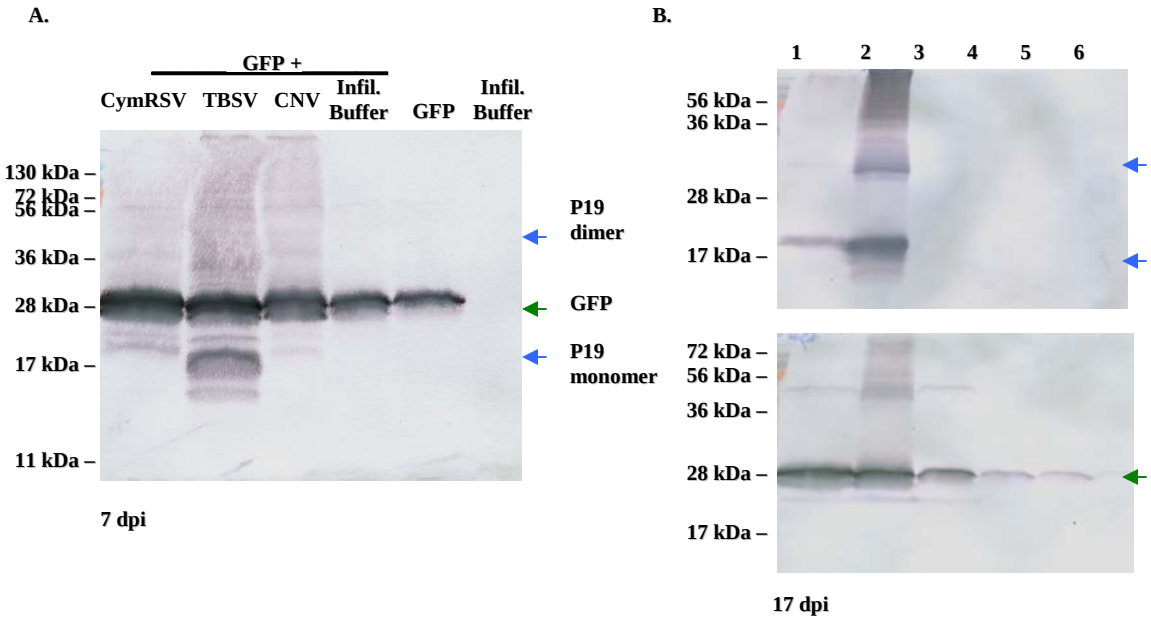

Fig. III-4. Detection of GFP and P19 from infiltrated *N. benthamiana leaves*.
(A) Western blot for detection of GFP for 7 dpi infiltrated *N. benthamiana* leaves, (B) 17 dpi *N. benthamiana* leaves. 1: CymRSV P19+GFP co-infiltration; 2: TBSV P19+GFP co-infiltration; 3: CNV P19+GFP co-expression; 4: GFP+infiltration buffer (equal volume) infiltration; 5: GFP *Agrobacterium* infiltration only; 6: infiltration buffer only (negative control). Arrows indicate positions of GFP (green), and of P19 monomer and dimmers (blue).

RNA silencing suppression by P19/R43W

The results in the previous section show that P19 of CymRSV, TBSV, and CNV effectively suppresses RNA silencing in the established transient assay. However, since each of these tombusviruses causes severe symptoms (Scholthof, 2006) their use for generating transgenic plants that constitutively express P19 was considered problematic. Considering our previous results that the P19/R43W mutant: i) does not cause a lethal necrosis in *N. benthamiana,* ii) prevents activation of VIGS and protects viral RNA from degradation, and iii) forms dimers that bind TBSV-specific siRNAs, it seemed a good candidate for biotechnological application in transgenic plants. The major question to address was whether P19/R43W could suppress RNAi of foreign genes in plants without causing deleterious symptoms.

As an initial screen for the feasibility of using P19/R43W, I first tested its functionality in the aforementioned described transient assay. Several T-DNA constructs were tested as possible vehicles to express this mutant protein *in vivo* by first examining their ability to transiently express wild-type P19. These constructs [pCB301-P19, pJL-P19, and pCass4N-P19 (Fig. III-2)] originated from different research groups (see Materials and Methods), yet they were all made with the TBSV *p19* gene from our laboratory. (Note: The P19 expressing pKYLX7 construct used in the previous sections was not yet available at the onset of these experiments.) Western blot analyses of agroinfiltrated *N. benthamiana* leaves showed that pCass4N-P19 yielded the highest levels of P19 especially when introduced with *Agrobacterium* strain EHA (Fig. III-5). Based on these results, pCass4N-P19 was used to introduce a mutation for expression of P19/R43W. Transient expression levels obtained upon agroinfiltration show that the accumulation of P19/R43W was measurably lower than that observed for wild-type P19

(Fig. III-5). Again, as observed for wtP19, P19/R43W transient expression on leaves of *N. benthamiana* was higher when using *Agrobacterium* strain EHA compared to strain C58 (Fig.III-5).

Even though the T-DNA constructs tested thus far are suitable for transient expression they lack a selectable marker, such as herbicide or antibiotic resistance that is needed when using *Agrobacterium* to transform tissue followed by selecting transgenic plants. Therefore, the pKYLX7 plant transformation construct expressing P22/P19 was tested. Surprisingly, upon agroinfiltration of this construct P19 accumulation was very low (Fig. III-5), presumably due to the high level of translation initiation from the upstream start codon for P22 expression (Scholthof et al., 1999), suggesting it would not be a suitable candidate for plant transformation.

The next question to address was whether the observed levels of P19 and P19/R43W were sufficient to elevate expression of a co-introduced foreign gene. This again was tested by co-infiltration of the P19 expression constructs with *Agrobacterium* expressing GFP. As shown in Fig. III-7, all agroinfiltrated *N. benthamiana* leaves with either wtP19 or P19/R43W expression enhanced and extended the level of GFP expression. Co-expression of P19/R43W and GFP generated reduced GFP signals compared to those with wtP19 expression (Fig. III-6) which at first sight agrees with the lower protein levels (Fig. III-4). However, enhancement of GFP expression was very evident for co-infiltration of GFP-expressing cultures with pKYLX7-P22/P19 (Fig. III-6) even though P19 accumulation was very marginal for this construct (Fig. III-5). Several days later, green-fluorescent signals were faded in leaves only infiltrated with the GFP-expressing construct while it was still evident in leaves co-infiltrated with RNAi suppressors (Fig. III-6).

In summary, these tests showed that; i) P19/R43W effectively elevates foreign gene expression upon transient delivery, and ii) the plant transformation vector pKYLX7-P22/P19 provides a potentially good backbone for expression of P19/R43W because expression of P19 from this construct very effectively suppresses RNA silencing even when protein expression is relatively low. These studies establish the feasibility of expressing P19/R43W from the pKYLX plant transformation vector to obtain enhanced foreign gene expression in transgenic plants without killing the plant.

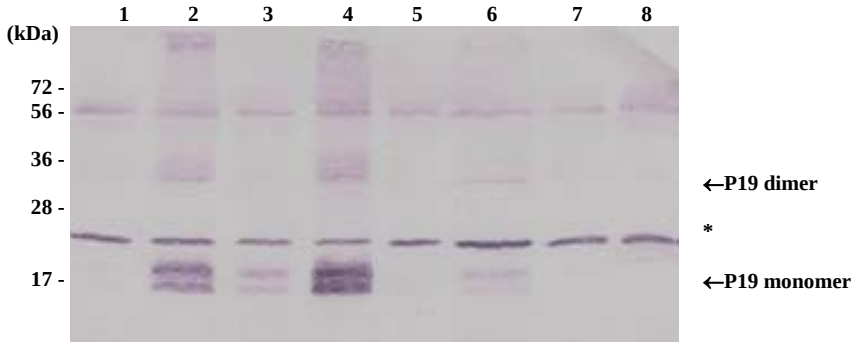

Fig. III-5. Detection of P19 in *N. benthamiana*, 3 days after agroinfiltration. Five P19-based constructs were tested in two *Agrobacterium* strains, EHA and C58. Lane 1: pCB301-P19 in GV3101; lane 2: pJL:P19 in GV3101; lane 3: pCass4N-P19 in C58; lane 4: pCass4N-P19 in EHA; lane 5: pCass4N-P19/R43W in C58; lane 6: pCass4N-P19/R43W in EHA; lane 7: pKYLX7-P22/P19 in C58, 8: Mock. Size markers are shown at the left. The position of P19 is indicated by arrow (for unknown reasons two forms of the monomers accumulated). An unidentified host protein cross-reacts with the antiserum, as indicated by the asterisk. EHA (EHA-101) is a disarmed version of *Agrobacterium tumefaciens* A281 (Hood et al., 1986b; Hood et al., 1986a) while C58 is a strain closer to wild-type *Agrobacterium* (Goodner et al., 2001; Wood et al., 2001).

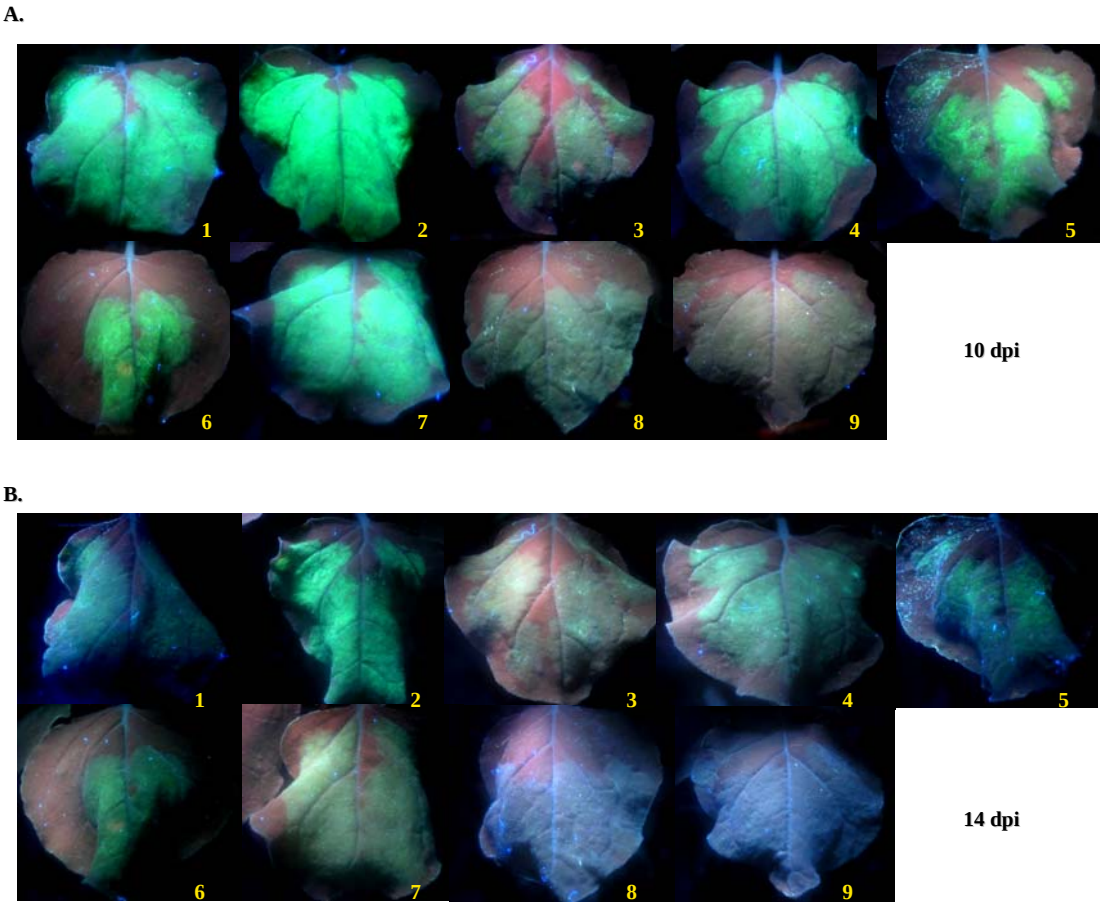

Fig. III-6. Comparison of GFP expression levels by different P19 constructs.
The pictures were taken at 10 (A) and 14 days (B) after *Agrobacterium* co-infiltration. Transient co-expression of the GFP and P19 constructs were at the same value of OD_{600}, respectively. 1: pCass4N-P19 (C58)+GFP; 2: pCass4N-P19 (EHA)+GFP; 3: pCass4N-P19/R43W (C58)+GFP; 4: pCass4N-P19/R43W (EHA)+GFP; 5: pCB301-P19+GFP; 6: pJL3-P19+GFP; 7: pKYLX7-P22/P19+GFP; 8: GFP-expressing *Agrobacterium* only; 9: Infiltration with buffer alone (mock).

Preparation of P19/R43W-expressing transgenic *N. benthamiana*

In order to prepare a transgenic foreign protein expression system, some modifications were made to the pKYLX7-P22/P19 T-DNA construct. First, the start-codon for P22 was inactivated to solely express P19. Westen blot analyses showed that this new construct, pKYLX7-P19, yielded readily detectable levels of P19 expression (Fig. III-7A) and not P22 (data not shown) and in transient co-infiltration assays GFP expression was enhanced (Fig. III-7B). Mutations were then introduced to express P19/R43W from pKYLX-P19. Western blotting showed that this construct expressed P19/R43W (Fig. III-7A) and P19 was biologically active as it suppressed RNA silencing (Fig. III-7B). This construct was verified by sequencing prior to it's used for plant transformation. Transgenic *N. benthamiana* plants were regenerated at Ralph M. Parsons Foundation Plant Transformation Facility using routine transformation and selection protocols (David M. Tricoli, UC Davis, CA), similar to those used for the transformation and regeneration of plants expressing another virus (symptom causing) protein (Goldberg et al., 1991).

Fourteen *N. benthamiana* T0 plants were shipped to our laboratory. These were grown on light shelves in the laboratory. All plants grew to maturity, flowered, and set seed. This seed was collected from individual plants to yield T1 seed for future analyses. Others have attempted to generate wild-type P19-expressing plants but generally the levels of P19 were undetectable and plants were screened with RT-PCR to confirm the P19 transformation (Dunoyer et al., 2004; Siddiqui et al., 2008). In the present study, we were mostly interested in plants in which P19 could be detected. Therefore our screen of T0 plants was performed by western blotting of total protein extracts with P19-specific antibodies. Based on the protein profiles of our P19/R43W transgenic *N. benthamiana*

plants (Fig. III-8), three lines showed detectable levels of P19/R43W. Intriguingly, only the SDS-resistant dimeric form of P19 was detected in these plants, if any monomers were present they accumulated at much lower levels.

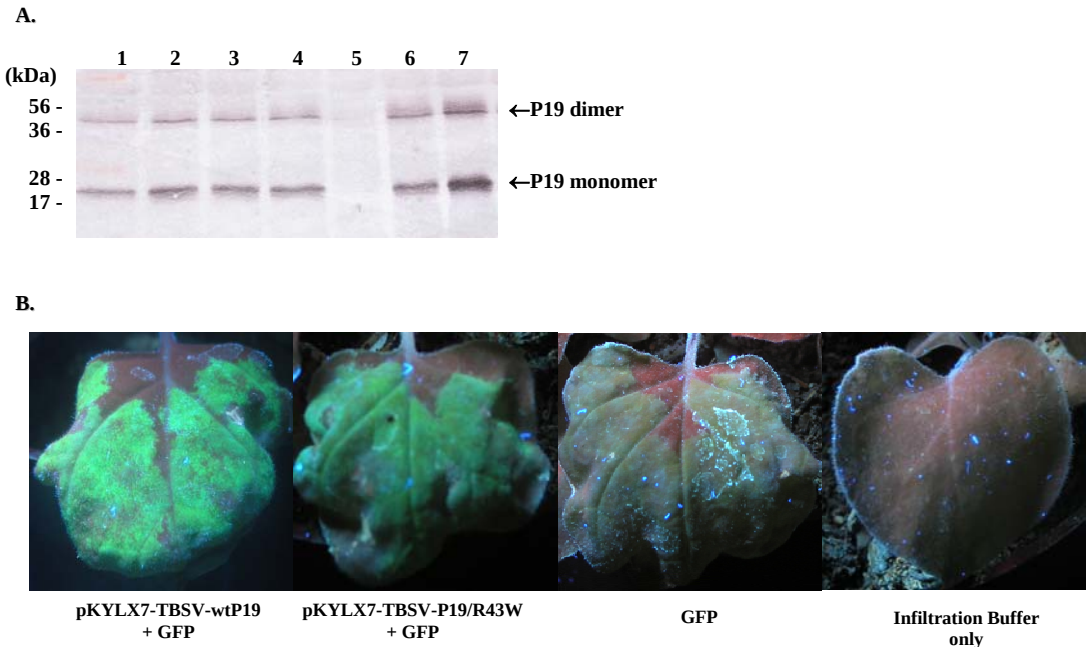

Fig. III-7. Detection of TBSV P19 in total protein extracts from 7 dpi *Agrobacterium*-infiltrated *N. benthamiana* leaves and GFP expression on TBSV P19 co-infiltrated leaves at 7 dpi. (A) Level of TBSV P19 was detected from *N. benthamiana*, 7 days after agroinfiltration. Lane 1: pKYLX7-P19/R43W line1 in C58; lane 2: pKYLX7-P19/R43W line2 in C58; lane 3: pKYLX7-P19/R43W line1 in EHA; lane 4: pKYLX7-P19/R43W line2 in EHA; lane 5: Mock (infiltration buffer only); lane 6: pKYLX7-wtP19 in C58; lane 7: pCass4N-wtP19 in C58. Lane 1, line 2, and line 3, line 4 indicate duplicate bacterial colonies. (B) GFP expression on the leaves co-infiltrated with a GFP-expressing construct and pKYLX7-P19, or pKYLX7-P19/R43W. All constructs were transformed into *Agrobacterium* strain C58 for this transient assay.

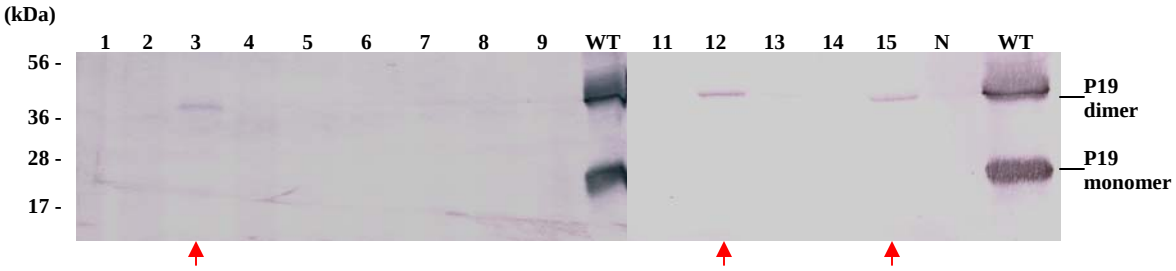

Fig. III-8. Detection of P19/R43W in total protein extracts from putative transgenic *N. benthamiana* T0 lines. Fourteen *N. benthamiana* plants were obtained from *Agrobacterium* transformation (number 10 is missing). All were tested for endogenous P19 expression by western detection. Three lines, P19/R43W-3, 12, 15, displayed detectable levels of P19 expression (shown with red arrows) that was predominantly present in the form of P19 dimers. Based on the different shipment dates, two separate SDS-PAGE and western experiments were performed 1-9 and 11-15. The levels of P19 generation from transgenic plants were compared to wt-TBSV inoculated plants (the right lane in both membranes and non-transgenic *N. benthamiana* (N).

Plant morphology and temperature effects

To determine if the T1 seeds represented transgenic lines, seeds of lines 3 and 12 were germinated on MS medium with 30 μg/ml kanamycin. The germination rate was ~95% for grown in the presence of kanamycin.

Previous reports have shown that transgenic expression of wild-type P19 in *Arabidopsis thaliana*, *N. tabacum*, and *N. benthamiana* often failed to yield detectable levels of P19, although the plants exhibited substantial deformations (Silhavy et al., 2002; Papp et al., 2003; Dunoyer et al., 2004; Scholthof, 2006; Siddiqui et al., 2008). These effects include variegated leaves, aberrant flower phenotype on *A. thaliana*, curled leaves on *N. benthamiana,* and compromised fertility. In the present study, we successfully established transformant lines expressing P19/R43W with minor physiological effects on *N. benthamiana* (Fig. III-9). For unknown reasons, some transgenic lines that did not accumulate detectable levels of P19 still showed symptoms varying from leaf curling and puckering to patchy necrosis.

Because the yield of P19/R43W protein in T1 plants was relatively low, it was questioned whether growing conditions, most notably temperature, could affect the accumulation. It is known that temperature affects protein stability and can also influence silencing (Szittya et al., 2003). For this purpose, T1 seeds were grown at ~25-28ºC or at ~18-20ºC, then germinated plantlets were pooled, proteins extracted, and expression profiles compared (Fig. III-10). The results indicated that plantlets germinated at ~18-20ºC had a relatively higher level of P19/R43W expression then those grown at higher temperatures. Interestingly, in contrast that what was observed for the mature T0 lines (Fig. III-8), for plantlets grown at ~18-20ºC the levels of P19 were also evident in monomeric form in addition to the SDS-resistant dimeric form (Fig. III-10).

Fig. III-9. Phenotypes of P19/R43W transgenic *N. benthamiana* lines.
Representative P19/R43W transgenic lines: 43-3, 43-12 displayed mild morphological changes on transgenic P19/R43W expressing *N. benthamiana* plants. Leaves of these transgenic plants only showed moderate wrinkling and blistering of leaves.

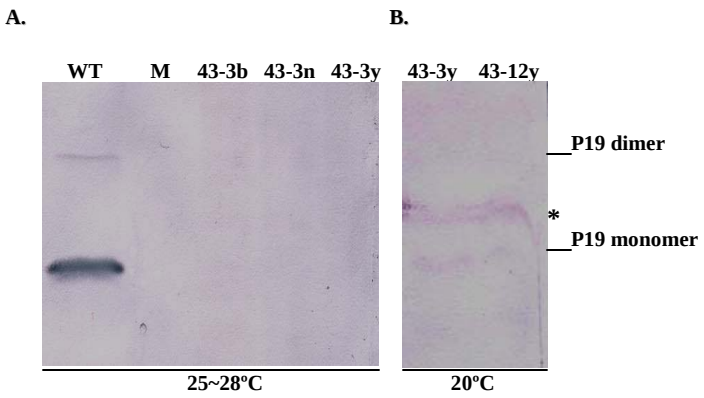

Fig. III-10. Detection of TBSV P19 from putative P19/R43W transgenic *N. benthamiana* T1 lines grown at ~25-28 ºC (A) and ~18-20ºC (B).
(A) Proteins were extracted from 43-3 T1 mature line with blistering (43-3b), normal leaves (43-3n) and seedlings (43-3y) at 25 ºC as shown in Fig. III-9. wtTBSV-infected (WT) and mock-inoculated (M) spinach at 25 ºC were used as positive and negative control for TBSV P19 detection. (B) P19 detection from 43-3 and 43-12 T1 plantlets was performed and showed the presence of monomeric form of P19. Asterisk (*) indicates a non-specific cross-interacting protein.

Preliminary results on the effect of transgenically expressed P19/R43W

Based on the western blot analyses of P19 (Fig. III-8), transgenic line P19/R43W-3 was selected for further examination. An alternative and quite sensitive method to determine if the transgenically expressed P19/R43W is active for suppression of RNA silencing is to infect these plants with a *Tobacco rattle virus* (TRV)-based VIGS construct that silences the plant-encoded phytoene desaturase gene (*pds*) (Liu et al., 2002b); a positive assay results in an easily discernable white bleaching phenotype (Fig. III-11). Transgenic *N. benthamiana* plants of the P19/R43W-3 line were agroinfiltrated with TRV-*pds* and the progression of the onset of silencing evidenced by bleaching was monitored (Fig. III-11). The infiltrated leaves of P19/R43W-transgenic plants displayed numerous small lesions which progressed to wilting of these leaves by 7 days after infiltration (Fig. III-12). Previously, I noticed the same effect when infiltrating non-transgenic *N. benthamiana* with a P19 expressing construct and TRV-*pds* during transient assays. Thus, this symptomatic phenotype is indicative of a biologically active P19/R43W. Moreover, infiltration of TRV-*pds* on the P19/R43W-3 transgenic line showed a delay in the onset of *pds* silencing (Fig. III-12).

Previous reports had shown that suppression of RNA silencing in *N. benthamiana* enhances the progression of TBSV infection (Omarov et al., 2006; Scholthof, 2006; Omarov et al., 2007; Scholthof, 2007). To test the susceptibility of P19/R43W transgenic plants to virus infection, they were inoculated with TBSV or with a TBSV vector expressing GFP to monitor the progression of infection. In both cases the spread of the infection seemed accelerated by 1-2 days in the transgenic plants compared to that observed in non-transgenic plants (data not shown). This indicated that early events in

TBSV infected cells benefit from the pre-existing presence of the suppression-active P19/R43W protein.

In summary, the P19/R43W-3 line expresses a biologically active suppressor of RNA silencing. My initial tests have shown that agroinfiltration of the GFP construct (Fig. III-2) into transgenic P19/R43W-3 *N. benthamiana* resulted in some, but not impressive enhancement of GFP expression compared to that obtained in non-transgenic plants (data not shown). Similar tests are currently being performed to determine if various combinations of plant age, light, and temperature can improve the performance of the transgenic lines to enhance expression of foreign genes.

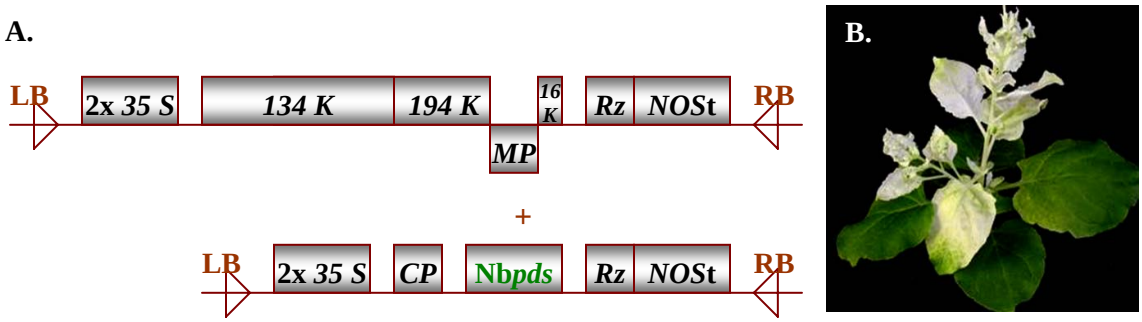

Fig. III-11. The TRV silencing vector to silence *phytoene desaturase* (Nb*pds*), provided by Dinesh-Kumar, Yale University. (A) The two genomic segments of the TRV vector as present between the left and right borders (LB and RB) on the T-DNA vector that can be launched with agroinfiltration. Expression is under control of the 35S promoter, the nos-poly(A) signal with an upstream ribozyme (Rz) sequence to yield infectious *in vivo* transcripts with authentic termini. (B) The silenced phenotype induced by the TRV-based Nb*pds* VIGS construct on *N. benthamiana*, 30 days after agroinfiltration.

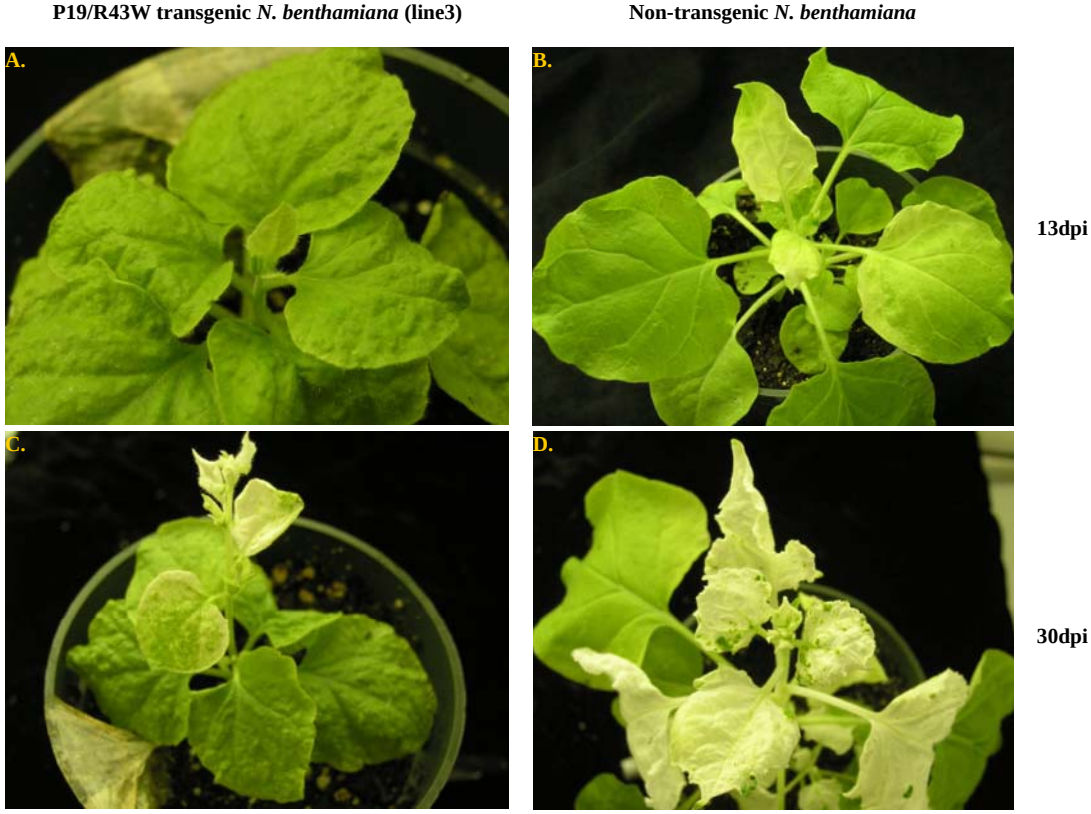

Fig. III-12. Silencing of *pds* by the TRV-VIGS system on P19/R43W transgenic line-3 and non-transgenic *N. benthamiana*. A, B: 13 days after infiltration with *Agrobacterium* expressing PDS. C, D: 30 days after TRV-*pds Agrobacterium* infiltration. Note: The slight puckering of leaves in transgenic plants is noticeable when comparing A and B.

Discussion

Transient expression of P19

A generally employed method to measure the ability of (viral) proteins to suppress RNA silencing uses GFP-transgenic *N. benthamiana* plants on which GFP is silenced upon agrioinfiltration with a GFP expressing T-DNA vector. If co-introduced potential suppressors are active, they will prevent the onset of GFP silencing on these plants (Voinnet et al., 1999). In 2003, Voinnet and Baulcombe reported a new convenient method to test the potential of proteins to suppress RNA silencing in plants that did not rely on the availability of transgenic plants (Voinnet et al., 2003). The novelty resided in the use of non-transgenic *N. benthamiana* plants and the observation that agroinfiltrated GFP-expressing constructs were also subjected to silencing even in absence of homologous transgenic copies. This provided the opportunity to co-agroinfiltrate the GFP T-DNA with constructs expressing potential suppressors to measure the enhancement and prolonged expression of GFP in presence of active suppressors. Importantly, prevention of RNA degradation was concluded to be the cause of this phenomenon (Voinnet et al., 2003). This co-agroinfiltration technique has now become a most attractive tool (Scholthof, 2007). Therefore, in this project I aimed to establish this technique in our laboratory by testing the ability of P19 from different tombusviruses to suppress RNA silencing.

The results based on GFP imaging and western blot analyses (Fig. III-3 and -4) show P19 of three tombusviruses (CymRSV, CNV, and TBSV) effectively suppress silencing of GFP expressed from an agroinfiltrated GFP-expressing T-DNA (Fig. III-2) in *N. benthamiana.* This resulted in elevated and extended levels of GFP accumulation that remained noticeable up to 2.5 weeks after infiltration. These results confirm the general

utility and repeatability of the test originally reported (Voinnet et al., 2003). Even though we did not perform precise quantitative analyses it seems we did not achieve the 50-fold increase reported earlier (Voinnet et al., 2003), but the effect was certainly more then 10-fold in our experiments. Our results also indicated that P19 of CymRSV was the most active *Tombusvirus* P19 tested (Fig. III-3 and -4). These results are intriguing because of the three P19 proteins tested, the CymRSV version is least symptomatic regarding the elicitation of necrotic local lesions due to a hypersensitive defense response (HR) on *N. tabacum* (C. Angel and J. E. Schoelz, personal communication). This agrees with earlier reports that the biological activity of TBSV P19 for virus invasion of plants can be genetically separated from its HR elicitation capacity (Chu et al., 2000; Qiu et al., 2002; Turina et al., 2003; Scholthof, 2006).

An unexpected finding was that the relatively low expression of P19 from pKYLX7-P22/P19 (Fig. III-5) still yielded quite impressive suppression of silencing based on GFP imaging. Previously, it was found in our laboratory that dosage of P19 was an important contributor to its activities for virus spread, symptom induction and suppression of VIGS (Scholthof et al., 1999; Qiu et al., 2002; Omarov et al., 2006). However, in the co-agroinfiltration test used in this study the effect of dosage might be less important. This may be related to the situation that during virus infection much more siRNA is produced compared to what is generated upon agroinfiltration (Silhavy et al., 2002; Vargason et al., 2003; Voinnet et al., 2003; Omarov et al., 2006), and thus more P19 is required to sequester the elevated amounts of siRNA during infection than during transient expression of non-replicating genes.

Transient expression of P19/R43W

Previous tests had shown that the mutant P19/R43W was a suppressor of VIGS, that it sequestered siRNAs and its attenuated symptom phenotype did not cause a lethal necrosis, instead the plants remain alive upon infection (Chu et al., 2000; Qiu et al., 2002; Omarov et al., 2006). To test if P19/R43W retained sufficient siRNA capturing capacity in the agroinfiltration test described above, a T-DNA construct designed for transient expression of P19/R43W was co-agroinflitrated with agrobacteria harboring GFP-expressing T-DNA (Figs. III-6 and -7). The results showed that in general P19/R43W did not accumulate to the same amount as wild-type P19 but the level was sufficient to obtain a mesurable increase and prolongation in accumulation of GFP compared to agroinfiltration in absence of the suppressor (Fig. III-5 and -6). In addition, GFP expression varied with different strains of *Agrobacterium*. For example, P19-expressing constructs in strain EHA showed more co-infiltrated GFP expression than C58 (Fig. III-6). Since EHA is a disarmed version of *Agrobacterium tumefaciens* compared to C58, the toxic effect caused by bacteria might influence P19 expression (Fig. III-6) and GFP expression (Fig. III-5). Such effects had been described previously (Wroblewski et al., 2005). Based on these positive results the p19/R43W mutation was transferred to a plant transformation vector (pKYLX7) commonly used in the laboratory. Use of this construct in co-agroinfiltration experiments confirmed its activity for suppressing silencing of GFP expression (Fig. III-7).

The results indicate that the P19/W43R mutant is active for suppression of RNA silencing, resulting in enhanced levels of a co-expressed foreign gene. Considering the reduced level of toxicity associated with this mutant compared to wild-type P19, this mutant was used for transformation of *N. benthamaina* to possibly provide a plant

expression platform debilitated in silencing of introduced foreign genes attractive for biotechnology.

P19/R43W transgenic *N. benthamiana*

The pKYLX7-P19/R43W construct was used for *Agrobacterium*-mediated transformation of *N. benthamiana*. This tobacco species was initially employed to confirm and demonstrate that the p19 mutant is biologically active for RNAi suppression. Other plants, such tomato are expected to be incorporated in future experiments to further establish the general usefulness of this tool. Fourteen potentially transgenic *N. benthamiana* lines were used for analyses and three of these accumulated detectable levels of P19 (Fig. III-8). The high germination rate of T1 seeds in the presence of kanamycin suggests that multiple copies of the transgene were present in the T0 lines because otherwise segregation would have resulted in a larger portion of the progeny that would no longer be kanamycin resistant. Genomic DNA extracted from the P19/R43W transgenic *N. benthamiana* plants was used for PCR to detect the presence of the integrated *p19*. The preliminary results indicated that several lines in which were unable to detect P19 protein did contain the *p19* insert (data not shown). Even though a thorough genomic analyses was not performed, it is possible that high copy number inserts frequently resulted in silencing of expression (transcriptionally or post-transcriptionally), thus possibly explaining the absence of protein accumulation in most lines.

Another explanation may reside in the discovery that temperature affected the level of P19/R43W accumulation. T1 seeds from line P19/R43W-3 grown at 20ºC yielded detectable levels of the P19 protein whereas in those grown at 25-28ºC the protein was not detected (Fig. III-10). It was previously reported that the suppression capacity of P19

is lost at higher temperature (Szittya et al., 2003). Thus, it is not inconceivable that at elevated temperatures *p19* expression is subjected to RNA silencing because the suppressor activity of the protein is compromised.

Transgenic expression of P19/R43W induced slightly altered *N. benthamiana* morphology

Recent reports indicated that wtP19-transgenic plants have altered leaf morphology, flowers, or were even unable to produce seeds (Dunoyer et al., 2004; Siddiqui et al., 2008). The transgenic *N. benthamiana* lines constitutively expressing P19/R43W had minor phenotypic differences with some oval, mildly puckered, and blistered leaves (Fig. III-9, and -12) that were not observed in non-transgenic plants. The yield of P19/R43W protein detected in the transgenic lines has 50-1,000-fold less than P19 expression during viral infection. This in itself could explain why the symptoms in the P19/R43W-transgenic lines are more attenuated than those elicited by this protein during infection (Chu et al., 2000; Omarov et al., 2006). However, in comparison to other studies that report on wtP19-transgenic plants (Papp et al., 2003; Dunoyer et al., 2004; Siddiqui et al., 2008), our study on the non-toxic but suppression active P19 mutant (P19/R43W) is the first to report the accumulation of readily detectable levels of protein without severe morphological effects on the plants. As mentioned above, in plants growing at high-temperature conditions (28°C) P19 expression could no longer be detected. Moreover, these same plants recovered from any mild morphological changes.

It has been suggested that some of the symptoms associated with P19 expression in plants may be related to the capacity of P19 to bind developmentally important microRNAs (miRNAs) (Papp et al., 2003; Dunoyer et al., 2004; Scholthof, 2006;

Siddiqui et al., 2008). This raises the possibility that the symptom attenuation associated with P19/R43W is related to a reduction in affinity for miRNA binding. In line with this hypothesis is that it was shown that the strength of siRNA binding by P19/R43W is reduced when compared to the binding of siRNAs by wild-type P19 (Omarov et al., 2006). Thus, it is possible that the weakened binding of siRNAs by P19/R43W is still sufficient to suppress RNA silencing while the reduced affinity for miRNAs minimizes developmental effects and thus viable seeds can be obtained from the transgenic plants.

Preliminary functionality tests

Initial experiments provided two lines of support for a conclusion that P19/R43W that is expressed in transgenic *N. benthamiana* is active, at least to a certain extent. First, the onset of VIGS mediated by TRV-*pds* is delayed based on the later appearance of RNA silencing-associated appearance of bleached leaves on *N. benthamiana* (Fig. III-12). Secondly, the transgenic plants exhibit an enhanced susceptibility to TBSV infection (data not shown).

Initial tests with older transgenic plants grown at 25-28ºC failed to show a substantial effect on the level and maintenance of GFP expression upon agroinfiltration of agrobacteria harboring GFP-expressing T-DNA. However, since those tests were performed it has become apparent that the P19 protein is only detectable at lower temperatures, and this may have affected the outcome substantially. Furthermore, in older plants the P19 accumulation was only evident as SDS-recalcitrant dimers (Fig. III-8) whereas in younger plants grown at 18-20ºC the protein also accumulates to detectable levels as monomers (Fig. III-10). It is not known if this is important but if in older plants

the P19 molecules are covalently linked, this may restrict their flexibility to effectively capture siRNAs. Further tests are required to test this possibility.

In conclusion, this represents the first report that a transgenically expressed *Tombusvirus* P19 was shown to accumulate to detectable levels in either *Arabidopsis* or *Nicotiana spp.* Unlike results obtained with wild-type P19, our plants exhibit a relatively normal phenotype, and initial experiments show promise that the P19/R43W protein is actively suppressing RNA silencing. Our tests show that possible ways to optimize this system may be by using young plants at lower temperatures, but varying other growing condition should also be considered. I am optimistic that we will be able to establish the right conditions to obtain high levels and extended maintenance of foreign protein expression without negative effects of RNA silencing. Thus we should be able to establish a system that is valuable to industrially produce favorite gene products *in planta*, and as a research tool for studies on RNA silencing in plants.

CHAPTER IV

DIVERSE BIOLOGICAL EFFECTS INFLUENCED BY PERTURBED INTERACTIONS BETWEEN TOMBUSVIRUS-ENCODED P19 AND siRNAs

Introduction

RNA interference (RNAi), also known as RNA silencing or post-transcriptional gene silencing (PTGS) is a conserved process in eukaryotes (Grishok et al., 2001) that serves as a regulatory mechanism to target specific RNAs for degradation and functions as a defense mechanism against viruses or invasive RNAs. The RNAi pathway is generally considered to be initiated with cleavage of the double-stranded (ds) RNA by DICER-like complexes (Bernstein et al., 2001) into duplex short interfering RNAs (siRNAs) of ~20-25 nucleotides (nt) (Hamilton and Baulcombe, 1999; Hamilton et al., 2002). Subsequently, these ds-siRNAs are associated with the RNA induced silencing complex (RISC), where one of the strands remains bound and contributes to recognition, and cleavage of targeted single-stranded (ss) RNAs (Omarov et al., 2006; Omarov et al., 2007; Scholthof, 2007).

To counter the silencing mechanism, viruses have evolved suppressors to circumvent the RNAi-mediated plant defense responses (Qu and Morris, 2005; Scholthof, 2006; Ding and Voinnet, 2007). These suppressors such as HC-Pro encoded by potyviruses (Kasschau et al., 2003; Chapman et al., 2004), 2b protein of cucumovirus (Ding et al., 1995; Brigneti et al., 1998), P19 of tombusvirses (Qiu et al., 2002; Omarov et al., 2006), P25 of potexvirus (Voinnet et al., 1999; Voinnet et al., 2000), coat protein (CP) of

carmoviruses (Qu and Morris, 2002; Qu et al., 2003), and three RNAi suppressors encoded by *Citrus tristeza virus* (CTV) (Lu et al., 2004), express non-structural as well as structural proteins. Nevertheless, most share the common feature that they were previously identified as pathogenicity factors or host range determinants (Scholthof, 2005). Among them, the 19 kDa protein (P19) encoded by *Tomato bushy stunt virus* (TBSV) is one of the best-studied suppressors (Takeda et al., 2005; Scholthof, 2006).

TBSV is the type member of the *Tombusvirus* genus (Family: *Tombusviridae*). It has a positive-sense ssRNA genome of ~4.8 kb encapsidated in isometric T=3 virus particles (Olson et al., 1983). TBSV has wide host range of infectivity among plant species (Martelli et al., 1988). The TBSV RNA genome contains five open reading frames (ORFs): *p33* and *p92* (replication), *p41* (coat protein), and the 3′-proximal genes known as *p22* and *p19* that encode a ~22 kDa (P22) and a ~19 kDa (P19) protein (Hearne et al., 1990; Scholthof, 2006; Scholthof et al., 1995). The *p19* ORF is entirely nested within the ORF for *p22*. P19 has multiple roles in pathogenesis and P22 is the cell-to-cell movement protein (MP) (Yamamura and Scholthof, 2005).

Most studies on the activity of P19-mediated suppression have been performed in *Nicotiana* species as well as *Arabidopsis* (not a host of TBSV). Based on previous bioassays in hosts, P19 activities include the elicitation of a hypersensitive response (HR) in *N. tabacum* (Chu et al., 1999), promoting cell-to-cell movement in *Capsicum annuum* (Turina et al., 2003), long distance spread in *C. annuum* and *Spinacia oleracea* (Scholthof et al., 1995a; Turina et al., 2003), as well as induction of severe symptom development in many hosts (Scholthof, 2006). Although P19 is dispensable for the initiation of TBSV infection in *N. benthamiana,* it is necessary for viral maintenance

(Chu et al., 2000; Qiu et al., 2002; Qu and Morris, 2002; Omarov et al., 2006; Scholthof, 2006).

TBSV is an unique model system to study RNAi because its replication is linked with accumulation of viral dsRNA-substrates (Scholthof, 2006). These abundantly generated dsRNAs accelerate DICER-mediated cleavage and result in readily detectable amounts of siRNAs that readily associate with P19 to inhibit viral RNA degradation via suppression of RNAi. Previous studies in our laboratory indicated that P19 was active as a dimer (Omarov et al., 2006; Scholthof, 2006) and X-ray crystallography of P19 showed that there are several positively charged amino acids on P19 dimers to electrostatically interact with duplex siRNAs (Fig. IV-1) (Vargason et al., 2003; Ye et al., 2003). This electrostatic interaction between P19 and siRNA is thought to be critical for the sequestration of siRNAs. Furthermore, the non-sequence-specific capture of siRNAs by P19 confers the ability of the protein to block RISC programming and suppress the consequent hydrolysis of any type of RNA that is targeted by RNAi (Omarov et al., 2006; Vargason et al., 2003).

Mutants that cause slight structural permutations can result in loss of siRNA binding, which is correlated with loss of suppressor activity (Omarov et al., 2006). However, these mutants also compromise binding of P19 to its interacting host factor Hin19, which could contribute to observed biological effects (Park et al., 2004). As such, it is not known if the siRNA binding sites predicted by the *in vitro* X-ray crystallography structure are important for any or all of the several *in vivo* biological activities. This reflects the main question of this study and therefore we focused on investigating the diverse biological/biochemical effects of mutations designed to precisely perturb the interaction between P19 and siRNAs while minimizing structural disturbances. For this purpose, we

selected thirteen sites on TBSV P19 which were predicted to contact siRNAs (Vargason et al., 2003; Ye et al., 2003) for mutagenesis, and these were examined for their effects on TBSV infection.

The results indicate that mutations affecting the periphery of the P19 dimer structure strongly attenuated symptoms on *N. benthamiana* whereas those affecting a central region caused severe leaf deformations and stunting. Biochemical tests showed that siRNA accumulation and binding was compromised for representative selected P19 mutants irrespective of the effect on symptoms. In addition, studies with hosts other than *N. benthamiana* showed that symptom induction and systemic spread in some hosts correlated with the capacity of P19 to bind siRNAs whereas in other hosts those biological features were not strictly associated with the ability of P19 to sequester virus-derived siRNAs. Intriguingly, one particular mutant not only caused the accelerated disappearance of TBSV RNA and proteins but also host RNA and proteins were degraded in *N. benthamiana* but not in spinach. In conclusion, compromising P19-siRNA binding sites impacts systemic invasion, symptom development, as well as virus and host material integrity in a host-dependent manner.

Material and methods

Inoculation and analysis of plant tissues. Transcripts were generated *in vitro* from full/partial-length pTBSV-100 cDNAs expressing P19 derivatives. These plasmids (1 μg) were linearized at the 3' terminus of the viral cDNA sequence by digestion with *Sma*I, and transcripts were synthesized by using T7 RNA polymerase. *N. benthamiana* plants were inoculated using standard procedures (Scholthof et al., 1993).

Site-directed mutagenesis. The QuikChange kit (Stratagene, La Jolla, CA) was used for site-directed mutagenesis and standard molecular biology protocols (Sambrook et al., 1989) were followed for the isolation and manipulation of plasmid DNA. The plasmid used to generate mutants was a pUC119 phagemid derivative with one amino acid substitution of P19/K60A on full-length TBSV cDNA insert. All derivative constructs were derived from amino acids substitution on P19, and were carefully designed to keep P22 intact.

RNA analysis. Total RNA was extracted by grinding ~200 mg leaf material (inoculated or systemically infected leaves) on ice in 1 ml of extraction buffer (100 mM Tris-HCl, pH 8.0, 1 mM ETDA, 0.1 M NaCl and 1% SDS). The homogenates were immediately extracted twice with phenol/chloroform (1:1, vol/vol) and total RNAs were precipitated with 8 M lithium chloride solution (1:1, vol/vol) at 4 $^{\circ}$C for 15-25 minutes. The resulting pellets were washed with 70% ethanol then resuspended in RNase-free distilled water. Approximately 10 μg of total RNAs were separated on a 1% agarose gel in 1× Tris-borate-EDTA (TBE) buffer and transferred to nylon membranes (Osmonics,

Westborough, MA) for northern hybridization analysis with [^{32}P]dCTP-labeled TBSV-specific probes as previously described.

Immunoprecipitation. First, 1 g of fresh leaf tissue was swiftly pulverized in an ice-cold mortar with 1.5 ml of ice-cold extraction buffer [150 mM HEPES (pH 7.5), 200 mM NaCl, 1 mM EDTA, 2 mM DTT] containing protease inhibitor cocktail (Roche Diagnostics). The homogenate was filtered through cheesecloth and centrifuged twice at 10,000 xg at 4^{o}C for 15 min. Then, 800 µl of the supernatant was incubated with 2 µl of TBSV P19 rabbit polyclonal antibodies at 4^{o}C for 2 hr and 30 µl of ImmunoPure Immobilized Protein G agarose beads (Pierce, Rockford, IL) were then added. The samples were incubated for an additional 2 hr at room temperature. The beads were spun down and washed six times with ice-cold extraction buffer. The precipitated proteins were analyzed by sodium dodecyl sulfate polyacrylamide gel-electrophoresis (SDS-PAGE) followed by western blotting.

Detection of TBSV siRNAs. P19/siRNA complexes purified with IP were treated with 10% SDS (50 µl) at 65^{o}C for 15 minutes, followed by phenol/chloroform extraction and siRNAs were ethanol precipitated. Precipitated siRNAs were separated in 17% polyacrylamide gel (with 8 M urea), electro-transferred onto nylon membrane (Osmonics, Westborough, MA), and analyzed by hybridization with TBSV-specific dCTP-labeled probes at 42 ^{o}C hybridization. In addition, total RNAs extracted from infected plants were also analyzed by 17% acrylamide gel (with 8 M urea) and siRNAs were detected as previously described (Omarov et al., 2006).

Western blot analysis. Protein samples were separated by SDS-PAGE in 15% polyacrylamide gels and transferred to nitrocellulose membranes (Osmonics, Westborough, MA). The membranes were stained with Ponceau S (Sigma, St. Louis, MO) to verify the efficiency of protein transfer. The antisera against TBSV proteins were applied at the dilution of 1:5000, respectively. Alkaline phosphatase–conjugated goat anti-mouse/rabbit antiserum (Sigma) was used as the secondary antibody and applied at a dilution of 1:1000. The immune complexes were visualized by hydrolysis of tetrazolium-5-bromo-4-chloro-3-indolyl phosphate (BCIP) as the substrate in the presence of nitro-blue tetrazolium chloride (NBT). In some experiments, horseradish peroxidase-conjugated to goat-anti-mouse antiserum (Bio-Rad, Hercules, CA) was used as the secondary antibody at the dilution of 1:5000, and the immune complexes were visualized by using the enhanced chemi-luminescence detection kit (Pierce, Rockford, IL).

Results

Effect of siRNA contact site mutations on symptom development in *N. benthamiana*

The mutations indicated in Fig. IV-1 and Table 1 were introduced on the previously mutated infectious TBSV construct expressing P19/K60A that affected one potential siRNA binding site. This mutation somewhat attenuated symptoms on *N. bethamiana*, but had no noticeable effect on HR in *N. tabacum* or systemic invasion of spinach (Chu et al., 2000). Thus, in anticipation that cumulative mutations would exacerbate effects we selected this as the parental construct to add additional mutations. Since the ORF for translation of the P22 cell-to-cell movement protein entirely overlaps the *p19* ORF this limited the available options for the type of nucleotide substitution that could be introduced without changing *p22*. Consequently, mutations were made to result in the single amino acid replacements R18C, P37S, W39G, T40S, W42R, K67E, K71E, Q107P, S113C, R115W, S120G, S124P (Fig. IV-1) (Table IV-1), and certain mutations were combined for sites close to each other from a three-dimensional perspective (Fig. IV-1).

Based on symptoms, western blots, northern blots, or combinations of thereof, it was evident that all derivatives were able to initially establish systemic infections on *N. benthamiana*, which is consistent with the finding that the absence or presence of P19 has no discernable effects in *N. benthamiana* regarding replication, cell-to-cell movement and the initiation of a systemic infection. Furthermore, these non-lethal phenotypes were not reversed to lethal upon super-infection with wtTBSV (data not shown). This cross-protection is again in agreement with the conclusion that the plants were indeed systemically infected and that introduction of wtP19 in these plants does not reverse the programming of the already established anti-TBSV RISC.

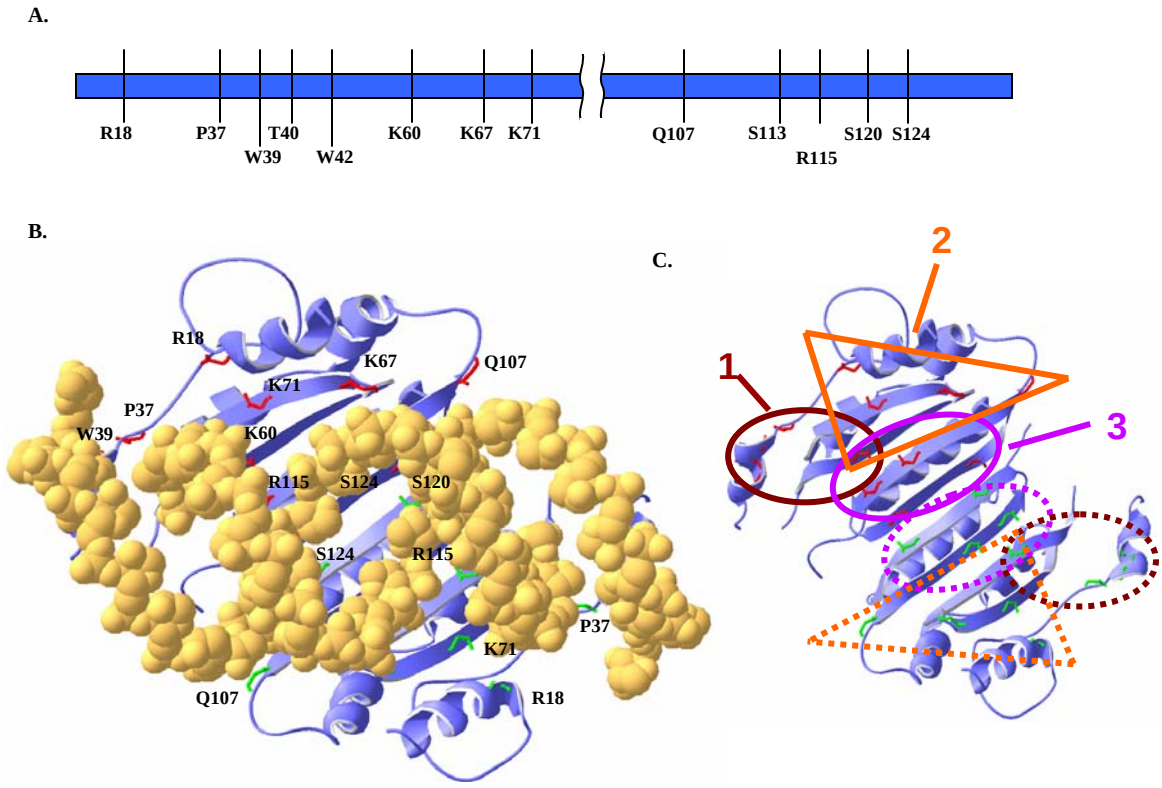

Fig. IV-1. Analysis of the correlation between P19/siRNA binding and pathogenesis of TBSV. (A) Diagram of selected P19 amino acids which include P19/R18, P37, W39, T40, W42, K60, K67, K71, Q107, S113, R115, S120, S124 to make single/combined amino acid substitutions and further investigate the effects on binding siRNAs and symptom development of TBSV. (B) The three-dimensional view of interaction between P19 dimer and siRNA structure is shown from the vertical aspect. (C) The combination of amino acid substitutions was categorized into three main groups, those located on the external (group 1), intermediate (group 2), and central regions (group 3) of P19 dimers. The parameters of P19/siRNA structure were downloaded from the NCBI Protein Data Bank (PDB) and analyzed by Swiss PDB Viewer. The images illustrate how P19 dimers bind the 21 nt duplex siRNA with reading heads (composed of tryptophan). The siRNA duplex is presented in yellow and the P19 dimer is displayed in blue. The targeted amino acids from different monomers of P19 are distinguished in red and green.

Table IV-1. Severity of symptoms associated with P19 mutations in *N. benthamiana* compared to parental P19/60

	18	37	39	40	42	60	67	71	107	113	115	120	124	Severity
P19/60	R	P	W	T	W	A	K	K	Q	S	R	S	S	+++
P19/18-60	C	P	W	T	W	A	K	K	Q	S	R	S	S	+++
P19/37-60	R	S	W	T	W	A	K	K	Q	S	R	S	S	++
P19/37-39-60	R	S	G	T	W	A	K	K	Q	S	R	S	S	+
P19/42-60	R	P	W	T	R	A	K	K	Q	S	R	S	S	+++
P19/37-39-40-42-60	R	S	G	S	R	A	K	K	Q	S	R	S	S	+
P19/60-67	R	P	W	T	W	A	E	K	Q	S	R	S	S	++
P19/60-71	R	P	W	T	W	A	K	E	Q	S	R	S	S	++
P19-18-60-71	C	P	W	T	W	A	K	E	Q	S	R	S	S	+
P19/60-107	R	P	W	T	W	A	K	K	P	S	R	S	S	++
P19/60-67-107	R	P	W	T	W	A	E	K	P	S	R	S	S	+
P19/60-113	R	P	W	T	W	A	K	K	Q	C	R	S	S	++++
P19/60-107-113	R	P	W	T	W	A	K	K	P	C	R	S	S	++++
P19/60-115	R	P	W	T	W	A	K	K	Q	S	W	S	S	++++
P19/60-107-113-115	R	P	W	T	W	A	K	K	P	C	W	S	S	+
P19/60-120	R	P	W	T	W	A	K	K	Q	S	R	G	S	+
P19/60-113-120	R	P	W	T	W	A	K	K	Q	C	R	G	S	+
P19/60-115-120	R	P	W	T	W	A	K	K	Q	S	W	G	S	++
P19/60-124	R	P	W	T	W	A	K	K	Q	S	R	S	P	+++
P19/60-120-124	R	P	W	T	W	A	K	K	Q	S	R	G	P	++
P19/60-115-120-124	R	P	W	T	W	A	K	K	Q	S	W	G	P	++++
P19/60-113-115-120-124	R	P	W	T	W	A	K	K	Q	C	W	G	P	++++

Note. Details of amino acid substitution on P19-siRNA binding sites. Thirteen sites on P19 were chosen to make amino acid substitutions which include R18C, P37S, W39G, T40S, W42R, K60A, K67E, K71E, Q107P, S113C, R115W, S120G, and S124P. The peripheral siRNA interacting sites of P19 which include R18, P37, W39, T40, W42, K60, K67, K71, and Q107P displayed the moderate infection and the subsequent recovery from TBSV infection. In addition, the binding sites on central domain of P19 dimer including S113, R115, and S124 showed the relatively aggravating symptoms. Nevertheless, there is one exception from this categorization which is P19/S120. Although P19/S120 is located in the center of the P19 dimer, the dramatic conformational change caused by substitution (S→G) may interfere with siRNA binding and pathogenesis.

In Table IV-1, the symptoms on *N. benthamiana* are indicated in five categories (number of plus signs), and Fig. IV-2 shows a representative for each category. The lethal necrotic symptom was only observed for *N. benthamiana* plants infected with TBSV expressing wtP19, typically resulting in severe symptoms on inoculated leaves starting at 3 dpi and upper leaves at 5 dpi, rapidly followed by apical necrosis and systemic collapse. TBSV expressing P19/K60A (parental construct for mutagenesis) showed attenuated symptoms, and as could be expected many P19 derivatives with additional mutations caused even milder symptoms (27 dpi). However, it was somewhat surprising that not all additional mutations had additive attenuation effects because some combinations of mutations caused more severe symptoms than observed for P19/K60A (Table IV-1, Fig. IV-2). There was no obvious correlation between the number of siRNA sites targeted for each mutant and the effect on symptoms. Comparison between symptom severity (Table IV-1) and the structural distribution of mutations (Fig. IV-1), indicated that substitutions occurring on the peripheral regions of the P19 dimer (domain 1) mostly resulted in attenuated symptoms. In contrast, changes on the central domain of P19 dimer (domain 3) caused mostly severe phenotypes (albeit less severe than for wtP19).

Extracts from infected plants were subjected to western blotting for the detection of P19 (Fig. IV-3). The profile seen for P19 in Fig. IV-3 was mirrored by accumulation profiles for CP and P22 (not shown), and evident at 5 dpi (Fig. IV-3) and 3 dpi (not shown). Even though the accumulation of P19 monomers was reduced for some mutants on the left hand side, the amount of P19 dimers was comparable. The exception relates to three mutants on the right with the S124P substitution (right side panel of Fig. IV-3). The strong reduction of P19 accumulation associated with these mutants was also observed for CP and P22 (not shown) indicating a rapid onset of RNAi-mediated clearance and

recovery. Considering the position of the S124P substitution, this may affect the stability of the P19 dimer interface thus leading to rapid P19 degradation. However, these explanations stand in intriguing contrast with the remarkable systemic symptoms (Table IV-1) observed for these mutants for which virus accumulation is so strongly reduced.

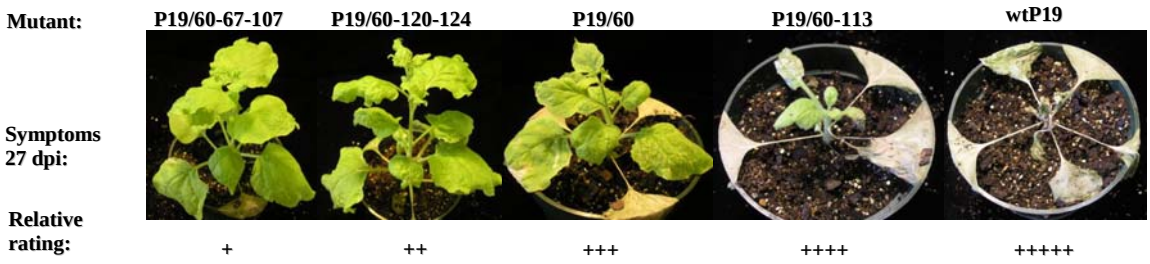

Fig. IV-2. Representative phenotypes of TBSV infections influenced by modifications on P19. The inoculated plants were categorized into different levels as also indicated on Table IV-1 to describe the severity of symptoms from of P19 derivatives on *N. benthamiana*. Based on the symptom development at 27 dpi, the parental construct (P19/60) exhibited the intermediate (+++) symptom while wt-TBSV which expressed wtP19 displayed severe (+++++) phenotype, P19/60-67-107 and P19/60-120-124 showed faint (+) and slight (++) TBSV infection, and P19/60-113 presented the moderately aggressive (++++) symptom development.

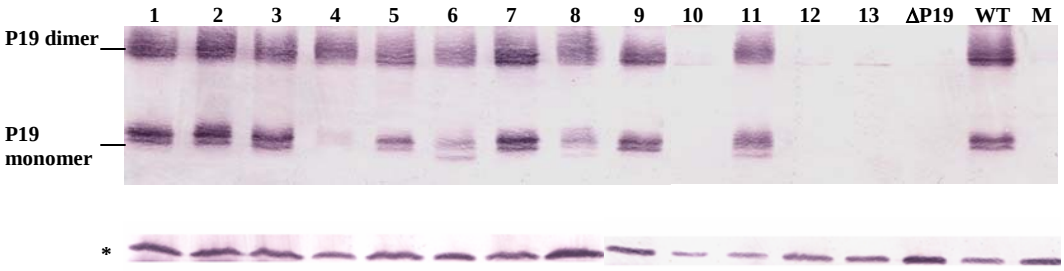

FIG. IV-3. Capability of P19 derivatives to accumulate the mutant P19 proteins within *N. benthamiana* upon infection. Western detection of P19 proteins from plant tissues at 5 dpi; (P19/60) (lane 1), derivatives P19/37-39-60 (lane 2), P19/37-39-40-42-60 (lane 3), P19/18-60-71 (lane 4), P19/60-67-107 (lane 5), P19/60-107-113-115(lane 6), P19/60-120 (lane 7), P19/60-113-120 (lane 8), P19/60-115-120 (lane 9), and P19/60-120-124 (lane 10), P19/60-113 (lane 11), P19-60-115-120-124 (lane 12), and P19/60-113-115-120-124 (lane 13). All these mutants were compared with P19 defective (ΔP19), wild-type P19 (WT) derivatives, and mock inoculation (M). Similar levels of P19 dimers were observed among most P19 mutants while amounts of P19 monomers differed. Nevertheless, P19/60-120-124, P19/60-115-120-124, and P19/60-113-115-120-124 were noteworthy for the absence of P19. Rabbit P19 antiserum was used for protein detection and the immune complexes were visualized by hydrolysis of the BCIP substrate. The unspecific ~23 kD host protein recognized by this P19 antiserum is used as a loading control, shown as an asterisk (*).

Effect of mutations on siRNA accumulation and association with P19

Based on the structure-symptom correlations (Fig. IV-1, Table IV-1) in combination with the reduced level of P19 accumulation for some mutants (Fig. IV-3), representative mutants were selected for detailed comparison with wtP19 and ΔP19. The selected mutants were P19/37-39-40-42-60 (affects domain 1 that includes the reading head that 'measures' the size of siRNAs, and causes symptom attenuation), P19/18-60-71 (affects domain 2 and results in attenuated symptoms), and P19/60-113-115-120-124 (affecting domain 3 and causing relatively severe symptoms). Prior to siRNA analyses, total proteins were collected from plants at 7 dpi and the western blot analyses for detection of P19 (Fig. IV-4, left panel) essentially verified what was observed at 5 dpi (Fig. IV-3). Moreover, for P19/18-60-71 an additional P19 mouse-antibody cross-reacting polypeptide was reproducibly observed that migrated between the dimer and monomer of P19 (Fig. IV-4, left and right panel). As was observed in Fig. IV-3 at 5 dpi, also at 7 dpi, no detectable levels of P19/60-113-115-120-124 were present (Fig. IV-4).

The detection of total TBSV-siRNAs (Fig. IV-4, left panel) revealed that in plants infected with mutants expressing P19/18-60-71, P19/37-39-40-42-60, P19/60-113-115-120-124, and ΔP19, less viral siRNAs accumulated compared to plants infected with virus expressing wtP19 (Fig. IV-4, left panel). In addition, ethidium bromide staining of agarose gels demonstrated that the total RNAs extracted from symptomatic plants contained an extra fast-migrating band (Fig. IV-4). When these bands were eluted and subjected to electrophoresis under denaturing conditions, northern blot analysis confirmed the presence of TBSV-specific 21-nt RNAs (Fig. IV-4).

Immunoprecipitation (IP) of *N. benthamiana* extracts with P19-specific antiserum was then performed to enrich the samples for P19 and to permit studying the siRNA

association for each selected P19 derivative. Western analysis of precipitated P19 (Fig. IV-4, right panel, top) displayed similar differential ratios of monomers and dimers observed for total extracts from selected P19 derivatives (Fig. IV-4, left panel). Most notable was that a P19 antiserum-reactive band was now present for P19/60-113-115-120-124 but it migrated above the P19 dimer; this appearance was reproducibly observed.

Analysis of siRNAs in IP samples showed that wtP19 was associated with TBSV-specific ~21-nt siRNAs whereas this was not detectable for P19/37-39-40-42-60, P19/18-60-71, and P19/60-113-115-120-124 (Fig. IV-4, right panel). Thus, there was no direct correlation between the association of P19 with siRNAs in these tests on the one hand, and the degree of (non-lethal) symptoms in *N. benthamiana* (Table IV-1). However, it is evident that the mutations do affect siRNA sequestration and that this eventually results in a recovery phenotype at several weeks after inoculation (Table IV-1), similar to what is known for P19 defective or null mutants (Omarov et al., 2006). The inability of mutants to effectively bind siRNAs is most obviously reflected by a reduced level of total siRNAs presumably because they have lost protection from nuclease otherwise provided by their binding to P19.

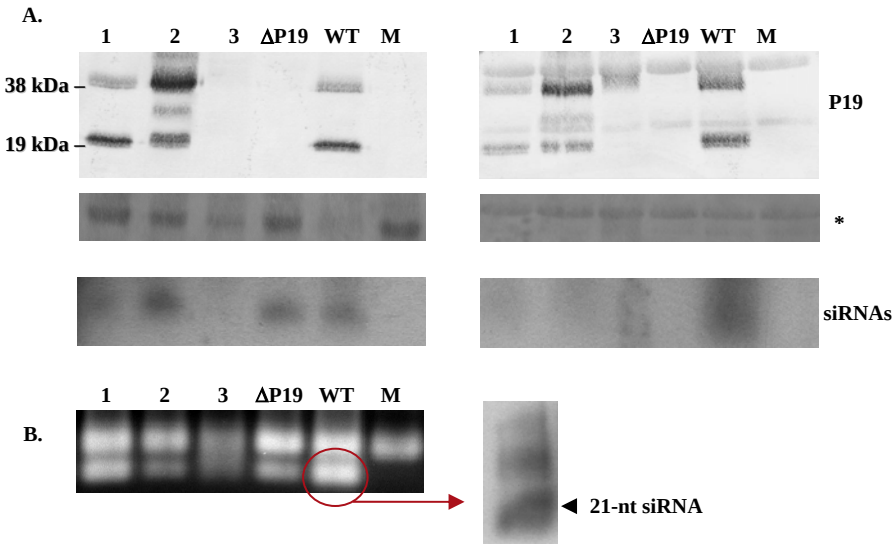

Fig. IV-4. Molecular characteristics of selected TBSV P19 mutants. (A) Western blot analysis of P19 from the total protein samples (left) and P19-associated IP complexes (right) from extracts of inoculated *N. benthamiana*. Total proteins and IP samples were extracted from 7 dpi *N. benthamiana* plants infected with TBSV expressing P19/37-39-40-42-60 (lane 1), P19/18-60-71 (lane 2), P19/60-113-115-120-124 (lane 3), ΔP19, wtP19 (WT). Rabbit P19 antiserum was used for precipitating complexes, mouse P19 antiserium was utilized for detecting proteins from these P19 derivatives and mock treatment (M). The signals for immune complexes were determined by development with alkaline phosphatase. Ponceau S staining after SDS-PAGE was used to compare sample loadings (indicated by the asterisk). The northern blot analysis of TBSV-derived small RNAs from total RNAs is shown in the left bottom panel; the right panel displays the siRNA detection from the immuno-precipitated RNAs. (B) The additional RNA signal in the total RNAs (marked by red circle) was observed at 7 dpi (left) and could be used as an indicator of TBSV infection based on its correlation with symptom development and protein detection. The subsequent denaturing gel electrophoresis confirmed that these small ds RNAs contain different small RNAs including 21-nt TBSV-derived siRNAs (right).

Host-specific effects of selected P19 mutants

If siRNA binding by P19 would be the dominant biochemical property required for all P19-mediated activities in all TBSV hosts then it could be surmised that the three mutants studied in detail in the above section would display similar defective phenotypes in each host when compared to infections with wild-type virus. To test this, we examined host-specific responses for these selected TBSV constructs by monitoring local lesion induction in *Cucurbita maxima* (cucumber), *N. edwardsonii, N. gossei, N. tabacum*, *Spinacia oleracea* (spinach), and *Vigna unguiculata* (cowpea). It is important to note that only in *N. tabacum* is P19 known to be the elicitor of an HR, whereas in the other plants the elicitor is one or more of the other viral proteins, or unknown. The effects of the mutations for systemic infections were compared for *N. benthamiana*, *N. excelsior,* and *C. annuum* (pepper) (Table IV-2). Symptom phenotypes were categorized as follows: symptoms comparable to those elicited by wild-type (+++++), symptoms absent (-), symptoms poor (+), symptoms between poor and wild-type (++, +++, ++++). Symptoms induced for selected plants are shown in Fig. IV-5.

The first noticeable result is that TBSV was only able to elicit local lesions on *N. gossei* or to induce systemic symptoms in pepper, when expressing wtP19, implying a correlation between the ability to sequester siRNAs and infection of these hosts. Another consistent finding was that the mutants P19/37-39-40-42-60, P19/18-60-71 behaved similarly in all species compared among each other by generally inducing mild symptoms. Nevertheless, P19/60-113-115-120-124 was generally more symptomatic (Fig. IV-5).

In contrast to the ability of TBSV to initiate a systemic infection on *N. benthamiana* in absence of P19 (Fig. IV-5), it was previously shown that P19 is needed for systemic

invasion on spinach (Scholthof et al., 1995a; Chu et al., 2000). Therefore, the accumulation of viral proteins, P33 and P19 was monitored in spinach for these mutants (Fig. IV-6). The results showed that the mutants accumulated both P33 and P19 to detectable level in inoculated leaves, only trace amounts of P19 were detected in upper spinach leaves for mutant P19/37-39-40-42-60 and P19/60-113-115-120-124. This accumulation of P19 (by P19/60-113-115-120-124) in spinach contrasts to what was observed in *N. benthamiana* (Fig. IV-3 and Fig. IV-4). Thus, these results suggest a differential level of the impact of P19-siRNA binding exists for these two hosts. Nevertheless, siRNA-binding mutants did not show detectable amounts of P33 (Fig. IV-6) and CP (data not shown) in upper spinach leaves, implying the importance of siRNA binding for full systemic invasion. The mutants had no effect on accumulation of Hin19, a host protein that interacts with P19 (Fig. IV-6).

Together these results suggest that mutagenesis of siRNA binding sites that prohibits the sequestration of siRNAs appears to prevent invasion and symptom induction in some hosts whereas in other species the capacity for siRNA binding is not strictly correlated with pathogenicity.

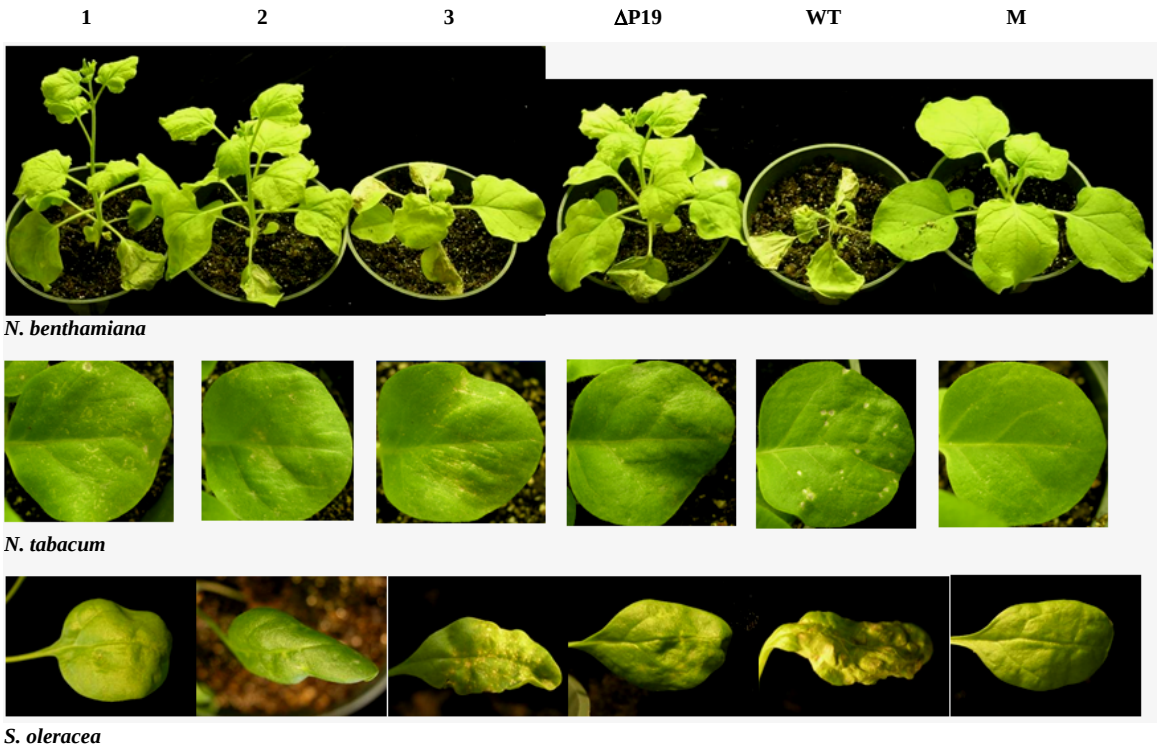

Fig. IV-5. Pathogenic responses on different host plants of TBSV.

Selected P19 derivatives were inoculated onto *N. benthamiana*, *N. tabacum*, and *S. oleracea* to observe the subsequent symptom generation. Selected P19 derivatives include P19/37-39-40-42-60 (1), P19/18-60-71 (2), P19/60-113-115-120-124 (3), ΔP19, wtP19 (WT), and mock treatment (M). Particularly, P19/60-113-115-120-124 (3) displayed more severe symptom compared to other P19/siRNA contact site and P19 defective mutants.

Table IV-2. Host-specific pathogenic effects associated with *p19* constructs

Construct	Local symptoms						Systemic symptoms		
	C. max.	***N. edw.***	***N. gos.***	***N. tab.***	***S. ole.***	***V. ung.***	***C. cap.***	***N. ben.***	***N. exc.***
WT-TBSV	+++	+++	+++	+++	+++	+++	+++	+++	+++
ΔP19	?	-	-	-	-	+++	-	+++	+++
(1) P19/37-39-40-42-60	+	-	-	+	++	+	-	+	+
(2) P19/18-60-71	+	-	-	-	++	+	-	+	+
(3) P19/60-113-115-120-124	+++	-	-	++	+++	++	-	+++	+++
Mock	-	-	-	-	-	-	-	-	-

Note. Pathogenic effects associated with selected P19 derivatives in different host plants. The host-specific pathogenic effects were tested for TBSV expressing P19/37-39-40-42-60, P19/18-60-71, P19/60-113-115-120-124, ΔP19, and wtP19 on *C. annuum*, *C. maxima*, *N. benthamiana*, *N. excelsior*, *N. gossei*, *S. oleracea*, and *V. unguiculata.*

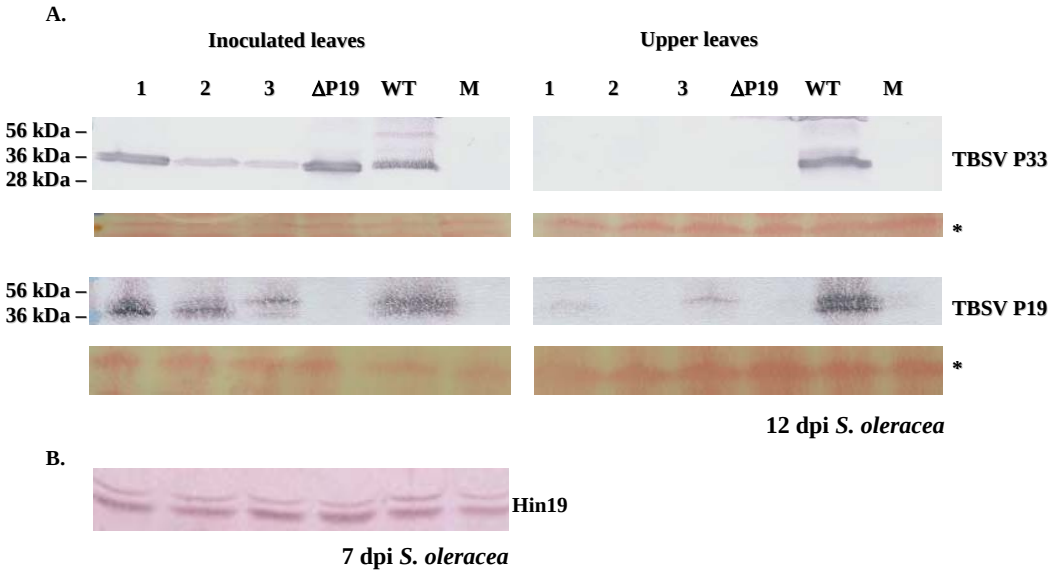

Fig. IV-6. Effects of P19 mutants on accumulation of virus in spinach. (A) Immuno-analyses of TBSV P33, P19, and Hin19 from inoculated and upper leaves of *S. oleracea*. TBSV P33 is the viral protein expressed in the early stage of TBSV infection which is used to confirm if P19 mutants are able to replicate. P19 was also detectable while only ΔP19 and mock treatment (M) were incapable to produce P19 on the inoculated tissues. On upper leaves, P19/37-39-40-42-60, P19/60-113-115-120-124, and WT showed P19 presence while P33 was only detectable for WT. The host proteins were used as the controls of SDS-PAGE after Ponceau S staining (marked with asterisk). (B) Western blot detection of Hin19, a host protein interacting with P19, from 7 dpi inoculated leaves.

Effects of specific mutations on the integrity of virus and host RNAs and proteins

Towards understanding the biochemical basis for the aberrant behavior of the P19/60-113-115-120-124 mutant, we decided to subject this mutant to closer scrutiny. First, to determine if the remarkable symptomatology associated with this mutant in *N. benthamiana* reflects an aberrant response, the mutant was also inoculated on *N. excelsior* which is distinct from *N. benthamiana*, but similarly susceptible for systemic infection. As evident in Fig. IV-7, infection of *N. benthamiana* and *N. excelsior* plants with TBSV expressing wtP19 leads to a lethal necrosis in both hosts. Even though infection with TBSV expressing P19/60-113-115-120-124 is not lethal, the symptoms, especially leaf deformations, are quite extensive and similar in both species (Fig. IV-7). Intuitively, the severe systemic symptoms associated with P19/60-113-115-120-124 contradict the observation that TBSV is undetectable in *N. benthamiana* (Fig. IV-4).

To determine the negative effects of mutants on viral RNA maintenance (i.e. RNA silencing), *N. benthamiana* samples were harvested at 3-5 dpi (Fig. IV-8) and 7 dpi (Fig. IV-9), and total RNAs were extracted. Accumulation of TBSV genomic RNA (gRNA), subgenomic RNA1 (sgRNA1), and subgenomic RNA2 (sgRNA2) was determined by northern blot hybridization. TBSV gRNA, sgRNA1, and sgRNA2 were detected at 3 dpi for plants infected with TBSV expressing P19/37-39-40-42-60, P19/18-60-71, ΔP19, and wtP19 (Fig. IV-8). However, much reduced levels of viral RNAs were detected for P19/60-113-115-120-124 at late time points with gRNA was the first to disappear (Fig. IV-8 and Fig. IV-9). For *N. benthamiana* plants infected with TBSV devoid of P19 expression (ΔP19), clearing of viral RNAs takes two weeks (Omarov et al., 2006). Thus, it seems that the P19/60-113-115-120-124 mutant has dramatically accelerated the impact of RNA silencing on RNA maintenance. This once more stands in contrast with the

remarkable symptoms (Fig. IV-5). Moreover, when examing total RNA it was reproducibly observed that host RNAs, including rRNAs, were present in reduced amounts and/or degraded in extracts from plants infected with virus expressing P19/60-113-115-120-124 (Fig. IV-9, middle). This was not due to degradation during the extraction procedure because mixing of other samples with the P19/60-113-115-120-124 sample during extraction did not result in degradation of other samples. Therefore, the reduction in levels of host RNA occurred in plants infected with TBSV expressing P19/60-113-115-120-124.

Even more noteworthy than the effects noticed on accumulation of host rRNAs, is that observed for the level of host proteins. When comparing total host protein amounts, it was consistently observed that host proteins were substantially degraded in *N. benthamiana* plants infected with virus expressing P19/60-113-115-120-124. In contrast, the degradation of RNAs and proteins were not observed in duplicated experiment in *C. annuum* (pepper) (data not shown) and *S. oleracea* (spinach) (Fig. IV-9). It is not clear how this mutation exerts these effects (whether it is mediated by protein-protein interactions or due to effects on miRNA performance) but it is evident that the P19/60-113-115-120-124 mutant can have disastrous host-dependent effects on the integrity of viral and host RNAs and proteins, and this property is probably linked to the severe deformations observed upon infection of *N. benthamiana*.

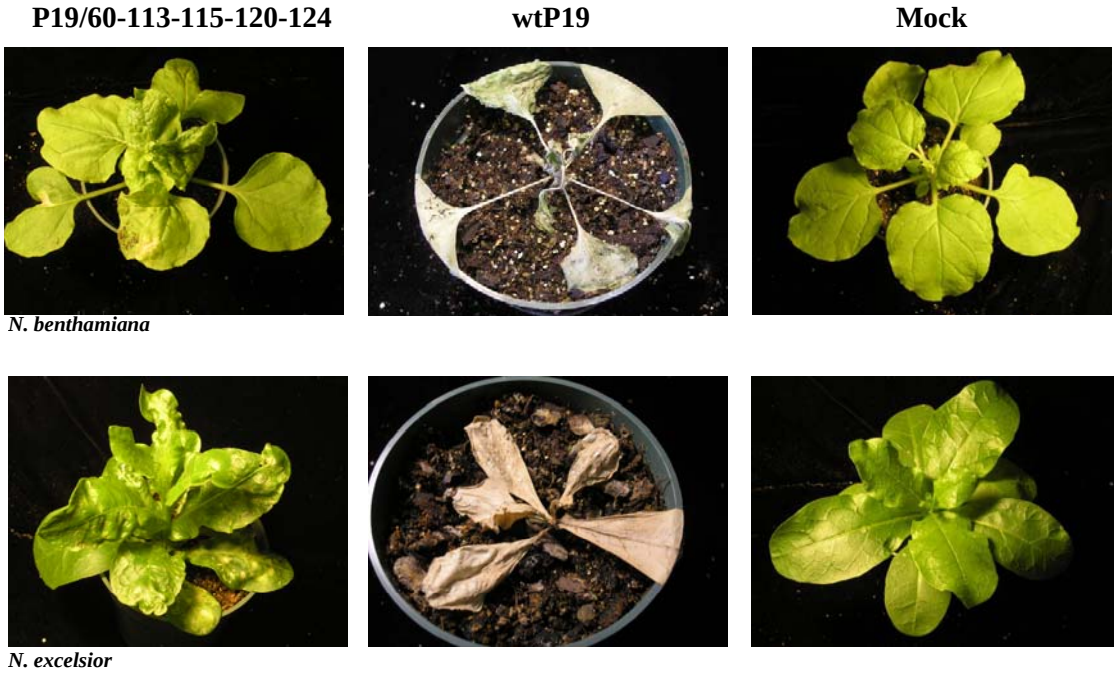

Fig. IV-7. Host-specific symptom development associated with P19/60-113-115-120-124. P19/60-113-115-120-124 is able to establish systemic infection on *N. benthamiana* and *N. excelsior*. TBSV expressing wtP19 resulted in death of both hosts. P19/60-113-115-120-124 generated saw-toothed, curling, bushy leaves with some lesions in *N. excelsior* (bottom left).

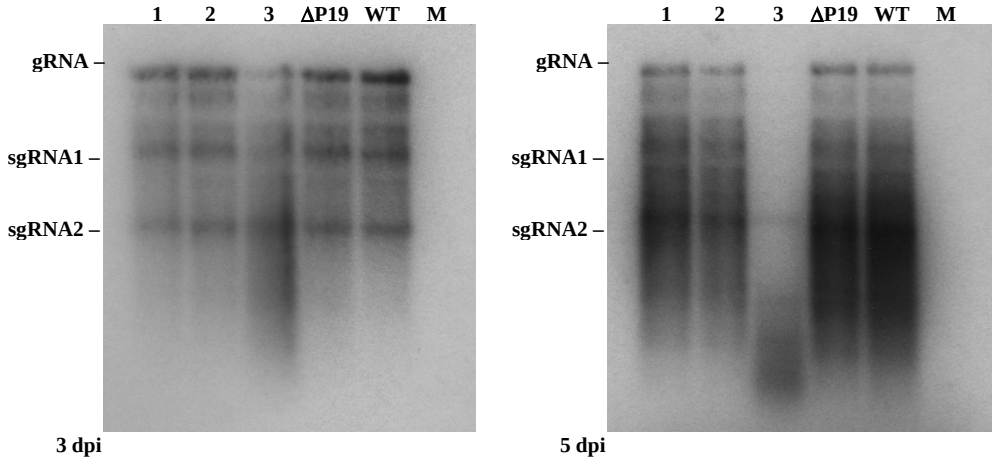

Fig. IV-8. Viral RNA maintenance in infected *N. benthamiana*.

Total RNAs were extracted from infected *N. benthamiana* 3 dpi (left) and 5 dpi (right) with TBSV expressing P19/37-39-40-42-60 (1), P19/18-60-71 (2), P19/60-113-115-120-124 (3), ΔP19, wtP19 (WT). For northern blot hybridization, dCTP-^{32}P labeled full-length TBSV cDNA was used for detecting viral RNAs from these P19 derivatives and mock treatment (M).

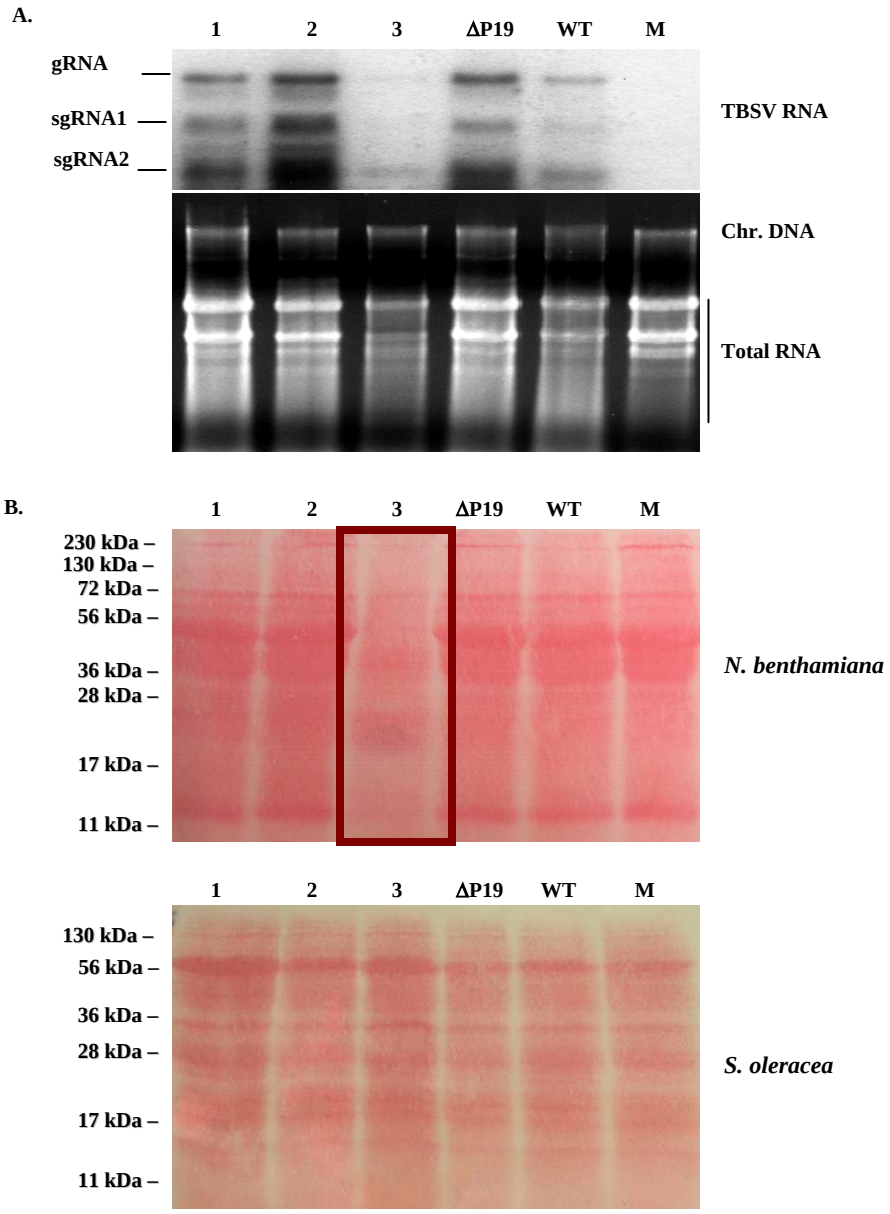

Fig. IV-9. Effect of P19/60-113-115-120-124 on host RNA and protein in *N. benthamiana* versus spinach. (A) The top panel shows a northern blot analyses for detection of TBSV RNAs in the total RNAs extracted at 7 dpi *N. benthamiana* plants infected with selected P19 derivatives- P19/37-39-40-42-60 (1), P19/18-60-71 (2), P19/60-113-115-120-124 (3), ΔP19, wtP19 (WT), and mock treatment (M). The middle panel shows the effects on host RNA integrity. (B) The upper panel shows Ponceau staining of total proteins for *N. benthamiana* and the lower panel shows the same for spinach. (These spinach plants were infected as determined by western blot.)

Discussion

Diverse symptoms are associated with siRNA binding mutants of P19 in *N. benthamiana*

Important properties that influence siRNA appropriation by P19 include: i) early and abundant accumulation of P19 upon infection (Scholthof et al., 1999), ii) the capacity of P19 to use hydrogen bonds, salt bridges, and hydrophobic interactions to form the tail-to-tail homodimer (Vargason et al., 2003; Ye et al., 2003; Park et al., 2004), iii) the proper structural positioning of tryptophane residues on the P19 reading structure to precisely measure 21-nt siRNAs (Omarov et al., 2006), and iv) the appropriate P19-siRNA binding via basic and polar amino acid interactions with the phosphate backbone and 2'-hydroxyl groups of dsRNA (Vargason et al., 2003; Ye et al., 2003).

In a previous biochemical study of P19 (Omarov et al., 2006) it was shown that mutations at positions 75 and 78 caused a structural perturbation that among other possible consequences, also prohibited the sequestration of siRNAs. This led to degradation of viral RNAs in infected *N. benthamiana* plants that subsequently recovered from infection several weeks after inoculation. The same study also showed that an R to W substitution at position 43 (P19/R43W) affected the interaction with TBSV-derived siRNAs. Even though P19/R43 was not predicted to represent an siRNA contact site, the mutation apparently compromised nearby sites (Trp^{39}, Thr^{40}, and Trp^{42}) (Fig. IV-1). Structural studies had shown that amino acid Trp^{39} (W^{39}) and Trp^{42} (W^{42}) on the P19 protein are necessary for proper electrostatic interaction with siRNA and conformational changes subsequently resulted in reduced affinity for siRNAs that also displayed exposed base pairs (Sagan et al., 2007). This binding was sufficiently unstable to lead to programming of an antiviral RISC that could be isolated and that specifically cleaved TBSV RNA *in vitro* (Omarov et al., 2007).

The aforementioned studies were performed with mutations that compromised the P19 structure and this caused a variety of biological effects in different host species (Chu et al., 2000; Turina et al., 2003). However, none of the mutations had been designed to specifically affect siRNA binding. Therefore, even though there was a correlation between the inability of P19 mutants to sequester siRNAs, and programming of RISC in *N. benthamiana* (Omarov et al., 2006; Omarov et al., 2007), other contributing effects due to structural perturbations could not be ruled out, such as improper association with host factors (Park et al., 2004). The purpose of the present study was to more precisely ascertain the role of siRNA binding for the various biological roles of P19 while avoiding the introduction of mutations that would affect dimer formation, or those on the surface that could potentially interact with other components, and to minimize non-specific structural perturbation. The targeting of predicted siRNA binding sites would also permit an *in vivo* verification of the *in vitro* structure prediction (Vargason et al., 2003; Ye et al., 2003).

That specific amino acid changes did substantially influence siRNA binding was shown *in vitro* by the alkylation of cysteine residues (Sagan et al., 2007). Therefore, we targeted thirteen predicted siRNA binding sites on P19 for substitutions, either individually or as combinations (Table IV-1). The structural distributions of the selected P19 residues can be categorized into three different groups (Fig. IV-1) either those affecting mostly peripheral residues on the P19 dimer (domain 1), those that involve the central domain of P19 (domain 3), whereas others modified residues in the intermediate region between the peripheral reading head and the central part of the P19 dimer (domain 2). Regardless of the substitutions, all of the mutants were infectious upon inoculation of

N. benthamiana and the early progress of systemic infection based on onset of symptoms, was not impeded for any of the mutants.

Mutations affecting domain 3 resulted in exacerbation of symptoms compared to those associated with P19/60 (domain 2) whereas those affecting domain 1 caused attenuation of symptoms (Table IV-1, Fig. IV-1). No consistent correlation was observed between the number of substitutions and effects on symptoms. The symptom attenuation and recovery phenotype previously observed for P19/R43W that was predicted to affect the proper positioning of W^{39} and W^{42} in domain 1 and thus the strength of the P19-siRNA association (Chu et al., 2000; Omarov et al., 2006), resembles the effect shown in the present study for the mutants in which precisely these residues W^{39} and W^{42} were substituted. The strong symptoms associated with substitutions in domain 3 and the effect of S124P on P19 accumulation suggest that this central region contributes to protein stability, perhaps by stabilizing the dimer.

At the early stage of infection (3 dpi), P19 could not yet be detected for all mutants in *N. benthamiana*, but at 7 dpi P19 (and other virus proteins) was readily detected, especially the SDS-recalcitrant dimer for most P19 mutants. P19/18-60-71 reproducibly displayed an additional P19 band with an intermediate molecular weight between P19 monomers and dimers (Fig. IV-4). Unexpectedly, the severe leaf deforming symptomatology associated with P19/60-113-115-120-124 was not related to P19 accumulation because as for other mutants carrying the S124P mutation, P19 protein was not detectable (Fig. IV-3). However, in concentrated samples the protein was eventually detected but in a dimeric form with a higher molecular weight than observed for wtP19 (Fig. IV-4) suggestive of a significant structural shift.

Upon further scrutiny of three selected mutants with combinatory substitutions, it was

evident that similar amounts of TBSV siRNAs were present in total RNAs of *N. benthamiana* plants infected with virus expressing P19/18-60-71 (domain 2) and P19/37-39-40-42-60 (domain 1) (Fig. IV-4). Quite remarkably these virus-associated ds-siRNAs were present in a distinct band of small RNAs that could simply be detected upon EtBr staining of agarose gels and that was specific for infected plants (Fig. IV-4). This represents a very rapid and convenient indicator for TBSV infection and the appearance of TBSV-induced siRNA production at various stages during infection. This method, as well as the traditional northern detection of siRNAs (Fig. IV-4), showed that the amount of siRNAs in *N. benthamiana* plants infected with the mutants was lower than observed for plants infected with virus expressing wtP19 suggesting that wtP19 was much more capable in stabilizing the integrity of siRNAs. The latter agrees with our finding that upon IP of P19, siRNAs co-purify for wtP19 but not at detectable levels for the mutants. These results suggest the residues on P19 that were predicted to bind siRNAs *in vitro* (Vargason et al., 2003; Ye et al., 2003), are also involved in binding virus-derived siRNAs during infection of plants. Substitutions of the siRNA binding sites in both domains 1 and 2 prevented siRNA sequestration, and both cause attenuation of symptoms culminating in recovery. In all, these data suggest that the RNAi machinery is activated and programming of RISC is allowed to occur because the mutants fail to sequester siRNAs. However, the correlation between symptom attenuation and compromised siRNA sequestration is less evident for the mutations in domain 3 that include the S124P substitution. The P19/S124P mutant causes quite severe symptoms (Fig. IV-5) while P19 or siRNA accumulation is hardly detectable (Fig. IV-4). Thus the correlation between inability of P19 mutants to sequester siRNAs and attenuation of symptoms (indicative of RNAi-mediated recovery) is not strict in *N. benthamiana*.

Not all host-specific P19-mediated activities rely on its capacity to bind siRNAs

P19 is dispensable for TBSV replication in all hosts tested, but depending on the plant species it is involved in different aspects of the infection processes (Scholthof, 2006). For instance, P19 has a crucial role in systemic TBSV invasion of pepper and spinach (Chu et al., 2000; Turina et al., 2003). The results in the present study showed that only wtP19 is active for pathogenesis on *N. gossei* and pepper, while all siRNA binding mutants were compromised. This implies that siRNA binding is crucial in these hosts. On the other hand, siRNA binding mutants were able to cause severe symptoms on spinach (Fig. IV-5) and accumulated TBSV RNA and protein (Fig. IV-6). However, the P19-siRNA binding site mutants were compromised for long distance spread in spinach based on a lack of accumulation of P33 (Fig. IV-6). Together the results suggest that the integrity of siRNA binding sites and associated siRNA-binding are required in some hosts whereas in other species other factors contribute to pathogenicity. There does seem to be a functional correlation between the ability to sequester siRNAs and long distance spread in spinach. The observation that for some mutant P19s can be detected in upper leaves while P33 is undetectable agrees with leaves that P19 can spread through spinach (H. Scholthof, unpublished data).

What factors other than siRNA binding could contribute to these observations? It is know that a certain type of RNA export protein (like Hin19) of *Arabidopsis* and *N. tabacum*, interacts with P19 (Park et al., 2004; Uhrig et al., 2004; Canto et al., 2006). From this, it seems reasonable to consider that Hin19 or other host factors that contribute to the function of P19 may be siRNA-binding independent. This assertion is supported by the finding that ALY proteins do not seem to be involved in silencing or P19-mediated suppression (Uhrig et al., 2004; Canto et al., 2006). In the present study, TBSV infections

caused by selected P19 derivatives or wtP19 did not show a difference in the accumulation of Hin19, but it is not known if the relevant interaction in all species involves a particular ALY protein and/or if mutations on siRNA binding sites affect the interaction of P19 with ALY proteins. Nevertheless, the incomplete conservation of selected P19/siRNA interacting amino acids among tombusviruses (Fig. IV-10) is indicative that some contribute in a virus-host specific manner.

Virus and host RNA and protein degradation associated with the S124P substitution

Why do mutants with the S124P substitution cause severe malformation symptoms? It has been suggested that part of the symptomatology induced by P19 may be caused by its capturing of miRNAs (Papp et al., 2003; Chapman et al., 2004). This could be the case for the mutants with the S124P substitution, but the P19 protein accumulation for this mutant is reduced to such an extent that it is not possible to test whether it has sequestered one or more specific miRNAs during the onset of infection. Yet, our results show that even though TBSV RNA accumulates to comparable levels for the mutants at 3 dpi, by 7 dpi the viral RNA has essentially disappeared from plants infected with P19/60-113-115-120-124 (Fig. IV-8 and Fig. IV-9). This suggests that the RNAi-mediated clearance of viral RNA that normally occurs for P19-defective mutants after 7-10 dpi is accelerated for TBSV expressing P19/60-113-115-120-124. Quite surprising is that the clearance is not restricted to viral RNA and proteins because host RNAs and proteins are also degraded in these inoculated *N. benthamiana* plants (Fig. IV-9). Furthermore, plant extracts from *N. benthamiana* plants infected with virus expressing P19/60-113-115-120-124 turn brown rapidly upon extraction and the pH of the material is 6, while it is 7 for extracts from plants infected with wild-type and other selected TBSV derivatives (data

not shown). Altogether the data show that failure of P19/60-113-115-120-124 to sequester siRNAs leads to RNAi-mediated recovery. Although this might agree with the accelerated disappearance of viral RNA, it contrasts with the severe symptoms that are associated with disastrous effects on host RNA and protein integrity. It is possible that the mutant protein triggers a reaction, either by protein-protein mediated interactions or by having gained affinity for specific miRNAs, which hyperactivates non-specific degradative events. Why the plant does not succumb to these events might be related to the rapid clearance of virus that re-establishes some sense of balance although the initially established deforming effects seem irreversible. It is also intriguing that the effect of this mutation on the integrity of viral and host materials in *N. benthamiana* is not evident in pepper or in spinach. The reason for this is still unknown, but it is just another example of the host-dependent effects of P19 (Scholthof, 2006).

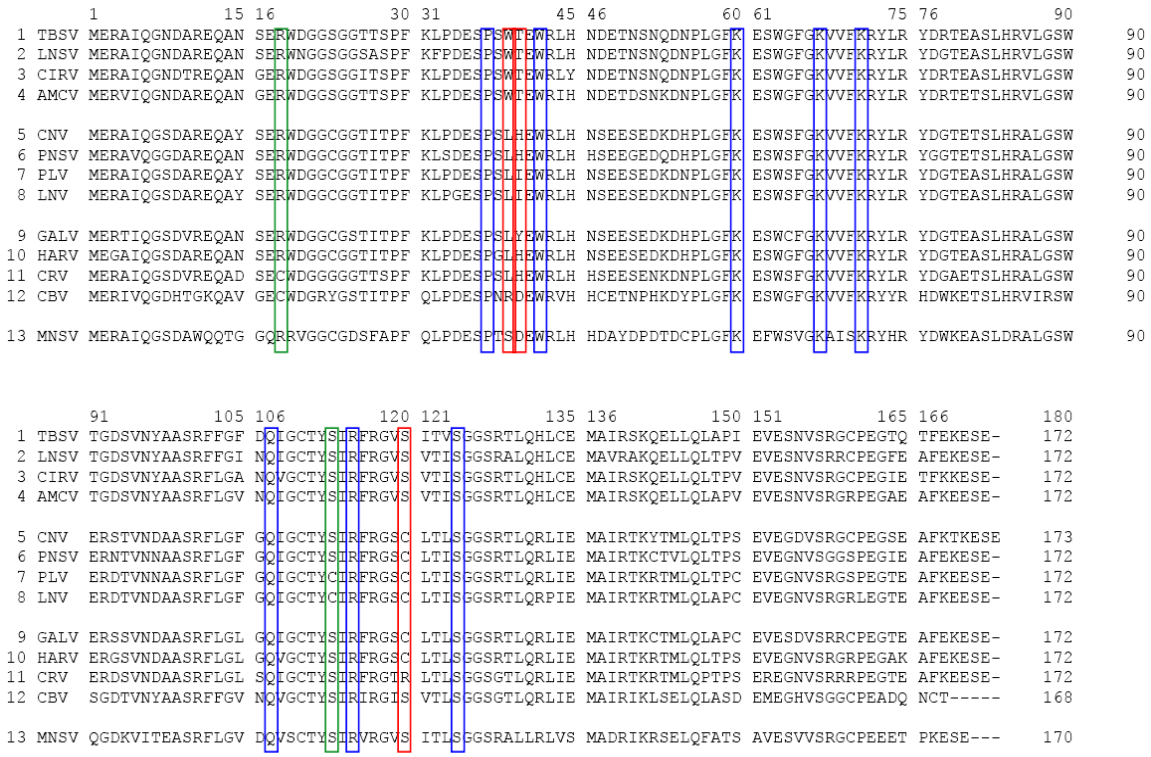

Fig. IV-10. Multiple alignment of tombusvirus P19s.
The selected siRNA contact sites on P19 displayed highly conserved (blue), moderately conserved (green), and non-conserved (red) patterns based on multiple aligned results.
The abbreviations of tombusvirus and their full names are listed as following: TBSV: *Tomato bushy stunt virus*; LNSV: *Lettuce necrotic stunt virus*; CIRV: *Carnation Italian ringspot virus*; AMCV: *Artichoke mottled crinkle virus*; CNV: *Cucumber necrosis virus*; PNSV: *Pelargonium necrotic spot virus*; PLV: *Pear latent virus*; LNV: *Lisianthus necrosis virus*; GALV: *Grapevine Algerian latent virus*; HARV: *Havel river virus*; CRV: *Cymbidium ringspot virus*; CBV: *Cucumber Bulgarian virus*; MNSV*: Maize necrotic streak virus*.

In conclusion, the results of this study show that: i) P19 is quite sensitive to mutagenesis of siRNA binding sites resulting in reduced amount of total TBSV-derived siRNA, loss of siRNA binding by P19, and loss of lethal necrosis on *N. benthamiana*, ii) siRNA-binding mutations on the central domain of P19 result in more severe symptoms compared to those affecting peripheral regions, iii) simple agarose gel-mediated detection of small RNAs that contain TBSV-siRNAs is a rapid indicator of infection, iv) integrity of siRNA binding sites is essential for infection of some hosts whereas in other plants this is less important and additional factors contribute, v) the S124P mutation on P19 leads to rapid degradation of viral and host RNA and proteins (including P19) in a host-dependent manner, and vi) P19/60-113-115-120-124 may cause more aggressive TBSV invasion even though it accelerates RNAi.

CHAPTER V

CONCLUSIONS, FINAL INTERPRETATIONS, AND FUTURE DIRECTION

Viral movement

Based on the studies described in Chapter II, clear visualization of TBSV invasion on subcellular, cellular, and plant levels was achieved. The cell-to-cell movement of TBSV was particularly focused on the cellular localization of GFP signals. This study reaffirmed that the capacity of virus to move through epidermis, mesophyll, and trafficking into phloem to result in systemic invasion, are all critical parameters to determine if a plant is a non-host (no cell-to-cell movement), local lesion host (mainly cell-to-cell movement), or systemic infection host (cell-to-cell movement and systemic spread) of TBSV regarding spread. The results also suggest that successful exit of initially inoculated epidermal cells is a critical determinant. The subcellular localization studies of P22 raised the possibility that single amino acid substitutions of P22, which showed a null phenotype (i.e. defective for movement), caused an aberrant distribution of P22 throughout the cell instead of it mainly being located at cell membranes.

Remaining questions are whether these substituitions on P22 influence the interaction with host factors to support viral complexes to move via plasmodesmata and what are those host factors? Furthermore, some reports indicate that viral movement proteins are required to form dimers and polymers to function. Therefore, determining the ability of P22 to form dimers and to analyze if substituitions on P22 are critical for dimerization and maintenance of the stable functional structure will further the understanding of how P22 functions to move from cell to cell. Another question I have is if these mutated forms

of P22 indeed are still able to bind and interact with viral nucleotides. P22-RNA binding assays, overexpressing or transient expressions of P22 derivatives, and further identification of other plant factors that interact with P22 can be used to study these subjects to benefit our understanding on viral movement. Another area of interest is to determine if there are any major structural differences of the thickness of cell wall, mesophyll, the water content of leaf tissues from non-host, local lesion host, and systemically susceptible plants?

Regarding the host range test with TBSV-GFP, I was also involved in, and interested in, a project examining the effect of CP sequence on the stability of TBSV gene vectors. The preliminary result showed that deletion of *cp* sequences downstream of *gfp* in TBSV-GFP significantly improved the velocity of viral movement and intensity of the infection by RNA transcripts (more and larger GFP spots), compared with results obtained with the original TBSV-GFP with ~1 kb CP DNA sequence downstream of the GFP gene. This agrees with previous studies that the *cp* sequence is sensitive to recombination and thus promotes rapid excision of foreign genes. These results also suggested that length of viral RNA may influence the efficiency of movement.

Intriguingly, simultaneous shut down of CP and P19 expression resulted in dramatically decreased green fluorescent signals (data not shown). These results, and others in our laboratory, suggest that presence of P19 supports or stabilizes GFP expression from TBSV. Other experiments have shown that TBSV constructs which retain the ability to form particles are less sensitive to RNAi-directed degradation than those devoid of CP expression. Therefore, although previous studies showed no direct interaction between these two TBSV proteins, there is a possibility that P19 and CP may

indirectly interact. It will be interesting to further investigate how CP and P19 together affect viral movement and spread.

Expressing P19 *in planta*

Endogenous P19/R43W production could be detected from crude protein extracts from leaves of transgenic *N. benthamiana* lines. Cooler growing conditions seemed a crucial factor to prevent aggressive RNAi and result in the achievement to detect P19. Assays on transgenic plants infected with TRV-*pds*, support that endogenous P19/R43W is responsible for causing necrotic lesions and preventing the induction of RNAi at the initial stage of infection. Presumably the low yield of P19 is insufficient to prevent thorough protection from RNAi. However, it may be also an advantage that this non-toxic but suppression-active mutant P19 in transgenic *N .benthamiana* plants still allows some basic levels of the RNAi mechanism to operate, so *N .benthamiana* will not be overly (hyper) sensitive to all pathogens. Persistent attempts will be needed to optimize growing conditions for these moderately suppressed plants to eventually be able to over-express genes on an industrial level for production of favorite proteins *in planta*.

In addition, the P19/R43W transgenically expressing *N. benthamiana* can be further used as a model to investigate the *in vivo* effects of P19. As shown in several reports, P19 sequesters miRNAs in *in vitro* systems. This endogenous P19 producing system can perhaps be utilized to confirm the connection between altered phenotype (development) of P19/R43W transgenic plants and *in vivo* sequestration of miRNAs. The anticipation is that the column purification or immuno-precipitation can be performed to pull down *in vivo* P19-associated complexes to prove that P19 is able to interact with miRNAs in this system. Consequently, it should be possible to confirm that the leaf blistering and

abnormal bushy phenotype of P19/R43W transgenic lines are caused by formation of some specific P19-miRNA complexes.

P19-siRNA contact sites

Based on the results in chapter IV, the siRNA contact sites on the P19 dimer are crucial for binding siRNA, aggressive symptom development, and RNA/protein maintenance in the TBSV-*N. benthamiana* system. The results showed that mutations affecting siRNA binding sites in a central region prevented siRNA binding and depending on the position of the mutation that could either aggravate or attenuate symptoms, in a host-dependent manner. Not all host responses correlated with siRNA-binding, but the RNA maintenance and long distance spread function appeared to depend on siRNA-binding.

In addition, a higher molecular weight virion-like signal of P19/60-113-115-120-124 was observed from crude plant extracts (TE extraction) upon native agarose gel electrophoresis when compared to virions from wild-type infected plants. Western blot analyses of TBSV CP and P19, followed by northern blots of TBSV RNAs showed that CP could be detected for the virion-like signals of all P19 derivatives. Simultaneously, P19 could not be detected for a P19 deficient (ΔP19) derivative while P19/37-39-40-42-60, P19-18-60-71, and wtP19 showed intense P19 signals associated with the virion-like bands. Meanwhile, the P19/60-113-115-120-124 mutant displayed a smeared immuno-signal, but there was no P19 detected specifically with virion-like signals. These are all interesting observations indicative of an interaction between virions and P19, in line with a suggested model in a previous section.

Subsequently, the degradation of viral/host proteins and RNAs brought out a question whether the changes on the P19 central region induced proteolysis and cell lysis. The preliminary examination on incubating crude TE extracts from P19/60-113-115-120-124 inoculated *N. benthamiana* tissues with either extracts from mock or wtP19 treatment did not show the dramatic protein degradation in these incubated samples. Therefore, the phenomenon of RNA/protein degradation can be concluded to occur inside infected cells and not during extraction. The results also showed that this non-specific RNA/protein degradation occurred in *N. benthamiana* but not in spinach. Hence, the future EM, subcellular and cellular localization of P19, *in vitro* P19-siRNA binding, as well as the P19-miRNA sequestration described previously will be useful to understand the mechanism behind these intriguing effects caused by altering the center of the P19 dimer.

Despite the above mentioned aspects that are presumably protein-related, I found some unexpected properties that cannot be ascribed to protein effects. As a control experiment, I inactivated the start codons for the three selected P19 mutants. As expected, for two of these the phenotypes were comparable to what is normally seen in absence of P19. Therefore, the phenotypes observed for these mutant P19 proteins are explainable as being due to protein effects. However, for P19/60-113-115-120-124, the mutation of the start codon rendered this mutant non-infectious (protoplast experiments have yet to be performed). Thus, it seems that part of the effects associated with the mutations may be due to structural effects on the RNA rather than protein. This agrees with an earlier finding that important ancillary elements reside in the P19 gene (Park et al., 2002). However, since in presence of P19 expression this mutant is infectious albeit very sensitive to RNA clearance, there must also be a protein-mediated effect. Dissecting these different contributions is a challenge in future experiments.

Concluding remarks

This research provides further evidence that the 3' proximal region of the TBSV ssRNA genome, with two nested ORFs, provides diverse functions including viral cell-to-cell movement, long distance spread, viral RNA accumulation, suppressing RNAi, and TBSV pathogenesis. This study proposes that movement out of epidermal cells is regulated by specific P22 residues and this ability is a critical host range determinant. Furthermore, this is the first time a mutant P19 was shown to be expressed in transgenic *N. benthamiana* plants to provide a host platform for biotechnological applications and for RNA silencing studies. Moreover, the critical effects influenced by the siRNA contact sites on the central domain of P19 dimers were identified. These findings allow us to go a step further towards understanding the mechanisms behind viral movement, suppression of RNAi, TBSV pathogenesis and diverse host responses.

REFERENCES

Anandalakshmi, R., Pruss, G.J., Ge, X., Marathe, R., Mallory, A.C., Smith, T.H., and Vance, V.B. (1998). A viral suppressor of gene silencing in plants. Proc. Natl. Acad. Sci. USA **95,** 13079-13084.

Ashby, J., Boutant, E., Seemanpillai, M., Groner, A., Sambade, A., Ritzenthaler, C., and Heinlein, M. (2006). *Tobacco mosaic virus* movement protein functions as a structural microtubule-associated protein. J. Virol. **80,** 12433-12433.

Asurmendi, S., Berg, R.H., Koo, J.C., and Beachy, R.N. (2004). Coat protein regulates formation of replication complexes during *Tobacco mosaic virus* infection. Proc. Natl. Acad. Sci. USA **101,** 1415-1420.

Balachandran, S., Hull, R.J., Vaadia, Y., Wolf, S., and Lucas, W.J. (1995). Alteration in carbon partitioning induced by the movement protein of *Tobacco mosaic virus* originates in the mesophyll and is independent of change in the plasmodesmal size-exclusion limit. Plant, Cell Environ. **18,** 1301-1310.

Beclin, C., Berthome, R., Palauqui, J.C., Tepfer, M., and Vaucheret, H. (1998). Infection of tobacco or *Arabidopsis* plants by CMV counteracts systemic post-transcriptional silencing of nonviral (trans)genes. Virology **252,** 313-317.

Bennett, C.W. (1940). Relation of food translocation to movement of virus of tobacco mosaic. J. Agric. Res. **60,** 361-390.

Bernstein, E., Caudy, A.A., Hammond, S.M., and Hannon, G.J. (2001). Role for a bidentate ribonuclease in the initiation step of RNA interference. Nature **409,** 363-366.

Brigneti, G., Voinnet, O., Li, W.X., Ji, L.H., Ding, S.W., and Baulcombe, D.C. (1998). Viral pathogenicity determinants are suppressors of transgene silencing in *Nicotiana benthamiana*. EMBO J. **17,** 6739-6746.

Brill, L.M., Dechongkit, S., DeLaBarre, B., Stroebel, J., Beachy, R.N., and Yeager, M. (2004). Dimerization of recombinant *Tobacco mosaic virus* movement protein. J. Virol. **78,** 3372-3377.

Bucher, G.L., Tarina, C., Heinlein, M., Di Serio, F., Meins, F., and Iglesias, V.A. (2001). Local expression of enzymatically active class I β-1,3-glucanase enhances symptoms of TMV infection in tobacco. Plant J. **28,** 361-369.

Callaway, A., Giesman-Cookmeyer, D., Gillock, E.T., Sit, T.L., and Lommel, S.A. (2001). The multifunctional capsid proteins of plant RNA viruses. Annu. Rev. Phytopathol. **39,** 419-460.

Canto, T., Uhrig, J.F., Swanson, M., Wright, K.M., and MacFarlane, S.A. (2006). Translocation of *Tomato bushy stunt virus* p19 protein into the nucleus by ALY proteins compromises its silencing suppressor activity. J. Virol. **80,** 9064-9072.

Carrington, J.C., and Whitham, S.A. (1998). Viral invasion and host defense: strategies and counter-strategies. Curr. Opin. Plant Biol. **1,** 336-341.

Carrington, J.C., Kasschau, K.D., Mahajan, S.K., and Schaad, M.C. (1996). Cell-to-cell and long-distance transport of viruses in plants. The Plant Cell **8,** 1669-1681.

Chapman, E.J., Prokhnevsky, A.I., Gopinath, K., Dolja, V.V., and Carrington, J.C. (2004). Viral RNA silencing suppressors inhibit the microRNA pathway at an intermediate step. Genes Dev. **18,** 1179-1186.

Chu, M., Park, J.W., and Scholthof, H.B. (1999). Separate regions on the *Tomato bushy stunt virus* p22 protein mediate cell-to-cell movement versus elicitation of effective resistance responses. Mol. Plant-Microbe Interact. **12,** 285-292.

Chu, M., Desvoyes, B., Turina, M., Noad, R., and Scholthof, H.B. (2000). Genetic dissection of *Tomato bushy stunt virus* p19-protein-mediated host-dependent symptom induction and systemic invasion. Virology **266,** 79-87.

Citovsky, V., Mclean, B.G., Zupan, J.R., and Zambryski, P. (1993). Phosphorylation of *Tobacco mosaic virus* cell-to-cell movement protein by a developmentally regulated plant cell wall-associated protein kinase. Genes Dev. **7,** 904-910.

Citovsky, V., Wong, M.L., Shaw, A.L., Prasad, B.V.V., and Zambryski, P. (1992). Visualization and characterization of *Tobacco mosaic virus* movement protein-binding to single-stranded nucleic acids. The Plant Cell **4,** 397-411.

Conrath, U., Klessig, D.F., and Bachmair, A. (1998). Tobacco plants perturbed in the ubiquitin-dependent protein degradation system accumulate callose, salicylic acid, and pathogenesis-related protein 1. Plant Cell Rep. **17,** 876-880.

Cronin, S., Verchot, J., Haldemancahill, R., Schaad, M.C., and Carrington, J.C. (1995). Long-distance movement factor: a transport function of the potyvirus helper component proteinase. The Plant Cell **7,** 549-559.

Dawson, W.O. (1992). *Tobamovirus*-plant interactions. Virology **186,** 359-367.

Desvoyes, B., and Scholthof, H.B. (2002). Host-dependent recombination of a *Tomato bushy stunt virus* coat protein mutant yields truncated capsid subunits that form virus-like complexes which benefit systemic spread. Virology **304,** 434-442.

Desvoyes, B., Faure-Rabasse, S., Chen, M.H., Park, J.W., and Scholthof, H.B. (2002). A novel plant homeodomain protein interacts in a functionally relevant manner with a virus movement protein. Plant Physiol. **129,** 1521-1532.

Ding, B., Haudenshield, J.S., Hull, R.J., Wolf, S., Beachy, R.N., and Lucas, W.J. (1992). Secondary plasmodesmata are specific sites of localization of the *Tobacco mosaic virus* movement protein in transgenic tobacco plants. The Plant Cell **4,** 915-928.

Ding, S.W., and Voinnet, O. (2007). Antiviral immunity directed by small RNAs. Cell **130,** 413-426.

Ding, S.W., Li, W.X., and Symons, R.H. (1995). A novel naturally occurring hybrid gene encoded by a plant RNA virus facilitates long-distance virus movement. EMBO J. **14,** 5762-5772.

Ding, S.W., Li, H.W., Lu, R., Li, F., and Li, W.X. (2004). RNA silencing: a conserved antiviral immunity of plants and animals. Virus Res. **102,** 109-115.

Duggal, R., Lahser, F.C., and Hall, T.C. (1994). *Cis*-acting sequences in the replication of plant-viruses with plus-sense RNA genomes. Annu. Rev. Phytopathol. **32,** 287-309.

Dunoyer, P., Lecellier, C.H., Parizotto, E.A., Himber, C., and Voinnet, O. (2004). Probing the microRNA and small interfering RNA pathways with virus-encoded suppressors of RNA silencing. The Plant Cell **16,** 1235-1250.

Dykxhoorn, D.M., and Lieberman, J. (2006). Silencing viral infection. PLoS Med. **3,** 1000-1004.

Fire, A., Xu, S.Q., Montgomery, M.K., Kostas, S.A., Driver, S.E., and Mello, C.C. (1998). Potent and specific genetic interference by double-stranded RNA in *Caenorhabditis elegans*. Nature **391,** 806-811.

Gallitelli, D., Hull, R., and Koenig, R. (1985). Relationships among viruses in the *Tombusvirus* group - nucleic acid hybridization studies. J. Gen. Virol. **66,** 1523-1531.

Gamarnik, A.V., and Andino, R. (1998). Switch from translation to RNA replication in a positive-stranded RNA virus. Genes Dev. **12,** 2293-2304.

Goldberg, K.B., Kiernan, J., and Shepherd, R.J. (1991). A disease syndrome associated with expression of gene-VI of *Caulimoviruses* may be a nonhost reaction. Mol. Plant-Microbe Interact. **4,** 182-189.

Goodner, B., Hinkle, G., Gattung, S., Miller, N., Blanchard, M., Qurollo, B., Goldman, B.S., Cao, Y.W., Askenazi, M., Halling, C., Mullin, L., Houmiel, K., Gordon, J., Vaudin, M., Iartchouk, O., Epp, A., Liu, F., Wollam, C., Allinger, M., Doughty, D., Scott, C., Lappas, C., Markelz, B., Flanagan, C., Crowell, C., Gurson, J., Lomo, C., Sear, C., Strub, G., Cielo, C., and Slater, S. (2001). Genome sequence of the plant pathogen and biotechnology agent *Agrobacterium tumefaciens C58*. Science **294,** 2323-2328.

Grishok, A., Pasquinelli, A.E., Conte, D., Li, N., Parrish, S., Ha, I., Baillie, D.L., Fire, A., Ruvkun, G., and Mello, C.C. (2001). Genes and mechanisms related to RNA interference regulate expression of the small temporal RNAs that control *C. elegans* developmental timing. Cell **106,** 23-34.

Hamilton, A., Voinnet, O., Chappell, L., and Baulcombe, D. (2002). Two classes of short interfering RNA in RNA silencing. EMBO J. **21,** 4671-4679.

Hamilton, A.J., and Baulcombe, D.C. (1999). A species of small antisense RNA in posttranscriptional gene silencing in plants. Science **286,** 950-952.

Hearne, P.Q., Knorr, D.A., Hillman, B.I., and Morris, T.J. (1990). The complete genome structure and synthesis of infectious RNA from clones of *Tomato bushy stunt virus*. Virology **177,** 141-151.

Heinlein, M. (2002). The spread of *Tobacco mosaic virus* infection: insights into the cellular mechanism of RNA transport. Cell. Mol. Life Sci. **59,** 58-82.

Heinlein, M., Epel, B.L., Padgett, H.S., and Beachy, R.N. (1995). Interaction of *Tobamovirus* movement proteins with the plant cytoskeleton. Science **270,** 1983-1985.

Heinlein, M., Padgett, H.S., Gens, J.S., Pickard, B.G., Casper, S.J., Epel, B.L., and Beachy, R.N. (1998). Changing patterns of localization of the *Tobacco mosaic virus* movement protein and replicase to the endoplasmic reticulum and microtubules during infection. The Plant Cell **10,** 1107-1120.

Hillman, B.I., Carrington, J.C., and Morris, T.J. (1987). A defective interfering RNA that contains a mosaic of a plant virus genome. Cell **51,** 427-433.

Hofius, D., Herbers, K., Melzer, M., Omid, A., Tacke, E., Wolf, S., and Sonnewald, U. (2001). Evidence for expression level-dependent modulation of carbohydrate status and viral resistance by the *Potato leafroll virus* movement protein in transgenic tobacco plants. Plant J. **28,** 529-543.

Hood, E.E., Helmer, G.L., Fraley, R.T., and Chilton, M.D. (1986a). The hypervirulence of *Agrobacterium tumefaciens* A281 is encoded in a region of pTiBo542 outside of T-DNA. J. Bacteriol. **168,** 1291-1301.

Hood, E.E., Chilton, W.S., Chilton, M.D., and Fraley, R.T. (1986b). Transfer DNA and opine synthetic loci in tumors incited by *Agrobacterium tumefaciens* A281 on soybean and alfalfa plants. J. Bacteriol. **168,** 1283-1290.

Hull, R. (2002). Matthews' plant virology. (London: Academic Press).

Jimenez, I., Lopez, L., Alamillo, J.M., Valli, A., and Garcia, J.A. (2006). Identification of a *Plum pox virus* CI-interacting protein from chloroplast that has a negative effect in virus infection. Mol. Plant-Microbe Interact. **19,** 350-358.

Kaido, M., Inoue, Y., Takeda, Y., Sugiyama, K., Takeda, A., Mori, M., Tamai, A., Meshi, T., Okuno, T., and Mise, K. (2007). Downregulation of the *NbNACa1* gene encoding a movement-protein-interacting protein reduces cell-to-cell movement of *Brome mosaic virus* in *Nicotiana benthamiana*. Mol. Plant. Microb. Interact. **20,** 671-681.

Kasschau, K.D., Xie, Z., Allen, E., Llave, C., Chapman, E.J., Krizan, K.A., and Carrington, J.C. (2003). P1/HC-Pro, a viral suppressor of RNA silencing, interferes with *Arabidopsis* development and miRNA unction. Dev. Cell **4,** 205-217.

Kawakami, S., Watanabe, Y., and Beachy, R.N. (2004). *Tobacco mosaic virus* infection spreads cell to cell as intact replication complexes. Proc. Natl. Acad. Sci. USA **101,** 6291-6296.

Kiselyova, O.I., Yaminsky, I.V., Karger, E.M., Frolova, O.Y., Dorokhov, Y.L., and Atabekov, J.G. (2001). Visualization by atomic force microscopy of *Tobacco mosaic virus* movement protein-RNA complexes formed *in vitro*. J. Gen. Virol. **82,** 1503-1508.

Koonin, E.V., and Dolja, V.V. (1993). Evolution and taxonomy of positive-strand RNA viruses - implications of comparative analysis of amino acid sequences Crit. Rev. Biochem. Mol. Bio. **28,** 546-547.

Lakatos, L., Szittya, G., Silhavy, D., and Burgyan, J. (2004). Molecular mechanism of RNA silencing suppression mediated by p19 protein of tombusviruses. EMBO J. **23,** 876-884.

Lakatos, L., Csorba, T., Pantaleo, V., Chapman, E.J., Carrington, J.C., Liu, Y.P., Dolja, V.V., Calvino, L.F., Lopez-Moya, J.J., and Burgyan, J. (2006). Small RNA binding is a common strategy to suppress RNA silencing by several viral suppressors. EMBO J. **25,** 2768-2780.

Lazarowitz, S.G., and Beachy, R.N. (1999). Viral movement proteins as probes for intracellular and intercellular trafficking in plants. The Plant Cell **11,** 535-548.

Liu, J.Z., Blancaflor, E.B., and Nelson, R.S. (2005). The *Tobacco mosaic virus* 126-kilodalton protein, a constituent of the virus replication complex, alone or within the complex aligns with and traffics along microfilaments. Plant Physiol. **138,** 1853-1865.

Liu, Y., Schiff, M., Serino, G., Deng, X.W., and Dinesh-Kumar, S.P. (2002a). Role of SCF ubiquitin-ligase and the COP9 signalosome in the *N* gene-mediated resistance response to *Tobacco mosaic virus*. The Plant Cell **14,** 1483-1496.

Liu, Y.L., Schiff, M., and Dinesh-Kumar, S.P. (2004). Involvement of MEK1 MAPKK, NTF6 MAPK, WRKY/MYB transcription factors, COI1 and CTR1 in *N*-mediated resistance to *Tobacco mosaic virus*. Plant J. **38,** 800-809.

Liu, Y.L., Schiff, M., Marathe, R., and Dinesh-Kumar, S.P. (2002b). Tobacco *rar1*, *eds1* and *npr1/nim1* like genes are required for *N*-mediated resistance to *Tobacco mosaic virus*. Plant J. **30,** 415-429.

Lough, T.J., Shash, K., Xoconostle-Cazares, B., Hofstra, K.R., Beck, D.L., Balmori, E., Forster, R.L.S., and Lucas, W.J. (1998). Molecular dissection of the mechanism by which potexvirus triple gene block proteins mediate cell-to-cell transport of infectious RNA. Mol. Plant-Microbe Interact. **11,** 801-814.

Lu, R., Folimonov, A., Shintaku, M., Li, W.X., Falk, B.W., Dawson, W.O., and Ding, S.W. (2004). Three distinct suppressors of RNA silencing encoded by a 20-kb viral RNA genome. Proc. Natl. Acad. Sci. USA **101,** 15742-15747.

Lucas, W.J. (1995). Plasmodesmata: intercellular channels for macromolecular transport in plants. Curr. Opin. Cell Biol. **7,** 673-680.

Lucas, W.J. (2006). Plant viral movement proteins: agents for cell-to-cell trafficking of viral genomes. Virology **344,** 169-184.

Lucas, W.J., and Lee, J.Y. (2004). Plant cell biology: plasmodesmata as a supracellular control network in plants. Nat. Rev. Mol. Cell Biol. **5,** 712-726.

Martelli, G.P., Gallitelli, D., and Russo, M. (1988). Tombusviruses. In The plant viruses, R. Koenig, ed (New York: Plenum Publishing Corp.), pp. 13–72.

Molnar, A., Csorba, T., Lakatos, L., Varallyay, E., Lacomme, C., and Burgyan, J. (2005). Plant virus-derived small interfering RNAs originate predominantly from highly structured single-stranded viral RNAs. J. Virol. **79,** 7812-7818.

Nagy, P.D., and Pogany, J. (2000). Partial purification and characterization of *Cucumber necrosis virus* and *Tomato bushy stunt virus* RNA-dependent RNA

polymerases: similarities and differences in template usage between tombusvirus and carmovirus RNA-dependent RNA polymerases. Virology **276,** 279-288.

Olson, A.J., Bricogne, G., and Harrison, S.C. (1983). Structure of *Tomato busy stunt virus* IV. The virus particle at 2.9 °A resolution. J. Mol. Biol. **171,** 61-93.

Omarov, R., Sparks, K., Smith, L., Zindovic, J., and Scholthof, H.B. (2006). Biological relevance of a stable biochemical interaction between the tombusvirus-encoded P19 and short interfering RNAs. J. Virol. **80,** 3000-3008.

Omarov, R.T., Ciomperlik, J.J., and Scholthof, H.B. (2007). RNAi-associated ssRNA-specific ribonucleases in *Tombusvirus* P19 mutant-infected plants and evidence for a discrete siRNA-containing effector complex. Proc. Natl. Acad. Sci. USA **104,** 1714-1719.

Oparka, K.J., and Cruz, S.S. (2000). The great escape: phloem transport and unloading of macromolecules. Annu. Rev. Plant Physiol. Plant Mol. Biol. **51,** 323-347.

Papp, I., Mette, M.F., Aufsatz, W., Daxinger, L., Schauer, S.E., Ray, A., van der Winden, J., Matzke, M., and Matzke, A.J.M. (2003). Evidence for nuclear processing of plant micro RNA and short interfering RNA precursors. Plant Physiol. **132,** 1382-1390.

Park, J.W., Desvoyes, B., and Scholthof, H.B. (2002). *Tomato bushy stunt virus* genomic RNA accumulation is regulated by interdependent cis-acting elements within the movement protein open reading frames. J. Virol. **76,** 12747-12757.

Park, J.W., Faure-Rabasse, S., Robinson, M.A., Desvoyes, B., and Scholthof, H.B. (2004). The multifunctional plant viral suppressor of gene silencing P19 interacts with itself and an RNA binding host protein. Virology **323,** 49-58.

Plasterk, R.H.A. (2002). RNA silencing: the genome's immune system. Science **296,** 1263-1265.

Qiu, W., Park, J.W., and Scholthof, H.B. (2002). *Tombusvirus* P19-mediated suppression of virus-induced gene silencing is controlled by genetic and dosage features that influence pathogenicity. Mol. Plant. Microb. Interact. **15,** 269-280.

Qu, F., and Morris, T.J. (2002). Efficient infection of *Nicotiana benthamiana* by *Tomato bushy stunt virus* is facilitated by the coat protein and maintained by p19 through suppression of gene silencing. Mol. Plant-Microbe Interact. **15,** 193-202.

Qu, F., and Morris, T.J. (2005). Suppressors of RNA silencing encoded by plant viruses and their role in viral infections. FEBS Lett. **579,** 5958-5964.

Qu, F., Ren, T., and Morris, T.J. (2003). The coat protein of *Turnip crinkle virus* suppresses posttranscriptional gene silencing at an early initiation step. J. Virol. **77,** 511-522.

Roberts, I.M., Wang, D., Findlay, K., and Maule, A.J. (1998). Ultrastructural and temporal observations of the potyvirus cylindrical inclusions (CIs) show that the CI protein acts transiently in aiding virus movement. Virology **245,** 173-181.

Robinson, R. (2004). RNAi therapeutics: how likely, how soon? PLoS Biol. **2,** E28.

Rubio, T., Borja, M., Scholthof, H.B., Feldstein, P.A., Morris, T.J., and Jackson, A.O. (1999). Broad-spectrum protection against tombusviruses elicited by defective interfering RNAs in transgenic plants. J. Virol. **73,** 5070-5078.

Sagan, S.M., Koukiekolo, R., Rodgers, E., Goto, N.K., and Pezacki, J.P. (2007). Inhibition of siRNA binding to a p19 viral suppressor of RNA silencing by cysteine alkylation. Angew. Chem. Int. Edit. **46,** 2005-2009.

Sambrook, J., Fritsch, E.F., and Maniatis, T. (1989). Molecular cloning: a laboratory manual. (Cold Spring Harbor, N.Y.: Cold Spring Harbor Laboratory).

Scholthof, H.B. (1999). Rapid delivery of foreign genes into plants by direct rub-inoculation with intact plasmid DNA of a *Tomato busby stunt virus* gene vector. J. Virol. **73,** 7823-7829.

Scholthof, H.B. (2005). Plant virus transport: motions of functional equivalence. Trends Plant Sci. **10,** 376-382.

Scholthof, H.B. (2006). The *Tombusvirus*-encoded P19: from irrelevance to elegance. Nat. Rev. Microbiol. **4,** 405-411.

Scholthof, H.B. (2007). Heterologous expression of viral RNA interference suppressors: RISC management. Plant Physiol. **145,** 1110-1117.

Scholthof, H.B., and Jackson, A.O. (1997). The enigma of pX: a host-dependent cis-acting element with variable effects on *Tombusvirus* RNA accumulation. Virology **237,** 56-65.

Scholthof, H.B., Morris, T.J., and Jackson, A.O. (1993). The capsid protein gene of *Tomato bushy stunt virus* is dispensable for systemic movement and can be replaced for localized expression of foreign genes. Mol. Plant-Microbe Interact. **6,** 309-322.

Scholthof, H.B., Scholthof, K.B.G., and Jackson, A.O. (1995a). Identification of *Tomato bushy stunt virus* host-specific symptom determinants by expression of individual genes from a *Potato virus X* vector. The Plant Cell **7,** 1157-1172.

Scholthof, H.B., Scholthof, K.-B.G., Kikkert, M., and Jackson, A.O. (1995b). *Tomato bushy stunt virus* spread is regulated by two nested genes that function in cell-to-cell movement and host-dependent systemic invasion. Virology **213,** 425-438.

Scholthof, H.B., Desvoyes, B., Kuecker, J., and Whitehead, E. (1999). Biological activity of two *Tombusvirus* proteins translated from nested genes is influenced by dosage control via context-dependent leaky scanning. Mol. Plant-Microbe Interact. **12,** 670-679.

Scholthof, K.-B.G., Scholthof, H.B., and Jackson, A.O. (1995c). The effect of defective interfering RNAs on the accumulation of *Tomato bushy stunt virus* proteins and implications for disease attenuation. Virology **211,** 324-328.

Seaberg, B.L. (2008). Host factors involved in viral movement through plants. In M.S. Thesis. Plant Pathology and Microbiology (College Station: Texas A&M University).

Siddiqui, S.A., Sarmiento, C., Truve, E., Lehto, H., and Lehto, K. (2008). Phenotypes and functional effects caused by various viral RNA silencing suppressors in transgenic *Nicotiana benthamiana* and *N. tabacum*. Mol. Plant-Microbe Interact. **21,** 178-187.

Silhavy, D., Molnar, A., Lucioli, A., Szittya, G., Hornyik, C., Tavazza, M., and Burgyan, J. (2002). A viral protein suppresses RNA silencing and binds silencing-generated, 21-to 25-nucleotide double-stranded RNAs. EMBO J. **21,** 3070-3080.

Simon, A.E., Roossinck, M.J., and Havelda, Z. (2004). Plant virus satellite and defective interfering RNAs: new paradigms for a new century. Annu. Rev. Phytopathol. **42,** 415-437.

Smith, K.M. (1935). A new virus disease of tomatoes. Nature **135,** 908-908.

Sokolova, M., Prufer, D., Tacke, E., and Rohde, W. (1997). The *Potato leafroll virus* 17K movement protein is pbosphorylated by a membrane-associated protein

kinase from potato with biochemical features of protein kinase C. FEBS Lett. **400,** 201-205.

Stuart, G., Moffett, K., and Bozarth, R.F. (2004). A whole genome perspective on the phylogeny of the plant virus family *Tombusviridae*. Arch. Virol. **149,** 1595-1610.

Szittya, G., Silhavy, D., Molnar, A., Havelda, Z., Lovas, A., Lakatos, L., Banfalvi, Z., and Burgyan, J. (2003). Low temperature inhibits RNA silencing-mediated defence by the control of siRNA generation. EMBO J. **22,** 633-640.

Takeda, A., Mise, K., and Okuno, T. (2005). RNA silencing suppressors encoded by viruses of the family RNA silencing suppressors encoded by viruses of the family *Tombusviridae*. Plant Biotechnol. **22,** 447-454.

Turina, M., Omarov, R., Murphy, J.F., Bazaldua-Hernandez, C., Desvoyes, B., and Scholthof, H.B. (2003). A newly identified role for *Tomato bushy stunt virus* P19 in short distance spread. Mol. Plant Pathol. **4,** 67-72.

Uhrig, J.F., Canto, T., Marshall, D., and MacFarlane, S.A. (2004). Relocalization of nuclear ALY proteins to the cytoplasm by the *Tomato bushy stunt virus* P19 pathogenicity protein. Plant Physiol. **135,** 2411-2423.

Vargason, J.M., Szittya, G., Burgyan, J., and Hall, T.M.T. (2003). Size selective recognition of siRNA by an RNA silencing suppressor. Cell **115,** 799-811.

Voinnet, O., Pinto, Y.M., and Baulcombe, D.C. (1999). Suppression of gene silencing: a general strategy used by diverse DNA and RNA viruses of plants. Proc. Natl. Acad. Sci. USA **96,** 14147-14152.

Voinnet, O., Lederer, C., and Baulcombe, D.C. (2000). A viral movement protein prevents spread of the gene silencing signal in *Nicotiana benthamiana*. Cell **103,** 157-167.

Voinnet, O., Rivas, S., Mestre, P., and Baulcombe, D. (2003). An enhanced transient expression system in plants based on suppression of gene silencing by the P19 protein of *Tomato bushy stunt virus*. Plant J. **33,** 949-956.

Waigmann, E., Lucas, W.J., Citovsky, V., and Zambryski, P. (1994). Direct functional assay for *Tobacco mosaic virus* cell-to-cell movement protein and identification of a domain involved in increasing plasmodesmal permeability. Proc. Natl. Acad. Sci. USA **91,** 1433-1437.

Waigmann, E., Cohen, Y., McLean, G., and Zambryski, P. (1998). Plasmodesmata: gateways for information transfer. Symp. Soc. Exp. Biol. **51,** 43-49.

Wang, H.L., Gilbertson, R.L., and Lucas, W.J. (1996). Spatial and temporal distribution of bean dwarf mosaic germinivirus in *Phaseolus vulgaris* and *Nicotiana benthamiana*. Phytopathology **86,** 1204-1214.

Whitham, S.A., Yang, C.L., and Goodin, M.M. (2006). Global impact: elucidating plant responses to viral infection. Mol. Plant-Microbe Interact. **19,** 1207-1215.

Wood, D.W., Setubal, J.C., Kaul, R., Monks, D.E., Kitajima, J.P., Okura, V.K., Zhou, Y., Chen, L., Wood, G.E., Almeida, N.F., Woo, L., Chen, Y.C., Paulsen, I.T., Eisen, J.A., Karp, P.D., Bovee, D., Chapman, P., Clendenning, J., Deatherage, G., Gillet, W., Grant, C., Kutyavin, T., Levy, R., Li, M.J., McClelland, E., Palmieri, A., Raymond, C., Rouse, G., Saenphimmachak, C., Wu, Z.N., Romero, P., Gordon, D., Zhang, S.P., Yoo, H.Y., Tao, Y.M., Biddle, P., Jung, M., Krespan, W., Perry, M., Gordon-Kamm, B., Liao, L., Kim, S., Hendrick, C., Zhao, Z.Y., Dolan, M., Chumley, F., Tingey, S.V., Tomb, J.F., Gordon, M.P., Olson, M.V., and Nester, E.W. (2001). The genome

of the natural genetic engineer *Agrobacterium tumefaciens* C58. Science **294,** 2317-2323.

Wroblewski, T., Tomczak, A., and Michelmore, R. (2005). Optimization of *Agrobacterium*-mediated transient assays of gene expression in lettuce, tomato and *Arabidopsis*. Plant Biotechol. J. **3,** 259-273.

Yamamura, Y., and Scholthof, H.B. (2005). *Tomato bushy stunt virus*: a resilient model system to study virus-plant interactions. Mol. Plant Pathol. **6,** 491-502.

Yang, S.J., Carter, S.A., Cole, A.B., Cheng, N.H., and Nelson, R.S. (2004). A natural variant of a host RNA-dependent RNA polymerase is associated with increased susceptibility to viruses by *Nicotiana benthamiana*. Proc. Natl. Acad. Sci. USA **101,** 6297-6302.

Ye, K., Malinina, L., and Patel, D.J. (2003). Recognition of small interfering RNA by a viral suppressor of RNA silencing. Nature **426,** 874-878.

Yoshii, A., Shimizu, T., Yoshida, A., Hamada, K., Sakurai, K., Yamaji, Y., Suzuki, M., Namba, S., and Hibi, T. (2008). NTH201, a novel class II KNOTTED1-like protein, facilitates the cell-to-cell movement of *Tobacco mosaic virus* in tobacco. Mol. Plant-Microbe Interact. **21,** 586-596.

Zeng, L.R., Vega-Sanchez, M.E., Zhu, T., and Wang, G.L. (2006). Ubiquitination-mediated protein degradation and modification: an emerging theme in plant-microbe interactions. Cell Res. **16,** 413-426.

Zou, G.M., and Yoder, M.C. (2005). Application of RNA interference to study stem cell function: current status and future perspectives. Biol. Cell **97,** 211-219.

VITA

Name: Yi-Cheng Hsieh

Address: 2132 TAMU, Dept. Plant Pathology and Microbiology,
Texas A&M University, College Station, TX 77843-2132

Email Address: yicheng_hsieh@yahoo.com

Education: Ph.D. in Plant Pathology, Texas A&M University,
College Station (August 2008)
M.S. in Entomology, National Taiwan University,
Taiwan (August 2000)
B.S. in Biology, Fu Jen Catholic University, Taiwan (August 1998)

Selected Awards:
Outstanding Graduate Student Award,
Plant Pathology and Microbiology, Texas A&M University, 2008
Graduate Student Research and Presentation Grant,
Association of Former Students and the Office of Graduate Studies,
Texas A&M University, 2008
Student Travel Award for ASV Annual Meeting, 2008
Student Travel Award for ASV Annual Meeting, 2007
Graduate Research Assistantship,
Plant Pathology and Microbiology, 2004- present
Graduate Assistantship (Non-teaching),
Plant Pathology and Microbiology, 2003-2004

Selected Publications:

Y. Hsieh, R. T. Omarov, and H. B. Scholthof. *In vitro* expression of non-toxic but RNAi suppression-active tombusvirus P19 on *Nicotiana benthamiana. Plant Journal*, in preparation.

Y. Hsieh, R. T. Omarov, and H. B. Scholthof. Diverse biological effects influenced by perturbed interaction between tombusvirus-encoded P19 and siRNAs. *Journal of Virology*, in preparation.

Y. Hsieh, B. T. Shaw, and H. B. Scholthof. Distinguished viral RNA accumulation and localization caused by defective dimerization on tombusvirus-encoded movement protein P22 (Journal, tbd).

C. Angel, **Y. Hsieh**, H. B. Scholthof, and J. Schoelz. Biological effects of tombusvirus P19 and P22 proteins agroinfiltrated in Nicotiana species, in communication.

Professional Activities:
Member of American Society for Virology, 2007-present
Member of American Phytopathological Society, 2005-present
Secretary, Taiwanese Student Association,
Texas A&M University, 2004
Member, Graduate Student Club, Plant Pathology and
Microbiology, 2003-present